Journal Pre-proofs

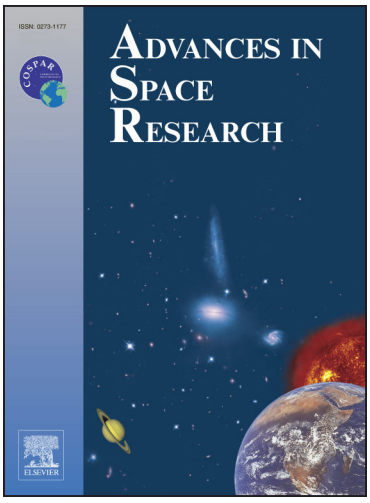


# Long-term Solar Variability: ISWAT S1 Cluster Review for COSPAR Space Weather Roadmap

Alexei A. Pevtsov, Dibyendu Nandy, Ilya Usoskin, Alexander A. Pevtsov, Claudio Corti, Laure Lefèvre, Mathew Owens, Gang Li, Natalie Krivova, Chitradeep Saha, Barbara Perri, Allan S. Brun, Antoine Strugarek, Maher A. Dayeh, Yury A. Nagovitsyn, Robertus Erdélyi

PII: S0273-1177(23)00682-8
DOI: https://doi.org/10.1016/j.asr.2023.08.034
Reference: JASR 16920

To appear in: *Advances in Space Research*

Accepted Date: 21 August 2023

Please cite this article as: Pevtsov, A.A., Nandy, D., Usoskin, I., Pevtsov, A.A., Corti, C., Lefèvre, L., Owens, M., Li, G., Krivova, N., Saha, C., Perri, B., Brun, A.S., Strugarek, A., Dayeh, M.A., Nagovitsyn, Y.A., Erdélyi, R., Long-term Solar Variability: ISWAT S1 Cluster Review for COSPAR Space Weather Roadmap, *Advances in Space Research* (2023), doi: https://doi.org/10.1016/j.asr.2023.08.034

Available online at www.sciencedirect.com

ScienceDirect

Advances in Space Research xx (2023) xxx-xxx

ADVANCES IN SPACE RESEARCH (a COSPAR publication)

www.elsevier.com/locate/asr

# Long-term Solar Variability: ISWAT S1 Cluster Review for COSPAR Space Weather Roadmap

Alexei A. Pevtsov[a,*], Dibyendu Nandy[b,c], Ilya Usoskin[d], Alexander A. Pevtsov[a], Claudio Corti[e,f], Laure Lefèvre[g], Mathew Owens[h], Gang Li[i], Natalie Krivova[j], Chitradeep Saha[b], Barbara Perri[k], Allan S. Brun[k], Antoine Strugarek[k], Maher A. Dayeh[l,m], Yury A. Nagovitsyn[n,o], Robertus Erdélyi[p,q,r]

[a] *National Solar Observatory, 3665 Discovery Drive, 3rd Floor, Boulder, CO 80303, USA*
[b] *Center of Excellence in Space Sciences India, Indian Institute of Science Education and Research Kolkata, Mohanpur 741246, West Bengal, India*
[c] *Department of Physical Sciences, Indian Institute of Science Education and Research Kolkata, Mohanpur 741246, West Bengal, India*
[d] *Sodankylä Geophysical Observatory and Space Physics and Astronomy Research Unit, University of Oulu, 90014 Oulu, Finland*
[e] *NASA Goddard Space Flight Center, Greenbelt, MD 20771, USA*
[f] *Physics and Astronomy Department, University of Hawaii at Manoa, Honolulu, HI 96822, USA*
[g] *Royal Observatory of Belgium, WDC-SILSO, STCE, Brussels, 1180, Belgium*
[h] *Department of Meteorology, University of Reading, Earley Gate, PO Box 243, Reading, RG6 6BB, UK*
[i] *CSPAR and Department of Space Science, University of Alabama in Huntsville, Huntsville, 35899, USA*
[j] *Max-Planck Institute for Solar System Research, Göttingen, 37077, Germany*
[k] *Université Paris-Saclay, Université Paris Cité, CEA, CNRS, AIM, Gif-sur-Yvette, 91191, France*
[l] *Southwest Research Institute, San Antonio, TX 78238, USA*
[m] *University of Texas at San Antonio, San Antonio, TX 78249, USA*
[n] *Central Astronomical Observatory of the Russian Academy of Sciences at Pulkovo, St. Petersburg 196140, Russia*
[o] *St. Petersburg State University of Aerospace Instrumentation, St. Petersburg 190000, Russia*
[p] *Solar Physics and Space Plasma Research Centre (SP2RC), School of Mathematics and Statistics, University of Sheffield, Sheffield, S3 7RH, UK*
[q] *Department of Astronomy, Eötvös Loránd University, Budapest, H-1117, Hungary*
[r] *Gyula Bay Zoltán Solar Observatory, Hungarian Solar Physics Foundation, Gyula, H-5700, Hungary*

Received 31 March 2023;

## Abstract

The Committee on Space Research (COSPAR) is updating its Roadmap on Space Weather. As input for this update, the COSPAR International Space Weather Action Teams (ISWAT) were asked to provide an overview of the current state-of-the-art and advancements since the last Roadmap (Schrijver et al., 2015), identifying gaps and opportunities for moving forward within the next 5 years — based on ongoing and planned missions, available modeling, and observational capabilities — and presenting an outlook beyond 5 years and recommendations on reaching long-term goals. While space weather is typically associated with short-term solar activity, knowledge of past solar variability observed and recorded through various parameters, including historical space weather events, informs us about the range of possible solar fluctuations. This long-term solar variability, belonging to the domain of space climate, is the prime focus of the ISWAT S1 Cluster. The goal of this paper is to describe the key objectives of the three S1 Action Teams, summarize the current state of knowledge of the topic that each team is focusing on, and identify the key science gaps that need to be addressed in each area.


*Keywords:* sunspot time series; solar total and spectral irradiance; large-scale heliospheric parameters; physical understanding of long-term variability; historical data preservation; long-term observations of the Sun

https://dx.doi.org/10.1016/j.jasr.xxxx.xx.xxx

## 1. Introduction

Life on Earth has been in existence from about 3.7–3.8 billion years ago (*e.g.*, Dodd et al., 2017). Over that time period, the solar total luminosity has increased by about 25% as compared to the modern-day Sun (*e.g.*, Ribas, 2009). By comparison, in modern days the total solar luminosity changes by about 0.1% over the 11-year sunspot cycle, indicating a very stable energy flow from the Sun to Earth — a prerequisite for a stable climate. Recent studies of stellar evolution also indicate that the early Sun may have exhibited cycle variability similar to that of modern times, albeit with larger amplitudes and different periods. Studies of solar analogs also suggest that after a star (Sun) enters the main sequence its magnetic activity gradually decreases until it is 6–7 Myr old (*e.g.*, Lorenzo-Oliveira et al., 2018). Thus, the magnetic activity on the Sun will continue similar to what we see today for another 1–2 Myr. Occasionally, this regular cycle variability is interrupted by extended periods of grand minima, the nature of which is still poorly understood. Thus, it is important to understand how solar activity is changing over long periods of time, what conditions affect the long-term variability and trigger the grand minima, and whether these changes could be predicted. The leading polarity of sunspot groups reverses between two consecutive cycles and, in relation to this, the polar fields change polarity shortly after the maximum of each sunspot cycle. This results in a 22-year magnetic (Hale) solar cycle. An analysis of solar activity reveals several other long-term periodicities, the strongest of which are the 90–100 years Gleissberg cycle (Gleissberg, 1939; see Hathaway, 2015 for a review) seen in sunspots and a quasi-210-year variability (sometimes referred to as Suess or de Vries cycle — see Usoskin, 2023) observed in cosmogenic isotopes time series (Suess, 1980; Hathaway, 2015). A 210-year variability may play a role in the recurrence of grand minima (*e.g.*, Tlatov & Pevtsov, 2017; Usoskin, 2023). The signature of all these periodicities is evident in many astrophysical channels, such as galactic cosmic rays (GCRs) and gamma-rays. Hale cycles directly affect the transport of GCRs in the heliosphere by changing the large-scale drift patterns (see, *e.g.*, Rankin et al., 2022 and Engelbrecht et al., 2022), producing a second-order effect in GCR modulation. Interactions of modulated GCRs with the solar photosphere and corona produce high-energy gamma-rays from the solar disk and halo, whose intensity is thus modulated over the solar cycle (see, *e.g.*, Linden et al., 2022 and Gutiérrez et al., 2022). The Sun also blocks high-energy GCRs, generating the so-called *Sun's shadow*, a depletion in the intensity of high-energy GCRs coming from the direction of the Sun. This shadow can be used to constrain coronal magnetic field models and it has been shown to vary with the 11-year and 22-year solar cycles (see, *e.g.*, Amenomori et al., 2000; Tjus et al., 2020; Aartsen et al., 2021). Most likely, the modulation of the Sun's shadow and high-energy gamma-rays is also present for longer periodicities. However, observations of these channels started only in the last couple of decades, so they have not been yet detected.

The Committee on Space Research (COSPAR) International Space Weather Action Teams (ISWAT) is a global center for community-coordinated collaborations to address challenges across the field of space weather. ISWAT activities are organized by Clusters and the Action Teams within Clusters. Cluster S1 focuses on reconstructing and establishing the ranges of variations of past solar activity, evaluating the extreme space weather and space climate episodes and, when possible, their impacts, helping to assess predictive models of solar activity ranging from solar dynamo and surface flux transport models to coronal and heliospheric field evolution models, and transition validated data-driven computational models to operational space weather (and space climate) forecasting tools. The Cluster is organized into three action teams: S1-01: Long-term solar variability; S1-02: Worst-case scenario for extreme solar events; and S1-03: Data sets of historical observations of solar and geomagnetic activity. In this paper, the leads of each Action Team and the research community were asked to provide a review of the current understanding of the research field, identifying the key outstanding questions and the current knowledge gaps, as well as the future research developments.

In Section 2 we review the observational and modeling aspects of sunspot time series, solar total and spectral irradiance, large-scale heliospheric parameters, and extreme solar events. Section 3 discusses the physical understanding of long-term variability, including solar cycle predictions and forcing on planetary environments. Section 4 addresses historical data preservation. Section 5 outlines the importance of continuity of long-term observations of the Sun, and Section 6 summarizes our review and high-level recommendations. Specific recommendations for each sub-field are provided at the end of each Section. Appendix A includes a list of acronyms used throughout the text.

## 2. Observational and modeling/theoretical aspects

Solar variability can be probed through the observation of various parameters available in different periods (length of the raw dataset) and timescales. The longest time series available is an index based on the number of spots and sunspot groups that appear on the Sun, called the sunspot number (Owens, 2013): it is available from the beginning of the 17th century. It enables the study of the long-term behavior of the Sun. Other solar-activity indices include, *e.g.*, the radio flux F10.7 (Tapping & Charrois, 1994), coronal index, etc. The spectral solar irradiance and the total solar irradiance have been directly measured since 1978 (see, *e.g.*, Ermolli et al., 2013; Kopp, 2016; DeLand et al., 2019 and references therein) and can be modeled before that using other long-term parameters, *e.g.*, sunspot (areas, positions, sunspot number) and plage (from white-light or Ca II K images) observations or cosmogenic isotope data (Solanki et al., 2013). The solar wind and heliospheric magnetic field have been directly measured by satellites for only a few decades

*Corresponding author.
*Email addresses:* apevtsov@nso.edu (Alexei A. Pevtsov), dnandi@iiserkol.ac.in (Dibyendu Nandy), ilya.usoskin@oulu.fi (Ilya Usoskin), aapevtsov@nso.edu (Alexander A. Pevtsov), corti@hawaii.edu (Claudio Corti)

Table 1. Key questions the S1 Action Teams are focused on.

| Question | Team | On the Web | Sections |
|---|---|---|---|
| What are the reliable estimates of long-term solar variability, based on proxy data, including uncertainty assessments? | S1-01 | Link | 2.1, 2.2, and 2.3 |
| Nature of the extreme events: What is an extreme event? How often can they occur? Does the Sun have a limit in producing extreme events? | S1-02 | Link | 2.4 |
| What is a comprehensive inventory of solar and geomagnetic datasets relevant for long-term space weather and space climate research; a standardized method for processing and preservation of historical data, their quality, and current state? What resources are needed to preserve these critical datasets? | S1-03 | Link | 4 |
| Physical understanding of long-term variability and its consequences | S1-01, S1-02 | | 3 |

(since late 1950s – early 1960s, Obridko & Vaisberg, 2017), but can be modeled over centuries and millennia through proxy data sources, *e.g.*, cosmogenic radionuclides. They are used, for example, to understand and anticipate solar eruptive events. Here we discuss only extreme solar events because of the focus on longer timescales of the ISWAT S1 Cluster.

In this section we present the available observations, their compilation, and different modeling approaches used to extend these observations back in time and/or through data gaps, and to estimate their uncertainties.

## 2.1. Sunspot number time series

### 2.1.1. Historical compilation of sunspot observations

The sunspot number (SN, Clette et al., 2014, 2015; Clette & Lefèvre, 2016) and group number (GN, Hoyt & Schatten, 1998a,b; Svalgaard & Schatten, 2016; Usoskin et al., 2016; Chatzistergos et al., 2017) are time series (1610 – present) that trace solar activity over more than 400 years. SN was computed in near real-time by Rudolf Wolf (1816–1893, Friedli, 2016) and his successors from 1849 onward and is a compilation of records from 1700 to 1848 (Friedli, 2016; Bhattacharya et al., 2023). Today it is produced and maintained by the WDC-SILSO[1]), since its transfer from Zürich to Brussels in 1981. For SN, the original formula of Rudolf Wolf for the daily sunspot number of a single observer is given by (Wolf, 1851, 1856):

$$\mathrm{SN} = k\,[(10 \times G) + S\,]\,, \qquad (1)$$

where $G$ is the number of sunspot groups on the solar disk on a given day, $S$ denotes the total number of individual spots within those groups, and $k$ is a normalization factor that brings different observers to a common scale ($k$ is the time-averaged ratio of daily SN of the primary reference observer to that of a secondary observer). Because there were about 10 spots per group on average in the nineteenth century, *i.e.*, $S \approx 10G$ (Waldmeier, 1968; Clette et al., 2014), the two parameters have about equal weight in SN. Despite its simplicity, historical SN time series may be non-uniform. Thus, for example, early observations by Wolf did not include small sunspots. In 1947, Waldmeier introduced unequal weights to sunspot counts to reflect their size and presence/absence of penumbra (Svalgaard et al., 2017). These non-uniformities are corrected in the most recent SN time series.

On the other hand, the group number series GN, built from the available raw source data, was compiled in 1995 (Hoyt & Schatten, 1998a,b). Its undeniable advantage is that it goes back to the first telescopic observations in 1610 (Vaquero & Vázquez, 2009; Arlt & Vaquero, 2020), and it is easier to compute with respect to SN. Because of the amount of work necessary to actually gather and compile all the data required for SN calculations, Hoyt & Schatten (1998a,b) created an index based on the number of groups which does not take the number of individual spots into account. In order for GN to be comparable with SN, Hoyt & Schatten (1998a,b) introduced a linear relationship where GN has to be multiplied by 12.08 to reach the level of SN. We note, however, that the approach of using SN as a proxy for GN needs to be taken with caution because the number of sunspots per group varies with phase of the solar cycle (*e.g.*, Tlatov, 2013). Georgieva et al. (2017) devised a correction function for the GN series that takes into account the changes in the number of sunspots per sunspot group from 1700–2017.

### 2.1.2. Observational data compilation

SN is a time series built by aggregating data from a number of observers with different quality and/or methods over a very long period of time (hundreds of years). The factor $k$ mentioned above is the key to assembling all data, but as the methods and understanding of the physics of the Sun evolved, so did the compilation methods.

Table 2 presents the evolution of the compilation methods of SN over time in Zürich and Brussels. From 1700 to 1848, SN was compiled from historical sources that can be found in the journals compiled by Rudolf Wolf (Wolf, 1848). From 1848[2] to 1876, Wolf used only his observations with gaps filled in by secondary observers (Bhattacharya et al., 2021, 2023). From 1877, Wolf introduced averaging of several observers for each daily observation.

For the historical part of the compilation, from 1700 to the 1850s, we can cite the example of Richard Carrington. Al-

[1] World Data Center – Sunspot Index and Long-term Solar Observations: https://www.sidc.be/silso/

[2] Wolf started observing from 1848, but only used his data from 1849.

though his observations are from 1853 to 1861, they happen at the very beginning of the consistent observations period and without Wolf's supervision, thus are a good representation of the historical part of the data. A recent study indeed shows that the counts of spots and groups made by Richard Carrington himself were biased by the goal of his studies. As his interest was the solar rotation (Carrington, 1863) he only counted the biggest spots and not the different umbras inside the penumbra as spots and also not all spots. In that sense, his counts were very different from modern sunspot counts and from Wolf counts over the same period (Bhattacharya et al., 2021).

Going back to the beginning of the GN series, with Galileo Galilei and Christoph Scheiner, there was a debate about the nature of sunspots (Carrasco et al., 2020). There was a significant change in the quality of sunspot drawings due to a new observation method used by Galileo from May, 1612. A student of Galileo, realized that one could project the solar image on a paper sheet in order to observe the Sun at any time of the day (Carrasco et al., 2020). This projection method greatly increased the number of groups recorded by Galileo. This fact can be seen from the comparison between the number of groups recorded by Galileo and Harriot (Carrasco et al., 2020).

Muñoz-Jaramillo & Vaquero (2019) describes the challenges encountered when trying to stitch together historical records, and thus when using said records. The challenge described here is mostly linked to the sparsity of coverage over certain key periods and can be partly overcome by adding more historical data to the time series as described in Arlt & Vaquero (2020) (see also the Belgian FARSUN project[3]). In addition to that, it is easy to see how the evolution in the knowledge of the historical observer and the contemporary interpreter can influence the counts, by, for example, comparing the extracted GN from Vaquero et al. (2016) to the GN from Hoyt & Schatten (1998a,b). It is even more sensitive when counting SN, which also contains the number of spots.

Considering the above-described possible inhomogeneities of the SN series, Hoyt & Schatten (1998a,b) decided to build a new series using the same method over the whole period. However, over time, when comparing SN and GN, it became evident that there were some discrepancies that were not linked to solar activity and could only be explained by investigating both sources closely (*e.g.*, Vaquero, 2007). In 2010, Frédéric Clette, Ed Cliver, and Leif Svalgaard launched a series of Sunspot Workshops[4] that led to a first recalibration of SN in 2015 and a series of reconstructions of GN (Clette et al., 2016b). Until 2015, SN was compiled following the method introduced by Wolf in 1849, perpetuated by his Zürich successors and passed on to Brussels in 1981 (Clette et al., 2007).

After this major update of the SN and GN series, a new relationship was determined (Clette et al., 2016b), based on GN from Svalgaard & Schatten (2016):

$$\mathrm{SN} = (17.8 \pm 0.4) \times \mathrm{GN} + (0.21 \pm 0.03) \times \mathrm{GN}^2. \quad (2)$$

There is currently an ongoing concerted effort to combine the strengths of all proposed methods to address their weaknesses (Clette et al., 2023). However, our community still needs to improve the compilation techniques, find better methodologies to quantify uncertainties, and, last but not least, continue the effort at recovering largely unexploited historical documents. The SN and GN series have now entered the era of modern data, and the goal is to include them in a versioning system, where the whole community can see both major updates to the data and the methods applied to compile them. We expect that a new, better, open-source, official sunspot number series will be released in late 2023 or early 2024 by the WDC-SILSO.

### 2.1.3. *Discussion of known issues and uncertainties*

Since 2011 and the beginning of the Sunspot workshops, we have learned a lot about both sunspot series, SN and GN. We know that before the recalibration effort started both series disagreed over certain specific periods: at the time of the creation of the SN series in 1850; at the end of the 19th century; at the beginning of the 20th century; around 1950; and in the most recent period, where a drift in SN could be seen. After this recalibration effort, documented in a Topical Issue (Clette et al., 2016b) and a recent review article (Clette et al., 2023) by an international team on *Recalibration of Sunspot Number Series*[5] at the International Space Science Institute, the situation has improved and there are fewer discrepancies in SN and GN time series. One of the remaining issues are the still imprecise uncertainties.

The GN series has been reconstructed using seven different methods (Hoyt & Schatten, 1998a,b; Cliver & Ling, 2016; Svalgaard & Schatten, 2016; Usoskin et al., 2016; Willamo et al., 2017; Chatzistergos et al., 2017; Dudok de Wit, personal communication). Figure 1 shows the results of these reconstructions for the 1700–2010 period. The reconstructions show larger differences mostly in the pre-Greenwich era (before 1867). They also have different time resolutions depending on the cadence of data employed: daily data (Cliver & Ling, 2016; Usoskin et al., 2016; Chatzistergos et al., 2017; Dudok de Wit, personal communication) or yearly data (Svalgaard & Schatten, 2016).

Hoyt & Schatten (1998a,b) created the first GN series in 1995 and an associated database. This series is known to suffer from many problems in data interpretation (Vaquero & Trigo, 2014) and compilation methods (Clette et al., 2014; Cliver, 2015). Cliver & Ling (2016) tried to reinterpret the Hoyt & Schatten database and created a revised GN that appears in blue in Figure 1. However, it still uses the old method of simple *k*-factors, which is known to introduce bias. Svalgaard & Schatten (2016) present a reconstruction of a complete GN series using a *backbone*[6] method. Contrary to the excessive

[3] Findability and Accessibility of historical (1610–1980) Raw Sunspot Numbers: https://www.belspo.be/belspo/brain2-be/project_p2_en.stm

[4] https://ssnworkshop.fandom.com/wiki/Home

[5] https://www.issibern.ch/teams/sunspotnoser/

[6] Backboning (after Svalgaard & Schatten, 2016): "*find a primary observer*

Table 2. Key dates in sunspot number observations from 1700. Before 1848, the number of observations per day was highly variable. For that period, information can be found in Hoyt & Schatten (1998a,b); Vaquero et al. (2016); Svalgaard & Schatten (2016); Cliver (2016). Table adapted from Dudok de Wit et al. (2016).

| Period | Description | Method | Time Coverage | Standard Observer |
|---|---|---|---|---|
| 1700–1748 | Historical sources gathered by Wolf | Crude yearly averages | Yearly | — |
| 1749–1817 | Idem | Standard and auxiliary observer (covering gaps) | Monthly only | Staudacher |
| 1818–1847 | Historical sources, Zürich observatory | Idem | Daily, partial coverage | Schwabe |
| 1848–1876 | Start of systematic observations by Wolf | Idem, crude counts, one to five observers | Daily, full coverage, one secondary station used for gaps | Wolf |
| 1877–1892 | Systematic observations, full counts | Two standard observers + auxiliary | Daily average of secondary stations for gaps | Wolf, Wolfer |
| 1893–1926 | Systematic observations | Idem | Idem | Wolfer |
| 1927–1980 | Zürich network[a] | Several standard observers + auxiliary | Daily average of standard observers; a few to ≈40 stations | Brunner, Waldmeier |
| 1981–2015 | SILSO network | Full network, pilot station, outlier removal | Daily average of ≈50 → ≈80 stations | Cortesi weighted counts |
| 2015– | SILSO network, transition to V2.0 | Idem | Daily average of ≈90 stations | Cortesi unweighted counts |

[a] The network of observers included both European and non-European countries.

use of *daisy chaining*[7] used in previous reconstructions, the backbone-method enables to actually minimize the number of links in the chain. Lockwood et al. (2016a,b) discuss the use of daisy chaining and the propagation of possible errors made on the linear fit between two observers. Usoskin et al. (2016) describe a method using the *active day fraction* (in a month) to compute an individual observational threshold for each observer that can be applied to a reference dataset (Greenwich data) in order to rescale (without overlap) all observers to a common reference. Despite the clear advantages, the approach may suffer from a hard-to-avoid dependency on the level of solar activity for non-overlapping observations. Willamo et al. (2017) tried to correct this method by addressing the known issues, but the dependency on the activity level still remains unresolved. Chatzistergos et al. (2017) developed a backbone reconstruction of group numbers that is based on the *correspondence matrices* described in Usoskin et al. (2016) instead of using a "simple" linear dependency between independent observers as in Svalgaard & Schatten (2016). The main drawback of this approach is that the dependency between the observers is poorly-defined at a higher number of groups. This could lead to underestimation of maxima of sunspot cycles. On the other hand, in previous reconstructions using $k$-factors taken from yearly values, such as in Svalgaard & Schatten (2016) or Cliver & Ling (2016), the cycle maxima are clearly larger than with other methods shown in Figure 1, *i.e.*, probably overestimated. A new method recently developed by Dudok de Wit (personal communication) employs tied ranking to combine the time series. The main drawback here is the need for a reference to do a conversion from the tied-ranking domain to the time domain. The selection of the reference may bias the result. Based on comparison with other methods (see Figure 1), it yields a time series which agrees reasonably well with other methods. Still, this new approach needs further evaluation.

At this time, all methods seem to perform reasonably well in reconstructing the GN series. None of the methods appears

*for a certain (long) interval and normalize all other observers individually to the primary based on overlap with only the primary (minimizing accumulation of errors)*".

[7] Daisy-chaining (after Svalgaard & Schatten, 2016): "*successively joining observers to the end of the series, based on overlap with the series as it extends so far (accumulates errors)*".

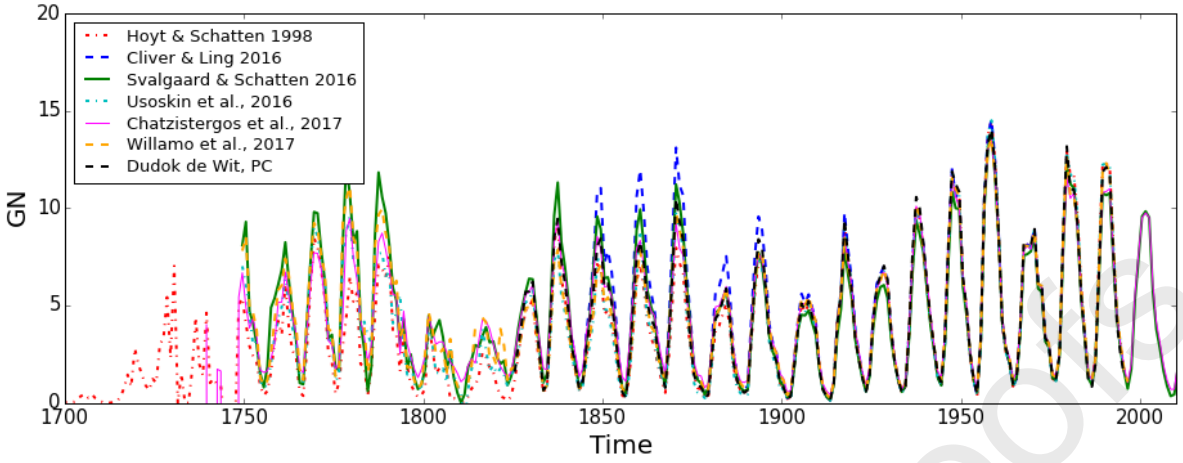


Fig. 1. Group number series from 1700 to 2010 provided by different teams.

to be superior, but it is clear that the original Hoyt & Schatten (1998a,b) series should not be used any longer. Some historical observational records used in the reconstruction of the original GN were misinterpreted, and the *k*-factors were sometimes incorrectly estimated.

The SN series, on the other hand, has been recalibrated for the period 1818–2015 with a small correction for the transition in 1850 between SN based on historical sources and the beginning of systematic observations by Wolf, an additional correction in 1947 due to the sunspot weighting introduced by Max Waldmeier, and a correction of the drift of the pilot station of the network at a later time. Also, in the historical SN — often referred to as *R* because Wolf called it the "*relative sunspot number*" (Izenman, 1985) — Wolfer and his successors applied a 0.6 factor to themselves in order to follow Wolf's scale. This scaling was abandoned in 2015 to follow Wolfer's scale and be comparable to other sunspot series, such as the Boulder Sunspot Number (*e.g.*, Feehrer, 2000) and National Solar Observatory (NSO) Sacrament Peak sunspot number (Carrasco et al., 2021a; see also link to "sunspot numbers data" in NSO's Historical Archive[8]). These corrections are described in Clette & Lefèvre (2016). However, recent works by Clette et al. (2021) and Bhattacharya et al. (2021, 2023) have shown that it is possible to correct the remaining inconsistencies by reconstructing the SN series from the available raw sunspot and group data. It is the case for the scale transfer from Schwabe to Wolf in 1849 (Bhattacharya et al., 2023) and the transition between Wolf and Wolfer over the 1860–1893 period (Bhattacharya, personal communication). WDC-SILSO SN2.1 time series has been recently described by Bhattacharya et al. (2023). The historical part of the next revision of the WDC-SILSO SN series (V3) will be released by the end of 2023, and is based on all available sunspot and group number data over the 19th and the beginning of the 20th century, including recently recovered data due to work by Drs. Hayakawa, Vaquero, and Arlt. Working versions will be based on simple *k*-factor daisy chaining, *i.e.*, reconstructed as Wolf would have done in the past, but the main version will be based on the method by Chatzistergos et al. (2017) developed for group numbers only, adapted to sunspot numbers. It will also include statistical uncertainties based on the properties of the distribution of data.

### 2.1.4. *Outstanding questions*

Computing SN and GN historical time series is never simple. First, the datasets are not homogeneous and could be affected by various observing biases, including changes in the observers' cohort with different levels of experience. Observing biases may also include differences in telescope aperture, the amount of scattered light (quality of optics and atmospheric seeing conditions), and even human vision (*e.g.*, Karachik et al., 2019). The effect of (small) telescope apertures could be different for SN, GN, and total area of sunspot groups (*e.g.*, Nagovitsyn & Georgieva, 2017). Second, data coverage is not homogeneous, with relatively good coverage in some periods and fewer or even no observations in other periods. Finally, the methods of reconstruction are still under development. The reconstruction methods described earlier all have their advantages and disadvantages that could affect the reconstruction differently over different periods. One could also argue that the total area of sunspots/groups is a better parameter as compared with SN and GN. The total group area is less sensitive to the loss of small sunspots (pores) due to observations with small aperture telescopes (*e.g.*, Nagovitsyn & Osipova, 2021). Also, the area of sunspots more closely represents a physical parameter such as the magnetic flux of active regions (*e.g.*, Ringnes & Jensen, 1960; Pevtsov et al., 2014). These methodology problems could be dealt with via further development of scientific, statistical, or analytical approaches.

[8] https://nso.edu/data/historical-archive/

### 2.2. Solar total and spectral irradiance time series

#### 2.2.1. Direct measurements and composite series

Solar irradiance is the radiative energy flux from the Sun incident on a plane of unit area perpendicular to the rays at the mean Sun-Earth distance (*i.e.*, 1 AU) outside of the terrestrial atmosphere. Total solar irradiance (TSI), earlier known as the *solar constant*, is the flux integrated over the entire spectral range, while spectral solar irradiance (SSI) is the flux per unit wavelength or within a given spectral interval.

Solar irradiance has been regularly monitored from space since 1978 (*e.g.*, Hickey et al., 1980; Willson et al., 1981; Willson & Hudson, 1988; Fröhlich, 2006, 2012; Kopp et al., 2016), albeit SSI measurements are significantly patchier than TSI, with gaps both in temporal and spectral coverage (Ermolli et al., 2013; DeLand et al., 2019; Woods & DeLand, 2021). The stability of the radiometers measuring TSI is sufficient to reliably recover the variability on timescales of minutes to the solar activity cycle. The typical amplitude of the variability measured over the last several decades is roughly 0.1% over the solar activity cycle and up to 0.3% on timescales of days to weeks (*i.e.*, due to the emergence and evolution of active regions and the modulation by the solar rotation). The potential change on longer timescales (secular variability) cannot be assessed with existing data.

Until now, measurements have been done by more than a dozen of individual instruments (Fröhlich, 2013), of which only a few survived more than a solar cycle (see, *e.g.*, Kopp, 2016; Montillet et al., 2022). Due to the difference in their absolute calibration, sensitivity changes, or interruptions in their operation (most famous being the so-called ACRIM[9] gap), their cross-calibration is not straightforward, hindering the construction of a composite record. A number of TSI composites have been constructed. The three "classical" ones are the PMOD[10] (Fröhlich, 2006), ROB[11] (Dewitte et al., 2004), and ACRIM (Willson, 1997; Willson & Mordvinov, 2003). Prior to the SoHO[12] launch in 1996, all these composites use essentially the same data, although in slightly different combinations and applying (or not) different corrections. Afterwards, the PMOD and ROB composites rely primarily on PMO6V[13] and DIARAD[14] radiometers on SoHO/VIRGO[15], while the ACRIM team continues with ACRIM-2 and later ACRIM-3. Updates and revisions of the PMOD and ACRIM composites were more recently published by Schmutz (2021) and Scafetta et al. (2019), respectively, but the changes are not significant. The reported secular change ranges from a rise between the activity minima in 1986 (solar cycles 21/22) and 2009 (solar cycles 23/24) in the ACRIM composite to a weak decline in PMOD. The rise in the ACRIM composite is, however, entirely due to the unaccounted slips in the Nimbus-7/HF data (Lee III et al., 1995), and is not featured by any other composite, models, or indeed alternative solar activity proxies.

In addition to these three TSI composites produced by different instrumental teams, two alternative composites were recently produced, essentially by statistical analysis and weighting of data from individual instruments (Dudok de Wit et al., 2017; Montillet et al., 2022). By their design, they do not provide any additional information on secular variability, although they provide statistical estimates of its uncertainty. Overall, no reliable conclusion on the minimum-to-minimum change in TSI during the period of measurements could be reached. Nevertheless, all composites suggest a marginal TSI decrease since 1996, and most even since 1978 (see Chatzistergos et al., 2023 for a detailed discussion).

SSI measurements have also been done since 1978 in the ultraviolet, with measurements in the visible and near-infrared being available only since 2003. The variability increases from roughly 0.1% over the solar cycle in the visible up to several tens percent in the ultraviolet, reaching about 100% around the Ly-$\alpha$ line at 121.6 nm (Floyd et al., 2003). While already earlier measurements pointed to the important role of the ultraviolet range for the overall irradiance variability, subsequent studies and observations showed that the radiation originating from the wavelengths below 400 nm contributes at least 50% to the TSI variability (Krivova et al., 2006; Woods et al., 2018; Dudok de Wit, 2022), and possibly significantly more (Harder et al., 2009; Haberreiter et al., 2017). The reevaluation of the SORCE/SIM[16] and SORCE/SOLSTICE[17] measurements used by Harder et al. (2009), and partly by Haberreiter et al. (2017), included a more careful analysis of the long-term instrumental stability. This led to slightly reduced estimates of the variability (*e.g.*, Woods et al., 2022; Dudok de Wit, 2022). However, the debate is not closed since longer uninterrupted SSI measurements with sufficient long-term stability are required. Related to this, in the infrared, between roughly 1300 and 2400 nm, models and observations suggest a variability in anti-phase with the solar cycle, but the exact spectral range and the magnitude of this anti-phase portion is also uncertain.

As the accuracy and the precision of the measurements vary with wavelength, the construction of an SSI composite record is significantly more challenging than in the case of TSI. The most recent composite is LASP GSFC SSI #3 by Woods & DeLand (2021), which is an update of the earlier versions by DeLand & Cebula (2008) and DeLand et al. (2019). It covers the spectral range 0.5–1600 nm over roughly the last two decades, and the ultraviolet range 120–500 nm back to 1978. For the quiet Sun it adopts the latest solar reference spectrum based on TSIS-1[18] SIM and the CubeSat Compact SIM data (Coddington et al., 2021), reported to be more accurate than earlier measurements used for the preceding and widely-used ATLAS-3[19] (Thuillier

[9] Active Cavity Radiometer Irradiance Monitor
[10] Physikalisch-Meteorologisches Observatorium Davos
[11] Royal Observatory of Belgium, previously known as RMIB, or IRMB in French, for Royal Meteorological Institute of Belgium
[12] Solar and Heliospheric Observatory
[13] Physikalisch-Meteorologisches Observatorium radiometer Version 6
[14] Differential Absolute Radiometer
[15] Variability of solar Irradiance and Gravity Oscillations
[16] Solar Radiation and Climate Experiment/Spectral Irradiance Monitor
[17] Solar Stellar Irradiance Comparison Experiment
[18] Total and Spectral Solar Irradiance Sensor – 1
[19] Atmospheric Laboratory for Applications and Science – 3

et al., 2004) and LASP WHI[20] (Woods et al., 2009) reference spectra. In particular, in the near-infrared the TSIS-1 spectrum is about 8%–10% lower. Also below 300 nm, the differences partly reach up to 10%.

### 2.2.2. Direct modeling

The variability of solar irradiance on timescales of minutes to hours is dominated by solar oscillations and granulation. On longer (except the evolutionary) timescales, it is driven by solar surface magnetism (Shapiro et al., 2017; Yeo et al., 2017). This means that the changes are the result of the perpetual competition between sunspot darkening and facular/network brightening. Thus, the task of the irradiance models is to adequately describe the contributions of the two components. For this, knowledge of the spatial distribution of the various magnetic features on the solar surface, as well as of their brightness, is needed.

Existing models can be divided into three classes: empirical, semi-empirical, and physical. The empirical models use linear regressions to link observational data representing sunspot darkening and facular brightening to direct irradiance measurements (*e.g.*, Willson et al., 1981; Hudson et al., 1982; Foukal & Lean, 1988; Chapman et al., 1996, 2013; Preminger et al., 2002; Wang et al., 2005; Wang & Lean, 2021; Coddington et al., 2016; Yeo et al., 2017; Chatzistergos et al., 2020a). Thus, these models are prone to take over all the uncertainties and problems of the irradiance measurements they rely on. While semi-empirical and physical models also employ solar observations to derive the surface coverage by sunspots and faculae, the brightness of these features (typically as a function of wavelength and solar limb distance) is computed using radiative transfer codes from solar model atmospheres. Semi-empirical models (*e.g.*, Fligge et al., 2000; Ermolli et al., 2003, 2011; Krivova et al., 2003; Penza et al., 2003; Fontenla et al., 2006, 2011; Wenzler et al., 2006; Ball et al., 2012; Yeo et al., 2014; Tagirov et al., 2019; Chatzistergos et al., 2021) use semi-empirical (thus the name of the model class) plane-parallel models, while the newest-generation physical models compute the emerging spectra from state-of-the-art 3D magnetohydrodynamics (MHD) simulations of the solar atmosphere. Currently, only one physics model exists (Yeo et al., 2017). While the semi-empirical models still contain at least one free parameter to scale the computed irradiance variations to the measurements, the SATIRE-3D[21] model by Yeo et al. (2017) does not require such scaling. This model reproduces about 97% of the TSI variability measured by SORCE/TIM[22] (Kopp et al., 2005), proving that solar surface magnetism is indeed the dominant mechanism driving the irradiance variability on timescales of days to decades. By model design, it is currently limited to the period covered by SDO/HMI[23] data.

[20] Whole Heliosphere Interval
[21] Spectral and Total Irradiance Reconstruction for the Satellite Era – 3D
[22] Total Irradiance Monitor
[23] Solar Dynamics Observatory/Heliospheric and Magnetic Imager

### 2.2.3. Long-term reconstructions

In order to reconstruct past irradiance variability, models, whether empirical or semi-empirical, require knowledge of the past evolution of the solar surface magnetism, *i.e.*, the surface coverage by various magnetic features at a given time. Whereas sunspot observations go back to 1610 (see Section 2.1), although with deteriorating quality, observations providing direct information on facular coverage are barely longer than space-borne irradiance measurements. Therefore, most of the available irradiance reconstructions for the last centuries use sunspot data. In general, there is a clear link between the emergence and evolution of sunspots and faculae, but there are also clear differences. Indeed, with growing activity the emergence rate of sunspots grows faster than that of faculae, and the emergence rate of yet smaller ephemeral magnetic regions changes even weaker (see, *e.g.*, Harvey, 1993; Foukal, 1993; Shapiro et al., 2014; Yeo et al., 2020a; Chatzistergos et al., 2022a; Nèmec et al., 2022). This is not accounted for by models relying on sunspot observations (see, *e.g.*, Krivova et al., 2021). The uncertainty of accounting for facular and network brightening prior to the satellite era leads to a high spread in the existing estimates of secular variability (see, *e.g.*, the review by Chatzistergos et al., 2023 and references therein). Using the only physical model SATIRE-3D (see Section 2.2.2) which does not require scaling to the measured TSI, and assuming that the global dynamo fully ceases during grand solar minima (*i.e.*, only the small-scale dynamo remains in action), Yeo et al. (2020b) set an upper limit of $2.0 \pm 0.7$ W/m$^2$ below the 2019 level on the possible decrease in TSI during a grand minimum, which reduces the range of the allowed amplitude by roughly a factor of two. This does not take into account any other (*i.e.*, non-magnetic) potential, yet unknown, mechanism of the irradiance variability. However, until now there has been no evidence that such a mechanism exists or is needed to explain existing observations.

Furthermore, to reduce the existing uncertainty in the secular variability, significant efforts have been recently put into digitizing, processing, calibrating, and analyzing the historical full-disc photographs of the Sun in the Ca II spectral line (see Chatzistergos et al., 2022b and references therein). Chatzistergos et al. (2020b) have presented the first composite of plage areas from 43 available datasets since the late 19th century. Being a good tracer of the solar surface magnetic field, Ca II images have the potential to provide the missing information and allow critical constraints on the secular variability (Chatzistergos et al., 2021).

Reconstructions going yet further back in time, before the start of telescopic observations of sunspots, use concentrations of cosmogenic isotopes in terrestrial archives, such as $^{10}$Be in ice sheets or $^{14}$C in ancient plants, as a proxy of solar magnetic activity. This is possible because cosmogenic isotopes are produced by galactic cosmic rays (GCRs), whose flux is modulated by the solar open magnetic flux (see Usoskin, 2023, and Sections 2.3.2 and 2.4.1). Since cosmogenic isotope data do not allow distinguishing between sunspots and faculae without further assumptions or models, reconstructions using such data need to be scaled in one way or another to either direct irradi-

ance measurements or to other reconstructions, *e.g.*, those based on sunspot observations. Therefore, they do not carry independent information on secular variability. Most models rely on linear regressions between cosmogenic data and modern measurements of either irradiance or other related quantities. Vieira & Solanki (2010) showed, however, that the relation is nonlinear. This is accounted for in the model by Vieira et al. (2011), more recently updated by Wu et al. (2018).

#### 2.2.4. Outstanding questions

The nearly four-and-a-half decades of space-based measurements of solar total and spectral irradiance returned invaluable information on the variability of what was previously considered to be the solar constant. In combination with extensive modeling efforts, this brought us a sound understanding of the mechanisms of irradiance variability. In particular, it has been ultimately shown that the variability on timescales of days to decades is driven by the ever-changing solar surface magnetic field. This allows reconstructions of past changes in solar irradiance provided appropriate proxies of the surface magnetism are available.

Yet, differences in the absolute calibration and unaccounted changes in instrument sensitivity do not currently allow a reliable estimate of the secular (*e.g.*, minimum-to-minimum) change in the TSI over the satellite era, while limited long-term stability as well as patchy wavelength and temporal coverage of spectral irradiance monitors lead to significant uncertainty in the solar cycle variability of solar near-ultraviolet (above around 250 nm), visible, and near-infrared irradiance. These uncertainties obviously also affect our ability to reconstruct past irradiance changes, aggravated by lack or insufficient quality and coverage of suitable proxies of solar magnetic activity in the past. The main open questions in irradiance studies include:

- What is the secular change in TSI over the period covered by direct space-borne measurements, that is since 1978?
- By how much can solar irradiance change on centennial and millennial timescales?
- What is the magnitude of the solar-cycle irradiance variability in the near-ultraviolet and near-infrared, and is the near-infrared variability in phase or anti-phase with the solar cycle?

Uninterrupted and at least partly overlapping, in both spatial and wavelength domains, monitoring of solar irradiance is absolutely imperative to answer these questions. High-resolution full-disc imagery at different wavelengths as well as synoptic magnetograms are important to gathering missing information on the radiative properties of different magnetic features, in particular the contrast of faculae/plage and network and its center-to-limb variation. The latter are crucial for understanding the impact of these features on the ultraviolet irradiance variability and for testing models of the spectral irradiance variability. Finally, preservation, recovery, digitizing, and careful processing of historic synoptic solar observations are indispensable to reconstructions of past irradiance changes.

### 2.3. Large-scale heliospheric parameters

The solar wind and heliospheric magnetic field (HMF) properties both evolve over the solar cycle and exhibit longer-term variations. Our information about these variations comes from direct in situ measurements, which reveal local variations, and proxy data, which typically relates to more global solar and heliospheric phenomena.

#### 2.3.1. In situ observations

Direct measurements of the solar wind and HMF at a single point in space and time can be made in situ with heliospheric spacecraft. Near-Earth solar wind observations stretch back to around 1964, with near-contiguous observations since 1996. Solar wind measurements are inherently local (*e.g.*, McComas et al., 2003), but the latitudinal invariance in the radial magnetic field component of the HMF observed by the Ulysses spacecraft (Smith & Balogh, 1995) means that the near-Earth HMF contains information about the global HMF. In particular, it can be used to estimate the total HMF content of the heliosphere (Owens et al., 2008), which is closely related to the open solar flux (OSF) which threads the source surface (Wang & Sheeley, 1995).

The total HMF approximately doubles between solar minimum and maximum, with secular variations showing a similar pattern to those seen in sunspots: a rise through the 60s and 70s to a peak in the late 80s and early 90s, and a decline since.

Solar wind speed and density in near-Earth space exhibit far less variation with the solar cycle. However, this is likely due to the local nature of the observations and the limited sampling of heliospheric latitude. Ulysses' observations revealed considerable variation in the solar wind speed over the solar cycle. At solar minimum, the mid- and high-latitude regions are dominated by fast (> 750 km/s) solar wind, with slow wind (~ 400 km/s) confined to the equatorial regions. At solar maximum, all latitudes exhibit fast wind (McComas et al., 2003). There are insufficient high-latitude observations to determine if there are secular variations in global solar wind speed.

#### 2.3.2. Proxy-based reconstructions

*Geomagnetic reconstructions.* Knowledge of the solar wind and HMF prior to the advent of in situ observations requires the use of more indirect proxy data. The most direct of such proxies comes from measurements of the Earth's own magnetic field, which date more than 170 years ago. As the Earth's field is disturbed from its equilibrium state by interaction with the local solar wind, it is possible to reconstruct the near-Earth solar wind conditions from ground-based magnetometer data (Feynman & Crooker, 1978). Owing to Earth's orbital variation and the highly variable out-of-ecliptic component of the HMF, such reconstructions are generally limited to annual timescales, to average out such effects. By using different geomagnetic indices based on observations from different geomagnetic latitudes, it is possible to deconvolve the influence from the HMF intensity and solar wind speed (Svalgaard & Cliver, 2010; Lockwood & Owens, 2011). At annual timescales, direct estimates of HMF intensity and solar wind speed based on

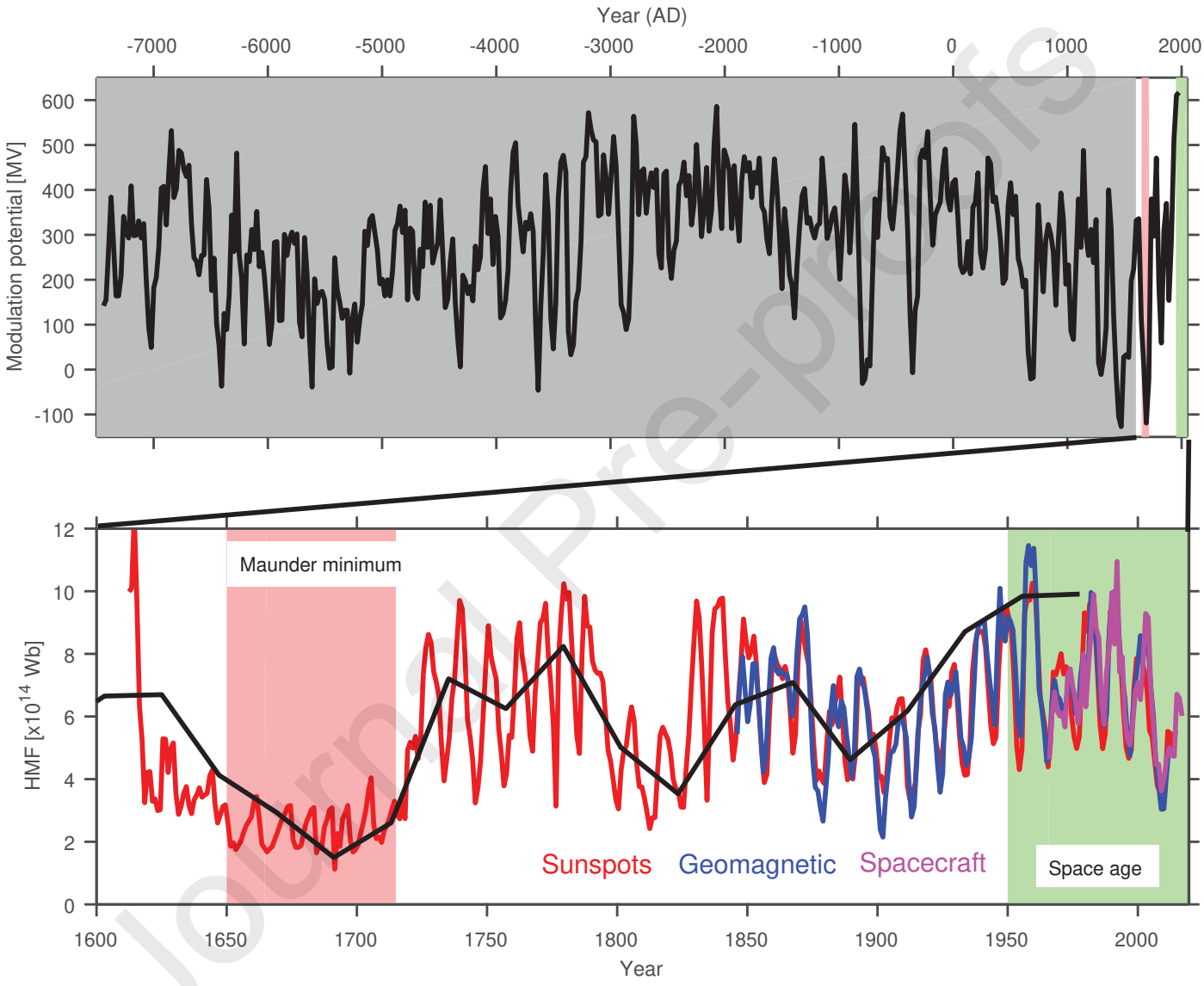


Fig. 2. Estimates of the heliospheric magnetic field from a number of proxy data sources. The top panel shows the heliospheric modulation potential, over the last 9,400 years, inferred from cosmogenic radionuclide records in tree trunks and ice sheets. This property is a proxy for the total heliospheric magnetic flux. Bottom: Total heliospheric magnetic flux, over the last 400 years, from spacecraft observations (magenta) and geomagnetic- (blue), sunspot- (red), and cosmogenic isotope- (black) based reconstructions. Figure taken from Owens et al. (2018).

geomagnetic indices correlate extremely well ($r$ = 0.94) with in situ observations (Owens et al., 2016). By assuming a Parker spiral magnetic field configuration, it is possible to reconstruct total HMF from geomagnetic observations (Lockwood et al., 2014). There is a strong upward trend in total HMF from the start of the 20th century, peaking during solar cycle 19 in the 1960s. The lowest values occur around 1900, which are comparable to 2010 solar minimum between solar cycles 22 and 23.

*Sunspot-based reconstructions.* As described in Section 2.1, the SN and GN time series provide an indirect measure of solar activity over the last 400 years. As sunspots are photospheric magnetic field structures, it follows that global SN has an indirect relation to total HMF. Using empirical regressions, it has been shown that there is a good correlation between HMF intensity and the square root of SN (Svalgaard & Cliver, 2005), using both 50 years of in situ observations ($r$ = 0.83) and 150 years of geomagnetic reconstructions ($r$ = 0.87, Owens et al., 2016). Caution should be taken, however, in extrapolating this regression outside the parameter range over which it is determined (*i.e.*, very high or low values of SN).

For a better understanding of HMF over the full range of variability, in particular, during anomalous conditions such as the Maunder minimum, it is necessary to use more physically constrained methods of relating SN to HMF. Solanki et al. (2000) proposed modeling the OSF, and hence total HMF, as a conserved quality. At annual timescales, the rate of OSF production is assumed to be related to SN, while a number of time constants control the rate of OSF decay. Owens & Lockwood (2012) further related the OSF loss to the tilt of the heliospheric current sheet. The agreement of sunspot-based estimates of HMF with in situ and geomagnetic estimates is slightly higher than when using the above-mentioned correlation between HMF intensity and the square root of SN. But, more importantly, it also reveals new behavior, such as the continued cycling of the HMF during the Maunder minimum (Owens et al., 2012).

Using the SN-based reconstructions of total HMF, the solar cycle 23/24 minimum is again estimated to have the lowest HMF intensity for around 100 years. HMF during the Dalton minimum (around 1700–1720) is estimated to have been around 20% lower, while values during the Maunder minimum (1645–1715) are likely to have been around 50% lower.

*Cosmogenic isotope-based reconstructions.* To reconstruct solar wind conditions prior to 1611, even more indirect proxies are required. Cosmogenic radionuclides, such as $^{14}$C and $^{10}$Be, are produced as a byproduct of nuclear collisions between cosmic-ray energetic particles and atoms in the Earth's atmosphere (Usoskin, 2023; see also Section 2.4.1). Since the cosmic-ray flux near Earth is modulated in the heliosphere and magnetosphere, measured concentrations of such nuclides in independently dated tree trunks and ice sheets can reveal a history of past solar activity. Section 2.4 describes how short-term variations in the radionuclide production rate can be related to sporadic extreme solar energetic particle events. But on longer timescales, the production rate is largely set by the intensity of GCRs reaching Earth (Beer et al., 2012). As this is modulated by the total HMF (with fewer GCRs reaching the terrestrial magnetosphere when the HMF is high), $^{14}$C and $^{10}$Be records can be used to estimate the total HMF or, more accurately, the open solar magnetic flux (Wu et al., 2018; Usoskin et al., 2021). Figure 2 shows that on long timescales (*e.g.*, 10–25 years), there is very good agreement between the radionuclide estimates of the HMF and those from more direct proxies. In particular, it highlights the value of the SN record, as the 400 years that it covers contains almost the full parameter range of variability of the HMF over the last 9,400 years (Acero et al., 2018).

### 2.3.3. Solar cycle variations and the global structure of the heliosphere

The continuous outflow of magnetized solar wind from the Sun creates a bubble-like cavity in the local interstellar medium (LISM), dubbed the heliosphere. At a large distance from the Sun, well beyond the outer planets, the supersonic solar wind slows down abruptly forming the termination shock. Upstream of the termination shock, the boundary between the LISM and the slowed-down solar wind is the heliopause, and is formed by the pressure balance of the LISM and that of the solar wind. As cold interstellar neutrals drift through the heliosphere, some become ionized through charge exchange or photoionization and are then picked up by the solar wind flow, becoming pick-up ions. Incoming cold interstellar neutral atoms interact with these pick-up ions and shocked solar wind in the heliosheath region, bounded by the termination shock and the heliopause, creating energetic neutral atoms (ENAs). These ENAs can now travel back to 1 AU unaffected by magnetic and electric fields, carrying inherent signatures of their progenitor ion populations (*e.g.*, Gruntman et al., 2001; Heerikhuisen et al., 2008), and providing a unique capability for remote-sensing of the heliospheric boundaries from Earth's orbit (*e.g.*, McComas et al., 2009).

In situ solar wind observables and remote ENA measurements complement each other in providing information about the structure of our heliosphere. The solar wind dynamic pressure, the product of the solar wind density and the square of the solar wind speed, determines the global size and the inflation status of the heliospheric cavity in the interstellar medium (*e.g.*, McComas et al., 2003), and directly controls the location of the termination shock and other heliospheric boundaries at the interstellar interface (*e.g.*, von Steiger, 2008). Furthermore, Ulysses observations showed that the dynamic pressure is mostly latitude invariant (McComas et al., 2008), meaning that measurements of near-ecliptic solar wind properties provide, to a great extent, an excellent proxy of the global status of the heliosphere, which can then be reflected few years (~2 to 4) later by ENA measurements (McComas et al., 2020; Zirnstein et al., 2018).

To date, remote measurements of ENAs, supported by in-ecliptic and latitudinal measurements of solar wind inferred from interplanetary scintillations (*e.g.*, Sokół et al., 2013) have enabled us to probe the vast distances of the heliosphere (*e.g.*, Zirnstein et al., 2018; Reisenfeld et al., 2021; Dayeh et al., 2014), creating a direct link between the solar output during

different phases of the solar cycle and the global status of the heliosphere as it responds later in time.

Recent results of long-term trends of the solar wind dynamic pressure (Sokół et al., 2021) showed that it exhibits a periodic behavior that largely affects the global structure of the heliosphere. The authors reported that the onset of each solar cycle is accompanied by a rapid increase of solar wind pressure. This pressure pulse happens about 4.7 yr from the beginning of each cycle, during the maximum phase of solar activity, and repeats with a period of ~10.2 yr. These repeating pulses of the solar wind dynamic pressure lead to subsequent periodic solar-cycle related variations of the ENA production in the heliosheath, beyond the termination shock.

Recent work by Dayeh et al. (2019, 2022) on long-term ENA variations found that the main heliospheric ENA structures in the sky (*e.g.*, the ENA ribbon and heliotail lobes) are persistent over all phases of the solar cycle and exhibit variations that can be tracked over different phases of the solar cycle. This motion enables predictions of the heliosphere global status during different solar cycle phases. Long-term variations in the dynamic pressure measured near 1 AU can thus provide good estimates of the global structure of the heliosphere.

Modulations of the solar wind caused by the long-term modulations of the solar magnetic field are difficult to model because of the disparity of scales between all the physical phenomena (the solar wind evolves over hours, the solar cycle over decades). However, quasi-static studies can go around this limitation, and provide useful insights on the structure of the inner heliosphere (Pinto et al., 2011; Réville & Brun, 2017; Perri et al., 2018; Hazra et al., 2021). These modulations can in return be correlated with various estimates, such as cosmic rays modulations (Perri et al., 2020).

In summary, the solar cycle-scale breathing pattern of the heliosphere and the subsequent ENA response enables us to probe the heliospheric boundaries and further examine the asymmetries in its structure (*e.g.*, Reisenfeld et al., 2021; Dayeh et al., 2014, 2022; Zirnstein et al., 2018, 2022). These predictions provide crucial constraints to the time-dependent heliospheric models.

#### 2.3.4. *Outstanding questions*

This field of research would benefit from having additional in situ and remote observations at high heliographic latitudes following the steps of a very successful Ulysses spacecraft (Wenzel et al., 1992). Examples of such observations include the Solar Orbiter (Müller et al., 2020) and a future over-the-poles mission (*e.g.*, Harra et al., 2022). These new data are needed for exploring the secular variations in global solar wind properties. High-latitude observations are also essential for solving the so-called *open flux problem* (Linker et al., 2017).

Sunspot-based reconstructions of solar wind may need to be improved for the periods of very low and high sunspot numbers, and a better understanding needs to be developed for the levels of HMF intensity during the periods of grand minima and their possible cycle variations.

Finally, a modeling of variations of solar wind due to the long-term modulation of the magnetic field in the heliosphere is important for developing a better understanding of long-term evolution of global structure of the heliosphere.

### 2.4. *Extreme solar events*

Our knowledge of the Sun, heliosphere, and solar-terrestrial relations becomes deeper and finer with the progress of scientific instrumentation and exploration methods. We are getting into finer details and smaller time- and spatial scales leading to a better understanding of the nature of physical processes which drive the solar variability. Modern space missions make it possible to study in situ conditions in the near-Sun environment, while precise multi-messenger observations allow us to look deeper, into regions unreachable for direct measurements. However, the amount and quality of data decrease going backwards in time. Ground-based or space-borne measurements of energetic particles from the Sun are available for 50–70 years, spectroscopic observations of the Sun for a century, and optical observations (or just counts of sunspots) for a few centuries. Direct, telescopic observations of the Sun started about four centuries ago in 1610. Since this period covers a broad range of solar variability, from the nearly spotless Maunder minimum (Eddy, 1976) in the second half of the 17th century (1645–1715) to the modern grand maximum (Solanki et al., 2004) of activity in the second half of the 20th century (1944–2009), a common paradigm was that our knowledge includes the full range of solar activity for the modern Sun. However, it has been discovered recently that the Sun occasionally produces extreme solar eruptive events which can be a factor 40–100 stronger than the strongest directly observed solar particle event of February 23, 1956 (*e.g.*, Miyake et al., 2019; Cliver et al., 2022; Usoskin et al., 2023). Since none of such extreme events took place during the last centuries, we have to rely on proxy data to study them, their parameters, and occurrence probability. The very fact of the existence of such events implies that we still do not possess the full knowledge of solar variability. The energy and timescales of the extreme solar events make them impossible to be studied using modern solar observations and in situ measurements, and require reliance on modeling of historical proxy data.

Until recently, it was believed that the ability of the Sun to produce extreme events was limited by the directly observed phenomena, but this paradigm has been changed, and the limits expanded by at least two orders of magnitude.

#### 2.4.1. *Events based on terrestrial proxy*

Energetic particles can initiate a nucleonic-electromagnetic-muon cascade in the Earth's atmosphere producing, as a byproduct, tracing amounts of radioactive nuclides. Those nuclides which are only (mainly) produced in the terrestrial system in this way, are called cosmogenic isotopes and are used to estimate the flux of energetic cosmic rays in the past, using records of cosmogenic $^{14}$C in independently dateable tree rings and $^{10}$Be and $^{36}$Cl in polar ice cores. This is the only known quantitative method of reconstructing solar activity for the pre-telescopic era (Beer et al., 2012; Usoskin, 2023).

Thousands of solar energetic particle (SEP) events have been registered during the recent decades, about 70 of them being

sufficiently strong and energetic to initiate nucleonic cascades in the Earth's atmosphere that can be measured by ground-based detectors, neutron monitors. Such events are called ground-level enhancements (GLEs, Poluianov et al., 2017) and were typically considered extreme SEP events. The greatest directly recorded SEP event was GLE #5 on February 23, 1956 where the response of some neutron monitors to the SEP event was 50 times larger (on the hourly scale) than the background count rate due to GCRs. However, even this strongest observed SEP event could not be detected by the cosmogenic-isotope method in the past (Usoskin et al., 2020).

This concept has been changed in 2012 when an anomalous peak in $^{14}$C abundance was detected in a Japanese cedar tree in a ring corresponding to the year 775 CE (Miyake et al., 2012). Despite different exotic ideas of its origin, including a supernova, a gamma-ray burst, and cometary impact, it was soon proven to be either a strong SEP event or a short (less than a few months) sequence of events (Usoskin et al., 2013) which occurred in the summer of 774 CE (*e.g.*, Sukhodolov et al., 2017; Uusitalo et al., 2018). Later, several more such events, called now extreme solar particle events (ESPEs), have been discovered (Miyake et al., 2013; Mekhaldi et al., 2015; Brehm et al., 2021, 2022; Paleari et al., 2022)), so that presently there are five confirmed ESPEs (7176 BCE, 5259 BCE, 660 BCE, 774 CE, and 993 CE) and three candidates (5410 BCE, 1052 CE, and 1279 CE). All these events are 20–100 times stronger than the strongest directly observed GLE #5, and their occurrence rate is of the order of one event per millennium, (1/500 – 1/2400) yr$^{-1}$. Interestingly, all these events, for which the 11-year cycle can be reconstructed, appeared near a maximum phase of the solar cycle of moderate strength (see a review by Cliver et al., 2022).

Since different cosmogenic isotopes have slightly different response functions to energetic particles, the energy spectrum of ESPEs can be roughly estimated (*e.g.*, Mekhaldi et al., 2015; Miyake et al., 2019). As shown recently by Paleari et al. (2022) and Koldobskiy et al., 2023, the energy spectrum of ESPEs is similar to those of strong GLE events, but a few orders of magnitude larger.

The existence and parameters of ESPEs make an enigma which cannot be answered with the present knowledge of solar physics — how so much energy can be stored and released on the Sun, how such extreme fluxes of energetic particles can be accelerated and transported to the Earth's orbit, what their terrestrial effects could be.

### 2.4.2. *Superflares on Sun-like stars*

The question of the maximum energy of solar flares is very important not only for solar physics, but also for practical applications. So far, the strongest measured solar flare was on November 4, 2003 (X35 in GOES/XRS[24] classification or $4.3 \times 10^{32}$ erg bolometric energy, Emslie et al., 2012), and an extrapolated statistical scaling suggested that once-per-millennium solar flares would have the maximum energy of $\sim 10^{33}$ erg (Gopalswamy, 2018; Aulanier et al., 2013; Kazachenko et al., 2017; Schmieder, 2018).

Maehara et al. (2012) reported a discovery, based on an analysis of tens of thousands of stars observed by the Kepler space-based telescope, that super-flares can occur on solar-type stars, and their energy can be $10^{34}$ – $10^{36}$ erg, *i.e.*, several orders of magnitude greater than the observed and theoretically expected solar flares. However, it is still unclear how reliably the results of an analysis of a large-ensemble data (around 5,000 stars) can be projected to a single star, our Sun, which is less active than the majority of the Sun-like stars (*e.g.*, Reinhold et al., 2020). Analyses of flaring stars in the Kepler data (and Gaia dataset) use different filters, whenever they are available, such as age, temperature, rotational period[25], metallicity, absence of companions (see, *e.g.*, Okamoto et al., 2021; Vasilyev et al., 2022), but other important parameters (*e.g.*, differential rotation, depth of the convection zone, meridional flow) cannot be defined straightforwardly for the stars. Sporadic cosmic rays, transients, or unresolved overlapping flaring objects can also contaminate the results (Vasilyev et al., 2022). Moreover, the sample of superflaring stars may be biased towards active stars with a resolved rotational period. If the Sun was observed from a distance, it would be unlikely to be included in the analysis because its rotation period can hardly be defined bolometrically (Reinhold et al., 2020). Thus, the projection of the large ensemble of Sun-like stars (~20,000 star × yr) to a single star is highly uncertain: the uncertainties of the projected superflares on the Sun are of the order of 20–100 in both energy ($10^{34}$ – $10^{36}$ erg) and occurrence probability (1/60 – 1/1500) yr$^{-1}$.

### 2.4.3. *Modeling extreme solar and stellar events*

The fact that large solar flares and fast coronal mass ejections often occur together and that superflares on solar-type stars have been detected by Kepler mission has raised the question of whether these superflares can be associated with energetic coronal mass ejections (CMEs) and stellar energetic particles (StEPs). Very recently, Veronig et al. (2021) reported the detection of sudden dimmings, caused by stellar CME mass loss, in the extreme ultraviolet and X-ray emissions associated with flares on cool stars. These detections are further benchmarked by Sun-as-a-star extreme ultraviolet measurements. Based on the strong association between solar filament eruptions and CMEs (*e.g.*, Marubashi, 1997; Webb, 2002; Green et al., 2018), filament eruptions could, perhaps, be used as indirect proxies for shock-generating ejecta on other stars. Namekata et al. (2022) reported a filament eruption from a superflare on a solar-type star. The inferred total mass ejected reaches $\sim 1.1 \times 10^{18}$ g, more than 10 times larger than the largest eruption at the Sun. It is conceivable that high-energy StEPs can be accelerated in such an eruption. Among other concerns, StEPs may impact the habitability of exoplanets around their stars (see, *e.g.*, Airapetian et al., 2020). It is therefore of interest to model

[24] Geostationary Operational Environmental Satellite/X-Ray Sensor

[25] For true solar-type stars, their rotational period usually cannot be determined. Thus, surveys limited to solar rotational periods may be biased towards stars whose rotational periods could be determined (and might be incorrect and in fact even represent more active stars, Reinhold et al., 2022).

these events in the context of treating these as extreme solar events and learn from the modeling effort which are the deciding factors of StEPs.

Ions and electrons are accelerated at the shock front via the diffusive shock acceleration mechanism (Axford et al., 1977; Bell, 1978a,b; Blandford & Ostriker, 1978; Krymsky, 1977)). Their energy can reach ~GeV/nucleon in certain events which are often associated with fast CMEs. However, the correlation between CME speed and SEP intensity and energy is not strong. This is due to the fact that many factors, including seed population, self-generated wave intensity upstream of the shock, and shock geometry, are all at work in deciding the characteristics of SEPs. This implies that modeling SEP and StEP events is a sophisticated task.

Early efforts of modeling SEP events have been taken by many researchers (*e.g.*, Lee & Ryan, 1986; Kallenrode, 1997; Kóta, 2000; Zank et al., 2000; Li et al., 2003, 2005; Ng et al., 2003; Luhmann et al., 2007, 2010; Vainio & Laitinen, 2007), addressing either the acceleration aspect or the transport aspect of SEP events. For example, in the work by Kallenrode (1997) and Luhmann et al., 2007, 2010, a source spectrum at the moving shock is assumed and the subsequent transport of SEPs in the solar wind is examined. These works focus more on explaining the time profiles of SEPs and can not provide an estimate of the maximum particle energy in SEP events. In comparison, the work of Lee & Ryan (1986), Zank et al. (2000), Li et al. (2003, 2005), and Ng et al. (2003) aimed to obtain the accelerated particle spectrum by solving Parker's transport equation at a propagating CME-driven shock in a self-consistent manner. Accelerated particles streaming upstream the shock amplify Alfvén waves and these waves in turn reflect particles across the shock front leading to further acceleration.

These early efforts, however, did not attempt a realistic description of the solar wind and the CME itself. Lee & Ryan (1986) and Ng et al. (2003) prescribed certain shock profiles and did not consider how the profiles evolve in the solar wind. Zank et al. (2000) and Li et al. (2003, 2005) employed the ZEUS MHD code to provide a description of both the pre-eruption solar wind and the CME-driven shock. They developed the 1D PATH[26] model which was later extended to 2D as the improved PATH model (iPATH, Hu et al., 2017). However, the CME shock is modeled more as a result of a pressure pulse instead of due to the ejection of plasma. Nevertheless, they showed that the evolution of the shock profile can impact the observed time profiles and spectra for observers at different locations. Hu et al. (2017, 2018) modeled the SEP events in a 2D geometry and examined the time profiles of SEPs at multiple locations that are separated longitudinally, finding that cross-field diffusion can be important for the initial phase of SEP events. Using the iPATH model, Fu et al. (2019) considered the effect of star rotation on the StEP observations. They showed that a faster-rotating star can lead to StEPs that have higher energies than slow-rotating stars.

As discussed in Section 2.4.2, our observations of superflares on solar-type stars are likely biased toward the more energetic ones. A particular question one is tempted to ask is what will be the StEP characteristics in these events. Observations have established that young solar analogs (G-type main sequence stars) are magnetically active (Güdel, 2007; Linsky et al., 2020; Airapetian et al., 2020). Large starspots covering up to 10% of a stellar surface, strong surface magnetic fields up to a few hundred Gauss, dense and hot X-ray bright corona, and massive fast winds and frequent flare activity are often reported for these stars (Sanz-Forcada et al., 2011, 2019; Güdel, 2007; Maehara et al., 2012; Shibayama et al., 2013; Kochukhov et al., 2020; Notsu et al., 2019; Airapetian et al., 2020). Since these superflares have fast CMEs associated with them, then it is conceivable that particles can be accelerated to very high energies in these star systems. Hu et al. (2022) examined how extreme events scale with the flare classes (or energy) for other stars using the iPATH model. By considering CMEs with speeds up to 7,500 km/s, Hu et al. (2022) demonstrated that protons up to 20 GeV can be accelerated in young stars with stronger magnetic fields. The model results suggest that the peak proton integrated flux, $F_p$ (in pfu), scales with the soft X-ray (1–8 Å) flare flux (as measured by GOES satellites in W/m$^2$), $F_{SXR}$. This result is in agreement with Cliver & D'Huys (2018), who found a good scaling between the peak proton flux at ~25 MeV and $F_{SXR}$ on a set of events from 1997 to 2016 associated with western hemisphere soft X-ray flares. These scaling relations are consistent with those of previous studies (Van Hollebeke et al., 1975; Belov et al., 2007). Earlier simulation results from Li et al. (2003, 2005) and more recently by Hu et al. (2022) provide a modeling basis to interpret future observations. We note that there might be an upper limit to this scaling set by saturation of the diffusive shock acceleration mechanism, the so-called *streaming limit*. In large SEP events, the streaming limit refers to the plateau in the ion time intensity profile prior to the shock passage (Reames, 1990; Reames & Ng, 1998; Tylka et al., 1999; Reames & Ng, 2010). Such a plateau has been suggested as an indication that the flux of the streaming protons is quenched by Alfvén waves that are generated and amplified by these streaming protons themselves. It reflects the ability of the shock to retain these particles for an extended period once they are accelerated. Numerical simulations (*e.g.*, Li et al., 2003, 2005; Verkhoglyadova et al., 2009, 2010) support this view point. More detailed simulations, perhaps those exploring more solar analogues, need to be systematically pursued, so that a clear projection to the "modern" Sun and space weather/climate applications at Earth can be obtained.

### 2.4.4. *Outstanding questions*

Models related to cosmogenic-isotope transport/deposition were primarily developed for slowly changing GCR-related production and may be invalid for fast ESPEs, potentially leading to large errors (see, *e.g.*, Koldobskiy et al., 2023 *vs.* Mekhaldi et al., 2015). Additionally, stellar-solar projections are done by extrapolating simple scalings leading to huge uncertainties in estimates of the superflare occurrence probability of the Sun (Notsu et al., 2019; Reinhold et al., 2020; Okamoto et al., 2021; Vasilyev et al., 2022). Thus, dedicated sophisti-

[26] Particle Acceleration and Transport in the Heliosphere

cated analysis methods need to be developed to eventually resolve the existing controversy between the results from solar (proxy) and stellar (direct) datasets and methods. Different reasons can be related to the large uncertainties, and several outstanding questions stand up in this respect:

- Do extreme solar events and stellar superflares reflect the same type of events?
- Does the Sun have limits in the energy of eruptive phenomena?
- Is there an intrinsic limit (streaming limit) in accelerating SEPs for extreme events?
- Can the statistics of stellar superflares be directly projected to the Sun?

Beyond purely academic questions, a crucially important one is related to the possible technological and societal consequences of such an extreme once-in-a-millennium event for our highly technological society.

## 3. Physical understanding of long-term variability and its consequences

The radiative and particulate output of the Sun varies across timescales ranging from orders of minutes and hours to evolutionary timescales. Extreme solar events like flares, prominences, coronal mass ejections, etc., regulate the space environmental conditions on short timescales and create what is known as space weather (Schrijver et al., 2015). On the other hand, slower, long-term solar activity fluctuations over decadal, centennial, and multi-millennial timescales manifest in the variation of solar wind properties, modulation of open solar flux and cosmic ray flux, and severity and frequency of extreme solar eruptive events, shaping space climate and eventually determining planetary habitability over evolutionary timescales (Nandy & Martens, 2007; Mursula et al., 2013; Nandy et al., 2021).

In this section we briefly discuss the long-term variabilities in the Sun's magnetic output, advances in predicting these variabilities, and its consequences on the planetary environments and habitability. Some related outstanding questions that need particular attention are also highlighted.

### *3.1. Solar magnetism as the heart of solar variability*

Solar dynamic activity is driven by the magnetic fields present in the Sun, which are observed in spatial scales as small as a few tens of kilometers, about the size of individual convective granules; large active regions that can be more than a few thousand kilometers in cross-section; and the global scale of the Sun (*e.g.*, the dipolar field). It is widely accepted that the Sun harbors a dynamo mechanism in its interior which converts the kinetic energy stored in turbulent convection and large-scale plasma flows — that pervade to the solar convection zone — into magnetic energy sustaining the large-scale magnetic fields against Ohmic dissipation (Brun & Browning, 2017; Charbonneau, 2020). Ultimately, the fluctuations in solar magnetic output that originate in the solar convection zone manifest as variations in diverse aspects of solar activity, from the short to long term, encompassing phenomena associated with space weather and space climate.

Plasma in the interior of the Sun is non-degenerate and quasi-neutral and the motion of the fluid is non-relativistic. Moreover, the collisional mean free path of the constituent particles is much shorter than the characteristic plasma length scales in this case. Such physical conditions enable one to describe the evolution of large-scale solar magnetic fields and plasma flows invoking the principles of MHD. The magnetic induction equation, describing the evolution of the magnetic field under the action of plasma flows and diffusion in such systems, is given by

$$\frac{\partial \vec{B}}{\partial t} = \vec{\nabla} \times \left( \vec{v} \times \vec{B} - \eta \vec{\nabla} \times \vec{B} \right), \tag{3}$$

where $\vec{v}$ signifies large-scale plasma flows and the magnetic diffusion is denoted by $\eta$. Typically, the entirety of this evolution of magnetic fields and flows is captured in the simultaneous solution of the above equation along with appropriate equations denoting the conservation of mass, momentum, and energy, as well as an equation of state.

Besides sustaining the cyclic regeneration of magnetic fields, a solar dynamo model should also emulate long-term observational features of the solar cycle, including the approximate 11-year periodicity, equatorward migration of the latitude of the emergence of sunspots, hemispheric asymmetry in sunspot emergence, poleward migration of the diffuse surface magnetic field, cyclic polarity reversal in the polar field, modulation in amplitude and duration of solar cycles beyond decadal timescales, etc., as well as episodes of grand minima and maxima in solar activity. Numerical simulations of the solar dynamo problem are challenging as they involve significantly large separation in temporal and spatial scales in a fluid medium with high turbulence caused by thermally driven convective fluxes. Attaining solar-like parameters characterizing the convection zone has remained elusive. Thus, the majority of solar dynamo models, to date, have depended on full MHD simulations with unrealistic parameter regimes, or simplifications and drastic truncations of the MHD equations, as well as assumptions about the internal flow components that are not observationally well constrained (Charbonneau, 2020). However, we note that differential rotation is rather well constrained in the solar convection zone (Charbonneau et al., 1999) and meridional circulation constraints are converging towards a single, one-cell deep circulation threading the solar convection zone (Rajaguru & Antia, 2015; Gizon et al., 2020).

In the following subsections, we discuss the current theoretical understanding of the long-term variability in solar activity, the possible origin of solar cycle fluctuations including occurrences of extreme solar activity phases such as grand maxima and grand minima episodes, and their implications on the evolution of planetary atmospheres and magnetospheres.

*3.1.1. Fluctuations in the solar cycle: observations and theory*

The solar cycle exhibits several periodicities that are indicative of the interplay of complex mechanisms involving stochastic perturbations, nonlinear processes, and feedback mechanisms (Hathaway, 2015; Brun & Browning, 2017; Charbonneau, 2020; Hazra et al., 2023; Mininni et al., 2000; Tobias, 1997, 2002; Ossendrijver, 2003; Weiss & Tobias, 2016). The most visible one is of course the variability in the quasi 11-year cycle or sunspot cycle, characterized by the minima and maxima of activity depending on the number of sunspots at the surface of the Sun. When we take into account the polarity of the solar magnetic field, we find a 22-year cycle, or Hale cycle, with a reversal of the dominant polarity at each pole every 11 years (Ossendrijver, 2003).

Finally, since we have observed sunspots for more than 400 years, we also have evidence of longer modulations of the general amplitude of solar cycles of around 100 years (Gleissberg cycle), as confirmed by cosmogenic-isotope data for several millennia (Peristykh & Damon, 2003; Beer et al., 2018; Usoskin, 2023). These cycles are stable at the scale of mankind, with reconstructions via cosmogenic isotope analysis up to 10,000 years in the past (Miyahara et al., 2010; Usoskin et al., 2021). However, there can be transitory disruptions such as grand minima (Usoskin, 2023). There are also asymmetries present in these cycles, with a north-south asymmetry in the sunspot numbers (Temmer et al., 2006), likely due to the large quadrupole component of the magnetic field (DeRosa et al., 2012), and an asymmetry in the rising and declining phases of each cycle (Clette & Lefèvre, 2012). These are mostly the elements we would like to understand and model to improve our forecasting: the minima and maxima dates of the cycles, the amplitude of a cycle, the transition from one cycle to another, and the possibility of disruptions.

The only theory that has managed so far to explain these behaviors is the dynamo theory (Moffatt, 1978). The dynamo mechanism relies on the MHD induction equation and describes how an electrically conducting fluid can maintain, or even amplify, its magnetic field against Ohmic dissipation, through the conversion of kinetic energy into magnetic energy. For reviews on the subject, see Brun & Browning (2017), Charbonneau (2020), Tobias (2021), and Hazra et al. (2023). The dynamo will cause the magnetic field to grow, usually until an equipartition state is reached and we have an equilibrium between the magnetic and kinetic energy densities. Saturation can also be seen as a nonlinear regime where the Lorentz force begins to back-react on the initial flow and thus modify the ingredients of the dynamo (such as the so-called Malkus-Proctor effect). Not all circumstances are conducive to a dynamo, as made famous by anti-dynamo theorems, such as Cowling's theorem (Cowling, 1933) that demonstrates that an axisymmetric field vanishing at infinity cannot be sustained by dynamo action. It can also be shown that no purely toroidal flow can act as a dynamo. Please note as well that a dynamo does not necessarily imply a cycle: it implies a sustained field, which can also be stationary (Strugarek et al., 2017). This provides important constraints on the magnetic field we expect in stars (see, *e.g.*, Brun et al., 2015b, 2022). In the case of the Sun, we do clearly see the existence of a cycle over timescales of more than 10,000 years and the formation of sunspots, which must have underlying fields which are well over the equipartition field that is estimated based on the classical notion of equipartition of energy between turbulent flows and magnetic fields.

Long-term quasi-periodic variations in solar activity can arise as a result of a variety of physical processes going on in the solar interior. Turbulent convection, rotation, and thermal gradients in the solar convection zone eventually drive large-scale flows, such as differential rotation and meridional circulation, and generate stochastic perturbations and noise in the system. Both the classical mean-field $\alpha$ effect source for the poloidal field arising due to helical turbulence (Parker, 1955) and the Babcock-Leighton mechanism for poloidal field generation (Babcock, 1961; Leighton, 1969) are subject to stochastic perturbations and nonlinear quenching, resulting in amplitude and period modulation; for a detailed discussion see the review by Bhowmik et al. (2023). Observations of bipolar magnetic active regions reveal large fluctuations in the tilt angle, plausibly due to the turbulent buffeting of rising flux tubes in the solar convection zone. This introduces perturbations in tilt angle, flux, pole separation, and the build-up of surface polar fields which are at the heart of the Babcock-Leighton solar dynamo. At the simplest level, the existence of a threshold for magnetic buoyancy instability itself may play a role in governing an upper bound on the field strengths of sunspots (Nandy, 2002).

Rotational shear in the solar convection zone plays a key role in the induction and amplification of large-scale toroidal fields. It is crucial to consider nonlinear mechanisms like the dynamical back-reaction of large-scale magnetic fields on large-scale plasma flows and turbulent diffusion. In mean-field models, this nonlinearity is typically captured by considering a direct feedback of Lorentz force upon the zonal flow (Bushby, 2006) and/or by a quenching term in the $\lambda$ effect (Küker et al., 1999). Various models have demonstrated that nonlinear back reaction of magnetic field on large-scale flow and turbulent diffusivity can induce a variety of modulation patterns in the cycle amplitude, including grand minima and parity modulations (*e.g.*, Beer et al., 2018; Knobloch et al., 1998; Wilmot-Smith et al., 2005; Jiang et al., 2009; Muñoz-Jaramillo et al., 2010; Weiss & Tobias, 2016). Following the idea that large-scale dynamos can produce small-scale helical fields that in turn quench the large-scale dynamo, a nonlinear helicity quenching mechanism can saturate the dynamo growth (Blackman & Brandenburg, 2002; Brandenburg & Subramanian, 2005). Another source of nonlinearity comes from the dynamical magnetic quenching of the toroidal fields, wherein, the Coriolis force fails to produce significant twist in strongly magnetized toroidal flux tubes under buoyant instability as they rise up rapidly through solar convection zone (D'Silva & Choudhuri, 1993; Dasi-Espuig et al., 2010; Kumar et al., 2019; Jha et al., 2020). Furthermore, the magnetic flux contents of anomalous active regions can potentially cause nonlinear suppression of polar field build-up (Talafha et al., 2022). It has also been argued that time-delay related dynamics, either in isolation (Wilmot-Smith et al., 2006; Jouve et al., 2010), or in the presence of stochastic fluctuation

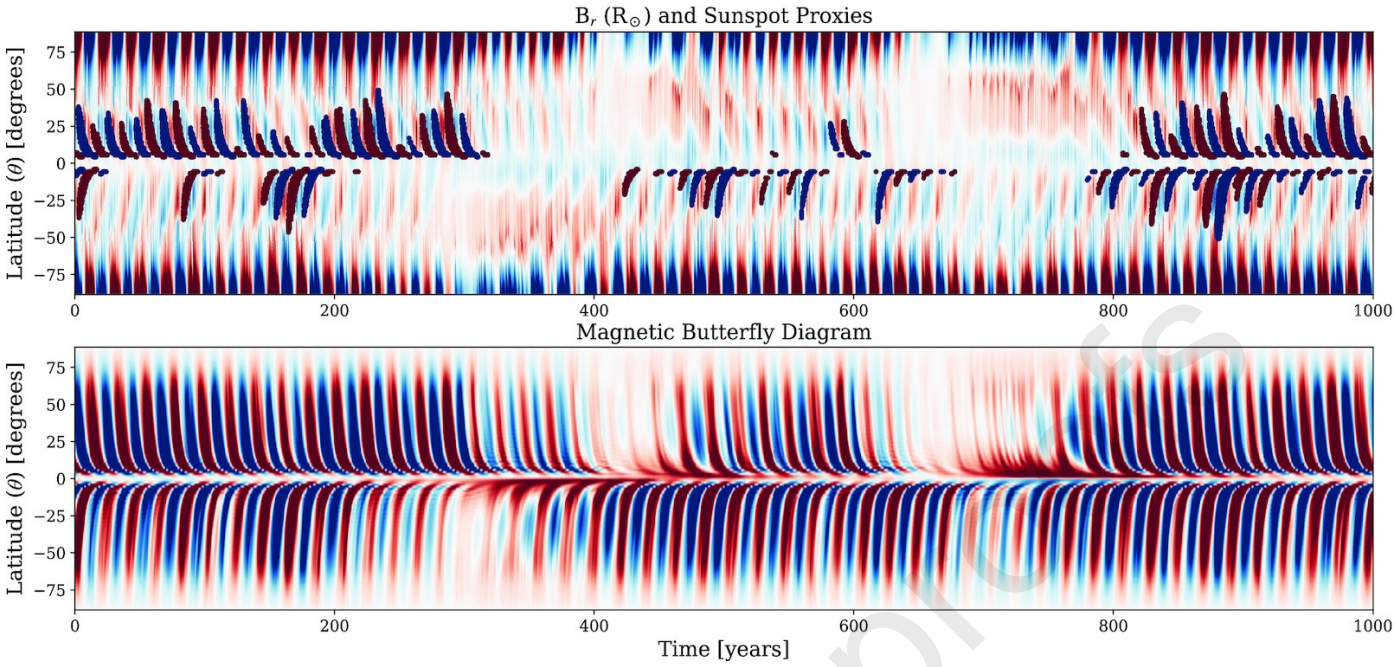


Fig. 3. Millennium timescale solar dynamo simulation from Saha et al. (2022) showing long-term modulation in solar activity, including grand solar minima-like phases, arising as a result of stochastic fluctuations incorporated in the poloidal sources. Top panel: simulated time series of the surface radial magnetic field variation (saturated to 1500 G) with sunspot eruption proxies confined to lower latitudes. Bottom panel: variation in the toroidal magnetic field (saturated to 150 kG) at the base of the solar convection zone.

or "magnetic noise", can lead to amplitude modulation and a variety of dynamical effects.

Figure 3 depicts simulated results of long-term modulation in solar cycles over a millennium timescale where the cycles are represented by alternating patterns of positive (red) and negative (blue) polarity of polar fields, while sunspot eruption proxies, shown as filled dots, are confined in mid-low latitudes. The hemispheric asymmetry can be seen in several places over the first 300 years and also in 400–650 year intervals. Episodes between 300–400 years and 650–800 years exhibit grand minima-like behavior. It is interesting to note the extended period of no polarity reversal in the Northern hemisphere during the 700–800 year period (see Saha et al., 2022 for further details).

### 3.1.2. *Dynamo modeling of long-term solar variability*

There are diverse approaches to dynamo modeling. The first one is the mean-field approach (see review by Brandenburg & Subramanian, 2005; Hazra et al., 2023). Here, the physical quantities are split between a mean and fluctuating part, which allows for the nonlinear terms in the induction equation to be simplified over an approximation of the mean electromotive force (Warnecke et al., 2016). This approach focuses on the large-scale generation of magnetic fields and uses prescriptions for the various physical quantities. The dynamo can then be described as a loop between two effects called the $\Omega$ and $\alpha$ effects. The $\Omega$ effect describes the linear winding of field lines by differential rotation and explains how to go from a toroidal to a poloidal large-scale field. The $\alpha$ effect describes the cumulative effects of small-scale turbulence which causes the magnetic field line to twist (hence the choice of the $\alpha$ symbol to describe it, reminiscent of a curl), and thus to generate toroidal components from poloidal, or vice-versa. A combination of these two effects ($\alpha - \Omega$, $\alpha^2 - \Omega$, and $\alpha^2$ dynamos) can then be made to oscillate between poloidal and toroidal states, and thus explain the solar cycle variability. The resulting models follow the Parker-Yoshimura rule (Parker, 1955; Yoshimura, 1975), which relates the direction of propagation of dynamo waves to the properties of turbulence and rotation. They are usually completed with an ad-hoc quenching to induce a level of saturation for the dynamo effect, mimicking the feedback of the Lorentz force. Some stochastic effects can be included to consider the fluctuations and asymmetries of the solar cycle (Warnecke et al., 2018). These models have been very successful, combining accuracy with speed, and functioning with limited resources (Roberts, 1972; Charbonneau, 2020). However, they require a complete description of the physical problem, fine-tuning of many of the model parameters, and do not include small-scales or nonlinear effects (except for those including the Malkus-Proctor effect or other nonlinear feedback; see Tobias, 1996, 1998 and Lopes et al., 2014).

Another approach is facilitated by highly parallel numerical simulations and consists of solving directly the MHD equation in global convective rotating simulations, with full nonlinear terms and turbulence (Gilman, 1983; Glatzmaier, 1984). This approach has the advantage of being fully self-consistent and includes nonlinear effects that allows for natural quenching or grand minima without manual fine-tuning. However, even with numerical optimisation, this method remains very costly and can only be used to compute a limited number of cycles, and probably not in real-time with the current machines (how-

ever, exa-scale supercomputers could possibly help overcome this limitation). It also suffers from some intriguing limitations. First, no model has been able to produce spots at this date, also known as the spotless dynamo paradox (Brun et al., 2015a). This may be due to the quite simplistic boundary conditions of the models that do not incorporate the solar atmosphere or just the numerical resolution limitations of the current models. Another limitation is the inability of these models to reproduce a solar case with solar parameters, especially the solar differential rotation (Brun et al., 2022), although an increase in numerical resolution and turbulence may be a promising way to solve this issue (Hotta et al., 2022). Despite these limitations, long-term variability has started to be studied as well with global 3D simulations, showing various types of modulations due to interactions between small-scale and large-scale flows and magnetic fields (Raynaud & Tobias, 2016).

An observationally motivated approach to solar cycle modeling is the Babcock-Leighton (Babcock, 1961; Leighton, 1969) paradigm which invokes the emergence of tilted bipolar sunspot pairs on the solar surface and the subsequent redistribution of their flux due to the action of near-surface meridional circulation, turbulent diffusion, and differential rotation, which ends up reversing and building up the polar field of the new cycle. In flux-transport Babcock-Leighton dynamo models, typically a deep, one-cell meridional circulation (Dikpati & Charbonneau, 1999; Nandy & Choudhuri, 2002), turbulent diffusion (Yeates et al., 2008) and turbulent pumping (Hazra & Nandy, 2016), either in combination or in isolation, play important roles in coupling the source regions for the poloidal field and the toroidal field across the solar convection zone (see also Jouve & Brun, 2007; Miesch & Teweldebirhan, 2016; Hazra et al., 2017; Kumar et al., 2019). In fact, at least for the Sun, observations clearly support the Babcock-Leighton mechanism as the primary driver of decadal to centennial-scale solar variability (Dasi-Espuig et al., 2010; Cameron et al., 2010; Jiang et al., 2014; Bhowmik & Nandy, 2018). Flux transport dynamo models based on the Babcock-Leighton mechanism incorporating stochastic fluctuations and nonlinearities have been quite successful in explaining at a qualitative level the long-term variability in the solar cycle, the occurrence of grand maxima and minima episodes, hemispheric decoupling, as well as parity modulation (see, *e.g.*, Hazra et al., 2014; Passos et al., 2014; Hazra & Nandy, 2019; Saha et al., 2022).

Please note that for stars which are more massive than the Sun, and hence have a different internal structure with an internal convective core, other dynamo mechanisms have been suggested, such as the Tayler-Spruit dynamo in the radiative interior (Spruit, 2002; Zahn et al., 2007; Jouve et al., 2015). In fact, it is still debated whether the Babcock-Leighton mechanism can explain the diversity of stellar scaling laws (Nandy, 2004) self-consistently (Brun et al., 2015b).

#### 3.1.3. Outstanding questions

Direct numerical simulations of solar dynamo mechanism involve the solution of the full set of MHD equations. However, these models still need to achieve solar-like parametrization. On the other hand, phenomenological flux transport dynamo models working in kinematic mode can successfully reproduce and explain a plethora of solar magnetic activities. One fundamental challenge that remains is to bring out the essence of the Babcock-Leighton mechanism in direct numerical simulations and thereby closing the gap between these two distinct classes of dynamo models, which is essential to better understand long-term solar magnetic activity.

Solar magnetic output varies across a wide range of timescales. Whether these variabilities originate primarily because of nonlinearities or the stochastic fluctuations in the dynamo mechanism is still not conclusively understood. Magnetic activity of the Sun over millennial timescales — as evident from direct observations and reconstructions — often exhibits intermittent quiescent phases sustained over extended periods known as grand solar minima. Understanding the transition of solar dynamo activity into such grand minima and the eventual recovery from these episodes in a predictive regime is another potential topic of interest.

### 3.2. Predicting the Sun's activity

#### 3.2.1. Current approaches to prediction of solar cycles

At the most fundamental level, the genesis of space weather and space climate — in essence — has its roots anchored in the Sun's convection zone, where the emergence, evolution, and dynamics of solar magnetic fields eventually govern the electromagnetic environment throughout the heliosphere. Therefore, accurately predicting and assessing our space environment is closely linked to comprehending the physics of the solar magnetic activity across different timescales — diurnal to decadal. As evident in the long-term observation of the Sun over the past few centuries, the most prominent and regular variation in solar activity is the 11-year sunspot cycle, typically referred to as the solar cycle. The task of predicting and forecasting the solar cycle is a major challenge in the field of heliophysics. Significant progress has been achieved in the last decade in developing such predictive capabilities. However, as evident in Figure 4, there is significant divergence in forecasts using multiple different methodologies, such as statistical correlations based on precursors of solar activity, time-series analysis of solar cycle observations, machine learning techniques, solar surface flux transport (SFT) models, solar dynamo models, etc. However, as demonstrated by Nandy (2021), physics-based forecasts for solar cycle 25 have converged to indicate a moderate-weak cycle similar to or slightly stronger than solar cycle 24.

Physics-based predictions of solar cycles typically involve the estimation of solar polar flux associated with the large-scale magnetic dipole moment of the Sun. The global axial dipole moment at the cycle minimum is shown to be strongly correlated with the peak amplitude of the following solar cycle and it also plays a crucial role in determining the subsequent dynamics of toroidal field generation (Muñoz-Jaramillo et al., 2013). Physics-based models rely upon studying the migration, decay, and dispersal of magnetic fields on the solar surface and in the convection zone, either by incorporating SFT processes or the large-scale dynamo mechanism in the solar interior, in order to calibrate the model parameters to hindcast past solar cycles and

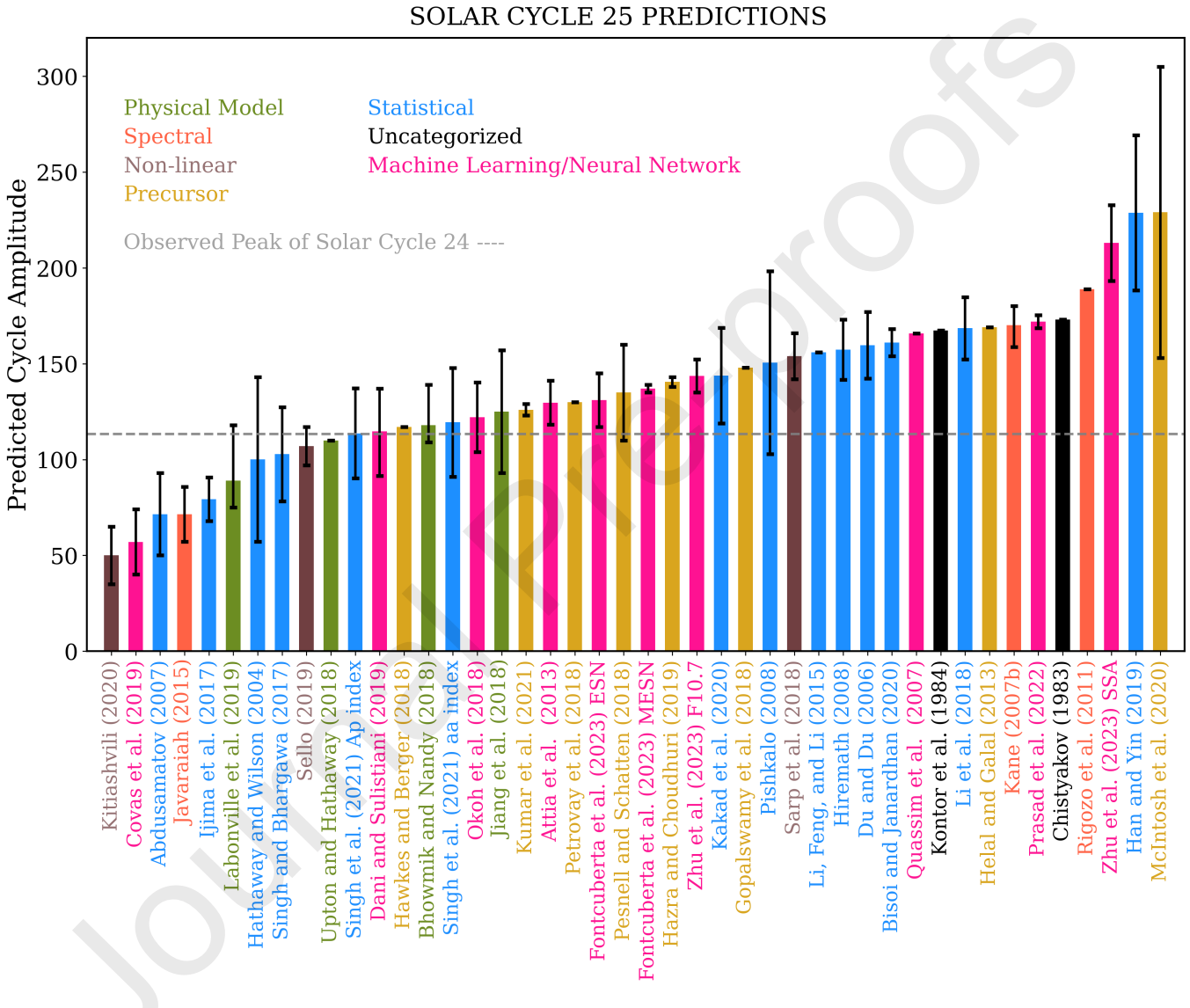


Fig. 4. Predictions of the peak amplitude of solar cycle 25 based on diverse methodologies by different groups (indicated in the plot and represented through distinct color bars). The heights of the bars indicate the predicted peak strength (scaled to conform to the new, revised sunspot time series following Nandy, 2021). The mean sunspot peak of all solar cycle 25 predictions is $136.74 \pm 40.0$ ($\pm 1\sigma$). The dashed line denotes the observed peak of solar cycle 24 (113.3 in the revised scale) for comparison. For references to all predictions listed in this figure, see Nandy (2021).

forecast the upcoming ones. Several works have been done in the last decade based on such models and significant progress has been achieved in predicting the solar cycles 24 and 25.

The earliest prediction of solar cycle 25 based on SFT models was presented by Cameron et al. (2016), where they utilized the synoptic magnetogram observations to simulate the descending phase of solar cycle 24 in the presence of stochastically-driven bipolar magnetic region emergence process and estimate the axial dipole moment at the following cycle minimum. Based on further correlations, they predicted the solar cycle 25 to be a moderate one. Hathaway & Upton (2016) and Upton & Hathaway (2018) predicted a weak to moderate solar cycle 25 using advective flux transport simulations with stochastic variations in the convective motion details, the active region tilt, and changes in the meridional flow profile. On the other hand, Iijima et al. (2017) claimed to detect a plateau-like characteristic in the solar axial dipole moment variations during solar minima and neglected any further assimilation of emerging bipolar magnetic regions into their model. Their prediction suggested a solar cycle 25 even weaker than solar cycle 24. Recently, Bhowmik & Nandy (2018) performed a century-scale simulation of solar cycles with the aid of SFT and axisymmetric, kinematic dynamo models, wherein they assimilated the observed statistics of emerging bipolar sunspot pairs during past solar cycles and presented a data-driven ensemble forecast of solar cycle 25, including the surface field distribution. Their prediction indicates a weak solar cycle 25 similar to, or slightly stronger than solar cycle 24. Lemerle & Charbonneau (2017) took a similar approach and coupled the surface magnetic field to the internal dynamo. Labonville et al. (2019) utilized the same model to assimilate the series of bipolar magnetic regions observed during past solar cycles and came up with an ensemble forecast of solar cycle 25, including its amplitude (weaker than solar cycle 24), rising and declining phases, and northern and southern asymmetry. In a similar approach, Hung et al. (2017) and Brun et al. (2019) have utilized variational data assimilation (4DVar) between a flux-transport dynamo model and the sunspot number and latitudinal variation of the line of sight magnetic field to forecast the next solar cycle. They also predicted a weak to moderate solar cycle 25.

Various statistical techniques using long-term solar observation data have been employed to forecast the strength and timing of solar cycle 25, wherein correlations between various feature parameters of the solar cycle are utilized (Hathaway & Wilson, 2004; Du & Du, 2006; Abdusamatov, 2007; Pishkalo, 2008; Li et al., 2015, 2018). Besides, Hiremath (2008) modeled solar cycles using autoregression by considering them as a forced and damped harmonic oscillator; Singh & Bhargawa (2017) performed a statistical test for the persistence of solar activity based on the Hurst exponent; Han & Yin (2019) implemented the Vondrak smoothing method to the descending phase of solar cycle 24; and Kakad et al. (2020) estimated the Shannon entropy related to the declining phase of the preceding solar cycle and used it to predict the amplitude of solar cycle 25.

In order to make solar cycle predictions, spectral analysis techniques of the sunspot number record have also been used under the presumption that the primary cause of variability in solar cycles is a long-term modulation caused by multiple frequency components. While Kane (2007) used spectral analysis of the sunspot time series to detect periodicity by the maximum entropy method, Rigozo et al. (2011) decomposed monthly sunspot number data into several levels and searched for periodicity by iterative regression at each level. Using the fast Fourier transform, maximum entropy method, and Morlet wavelet analysis techniques, Javaraiah (2015) studied the hemispheric asymmetry in the latitudinal distributions of sunspots to predict solar cycle 25.

Machine learning techniques have proven to be successful over the last decade at generating forecasts of time series, in general. This has led to a variety of machine learning and neural network models of different levels of sophistication (such as neuro-fuzzy approach, linear regression, random forest, radial basis function, support vector machine, and echo state network) being utilized for the prediction of solar cycle 25 (Quassim et al., 2007; Attia et al., 2013; Okoh et al., 2018; Covas et al., 2019; Dani & Sulistiani, 2019). One major issue with many of these approaches is their lack of grounding in the physics of the solar dynamo and the assumption that the past history of the long-term sunspot time series encodes memory capable of generating accurate future cycle forecasts. As discussed in Nandy (2021), the physics of fluctuations and flux transport timescales in the solar dynamo mechanism combine to limit the memory of the solar cycle to about one cycle, mainly relating the polar field at the minima of a cycle to the sunspot-forming toroidal field of the following cycle. In this context, a novel approach in using machine learning applications to solar cycle predictions has been utilized by Espuña Fontcuberta et al. (2023), who first apply multiple algorithms to the physics-based truncated Babcock-Leighton solar dynamo model of Hazra et al. (2014), select the best performing algorithm, and finally utilize this algorithm for solar cycle predictions. This bridges the gap between machine learning models applied simply to the sunspot time series and more physics-based approaches. However, we expect further refinements in the applications of machine learning algorithms, which are showing great promise now in "learning" the behavior of dynamical systems based purely on data inputs without a priori knowledge of the underlying mathematical equations.

In addition to an oscillatory component, solar dynamo may have an irregular component of different origin, such as: stochastic fluctuations in the meridional circulation(Karak & Choudhuri, 2013), emergence of a rogue active region that may "kill" the solar cycle (Nagy et al., 2017), and a simplified Duffing oscillator with abrupt transition from high amplitude to low amplitude and different frequency branches (Nagovitsyn & Pevtsov, 2020). These irregularities may complicate the long-term prediction of solar cycles.

### 3.2.2. *Outstanding questions*

Advances in assimilating observational data in the computational models has resulted in significant convergence in the physics-based predictions of solar cycle 25 as compared to the predictions for cycle 24. Nevertheless, the adopted predictive approaches still require significant improvements.

What is the best proxy for solar cycle predictions? What physical dynamo model of the solar cycle is most suitable for predictive purposes? How early and with what accuracy can we predict the solar cycle? Precise answers to these crucial questions can efficiently constrain the fundamental physics of solar magnetic cycles and help develop more accurate predictive capabilities.

### 3.3. Solar-planetary interactions

#### 3.3.1. Planetary forcing of solar cycles

In his letter to Carrington, Wolf (1859) suggested that 11-year variations in sunspots could be explained by the planetary influence, with Jupiter defining the amplitude and period of sunspot cycle, Saturn inducing the variations in these parameters, and Earth and Venus adding smaller scales "ripples" in sunspot variations. The idea of planetary forcing of solar cycle was later discussed in numerous papers (see, *e.g.*, Jose, 1965; Wolff & Patrone, 2010; Abreu et al., 2012; Scafetta, 2012; Okhlopkov, 2016; Stefani et al., 2016, 2019, 2021, and references therein). The idea was shown to be erroneous by De Jager & Versteegh (2005), Poluianov & Usoskin (2014), Holm (2015), Charbonneau (2022), Nataf (2022, 2023), Weisshaar et al. (2023), and Biswas et al. (2023). Horstmann et al. (2023) demonstrated that Rossby waves could, in principle, be excited in the tachocline by low-frequency planetary perturbations. However, the amplitude of these waves strongly depends on the frictional dampling, whose amplitude is not well-known. Recently, Cionco et al. (2023) analyzed the tidal forces related to Venus–Earth–Jupiter configurations based on the complete Sun's tide-generating potential, and found no presence of 11-year periods. Their results, however, do show periodicities of about 10 years and in the range of 11.7–11.9 years, which, perhaps, some may consider to be close enough to a period of the solar cycle, although none of these periodicities involve both Venus and Earth.

Interactions due to a larger mass planet closely orbiting a host star (hot Jupiter) or to a close binary system, whether stellar-planetary or stellar-stellar, may be important drivers for stellar cycles (*e.g.*, Wei, 2022; for a review, see Section 6.3 in Berdyugina, 2005), but it is not a case for the Sun.

#### 3.3.2. Long-term solar variability and forcing of planetary environments

Variations in the Sun's activity influence the space environments of the planets that it hosts. This forcing occurs over short to very long timescales, including the evolutionary lifetime of the solar system — studies of which have implications for planetary habitability (Lammer, 2013). The magnetic activity of stars — including that of the Sun — evolves with age (see Figure 5). This evolution is governed mainly by changes in stellar rotation rate due to the loss of angular momentum mediated through magnetically driven solar (stellar) winds (Réville et al., 2015; Matt et al., 2015). This in turn reduces the efficiency of the solar dynamo mechanism and regulates the intensity and topology of photospheric and coronal magnetic field distribution, including the severity and frequency of solar eruptive events as well as the Poynting flux transmitted to heat the solar (stellar) corona. In the grand scheme of things, the magnetic output of a solar-like star, therefore, reduces as the star ages (Nandy & Martens, 2007; Vidotto et al., 2014; See et al., 2019; Reiners et al., 2022). However, there is some recent evidence that, for slowly rotating stars with very large Rossby numbers that possibly yield an anti-solar differential rotation, the magnetic flux increases again. This has been shown observationally by Brandenburg & Giampapa (2018) and also found in numerical simulations of solar-type stars dynamo in Brun et al. (2022). It would be thus instructive to assess the magnetic flux trends of very slow rotators.

For far-out planets like those we encounter in the solar system, it is typically the activity of the star which has an impact on planetary atmospheres and evolution. Primary mechanisms of star-planet interactions include, but are not limited to, radiative forcing of planetary atmospheres (Haigh, 2007), thermal and/or non-thermal processes that influence planetary atmospheric escape (Gronoff et al., 2020), impacts of stellar wind and magnetic storms (Das et al., 2019; Basak & Nandy, 2021; Varela et al., 2022; Gupta et al., 2023); for a review see Nandy (2021).

Star-planet interaction is mediated by magnetic fields, and the presence or absence of a magnetosphere plays an important role (Zarka, 2007; Saur et al., 2013). It is believed that the existence of a magnetosphere is useful for the protection of planetary atmospheres against solar-stellar wind and storm impact (see Figure 6). Mars offers an interesting case study in this respect. It is conjectured that at about 1.5 billion years of age of the solar system, when the Sun was much more magnetically active, Mars had an active dynamo; the resulting Martian magnetosphere shielded its atmosphere from the relatively strong young Sun. Mars is thought to have had a warm moist atmosphere at this point in time which could have been suitable for hosting life. Subsequently, however, the cooling of the Martian core resulted in the loss of its global dynamo and large-scale magnetosphere. Following the sustained impact of solar radiation-driven sputtering processes, solar magnetic storms, and winds, the atmosphere of Mars likely eroded away (Basak & Nandy, 2021), influencing conditions for habitability (at least on or near the surface). Modeling such interactions leading to atmospheric mass losses at the global level is a challenging task. Such attempts are illuminating hitherto unanticipated physics of the interaction of stellar magnetized winds with planetary atmospheres. We note that these studies, which can be constrained by observations in the solar system, also inform and guide the development of models of star-planet interactions in exoplanetary systems (Strugarek, 2017).

#### 3.3.3. Outstanding questions

Solar cycle forcing by planetary tides is a recurrent topic, despite being rejected by numerous studies. Still the question remains open for other solar-like stars hosting closer and more massive planets.

Understanding the magnetic interaction of (exo)planets with their host stars is an important emerging field of study which transcends the boundaries of the solar system and has profound implications for exoplanetary space weather and the search for habitable exoplanets.

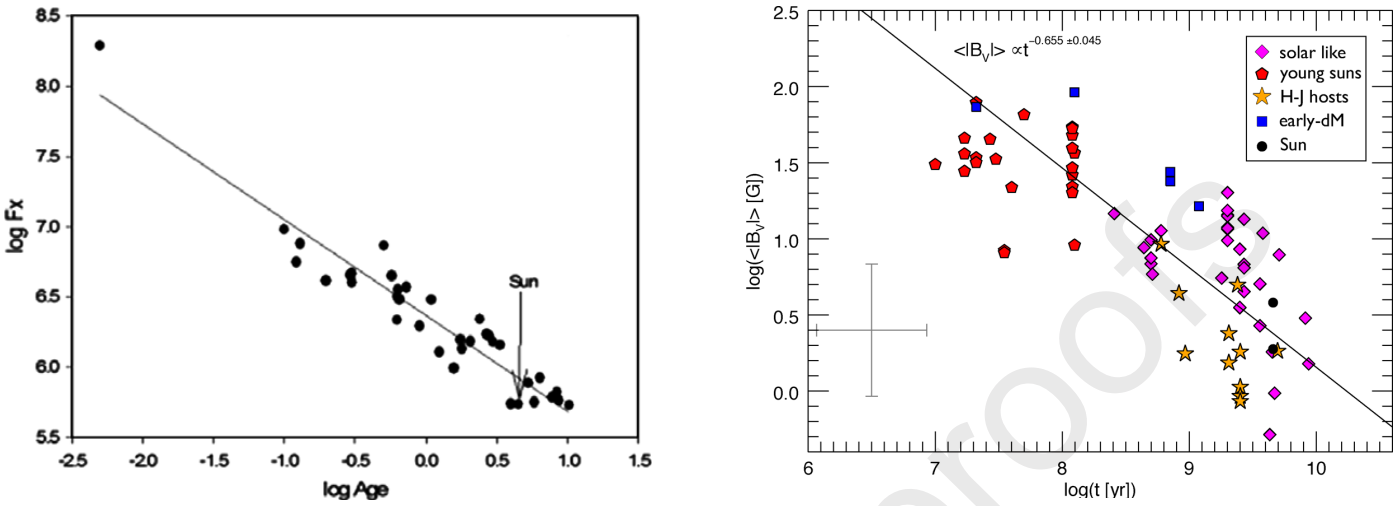


Fig. 5. Left (reproduced from Nandy & Martens, 2007): The stellar coronal X-ray emissions decrease as the stellar age increases (x-axis; in log of Gyrs). Right (reproduced from Vidotto et al., 2014): The average large-scale stellar magnetic field strength is negatively correlated with the stellar age (x-axis; in log of yrs). Typical errors in estimation of stellar magnetic field and age are represented by gray vertical and horizontal error bars, respectively. A detailed description of this figure can be found in Vidotto et al. (2014). These observations of stronger magnetic output at young stellar ages suggest that the environment of the early, young Sun was relatively extreme, with more energetic storms, winds, and radiative output creating an intense space environment for Earth and other solar system planets. Note that for very young stars a saturation in activity is also observed which is not captured in this sample (see, *e.g.*, See et al., 2019).

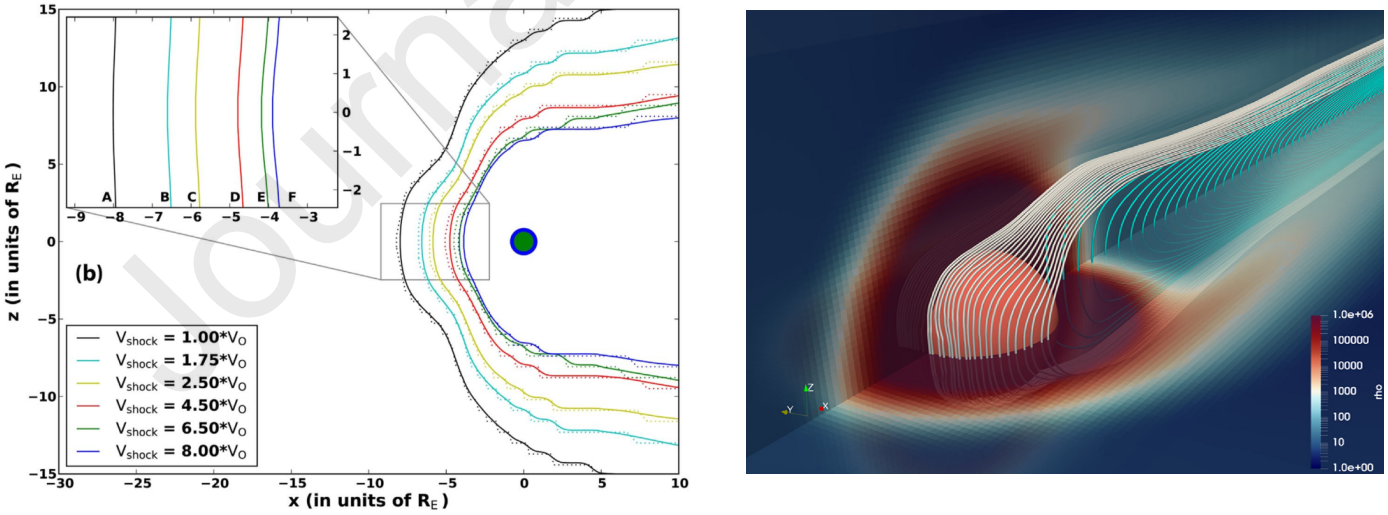


Fig. 6. Left: Magnetopause boundary approaches towards the planet with increasing speed of the magnetized stellar wind, as shown in simulations performed by Das et al. (2019). Right: A simulated 3D view of the steady-state imposed magnetospheric configuration of a planet without an intrinsic magnetosphere. The stellar wind eventually strips off the atmosphere of the planet in the course of its evolutionary timescale (Basak & Nandy, 2021).

In fact, how the evolving solar activity impacted Earth's environment and the emergence of life is a pertinent question. As such, the very concept of planetary habitability, that today takes into consideration mostly the irradiating flux from the host star, will have to be refined to encompass the important effect of secular evolution of the magnetism of the host star and of the planet, as our understanding of these interactions progresses in the coming decade.

## 4. Historical data preservation and curation

Over the past centuries, the astronomical/heliophysics community has accumulated a significant heritage of recorded observations of solar events. Those records contain irreplaceable information about long-term evolutionary and non-evolutionary changes in our closest star and its surroundings (heliosphere). Unfortunately, recent history already provides examples of irreplaceable loss or "close calls" for such historical data. Thus, the preservation and digitization of all important historical records are vital. It is imperative that the community and international funding agencies work together on recognizing the gravity of the situation and developing comprehensive long-term planning supported by adequate resources to prevent irreplaceable loss of this data. The importance and urgency of this issue have been recognized by, *e.g.*, General Assembly XXX of the International Astronomical Union in its Resolution B3: "*on preservation, digitization and scientific exploration of historical astronomical data*", US Decadal Survey on Astronomy and Astrophysics 2020 (National Academies of Sciences, Engineering, and Medicine, 2021; see also Pevtsov et al., 2019).

### *4.1. A comprehensive inventory of solar and geomagnetic datasets relevant for long-term space weather and space climate research*

Both historical and more modern observations of the Sun are available to researchers and the general public via various datasets. The datasets based on NASA spacecraft data are better organized, although, due to the preferences of research communities, the data from different heliophysics and geophysics sub-fields are using different formats and metadata. The data can be accessed via the NASA Heliophysics Data Portal (see the first entry in Table 3). The dataset is organized by a mission (or spacecraft), and it even includes some ground-based instruments. Non-NASA data are less well organized, although NOAA's National Centers for Environmental Information (NCEI) contains a good collection of solar and heliospheric data.

Traditionally, historical datasets are maintained by projects that were involved in their collection or digitization. This decentralized approach does not guarantee a long-term curation of the datasets. Even for large observatories, historical datasets could be in danger of neglect as the priorities change and funding sources "dry out". For example, as the NSO relocated to Colorado from its previous locations at New Mexico and Arizona, only selected historical data were transferred. Other data were either left behind to new observatory operators or were transferred to some other users. Some historical data accumulated by NOAA in its Boulder, Colorado location were given away to individuals as new priorities for the warehouse led to the reduction of available space. Digitized observations of Ca K line taken at Mount Wilson Observatory (MWO) were partially lost as the data server was turned off due to a lack of understanding of the importance of the data and a lack of funding. Some MWO data were recovered using copies made by members of the international research community for their individual projects.

The datasets maintained by individual projects are much harder to find and could be highly non-uniform with respect to the data format and metadata. Some data are provided as ASCII tables in the attachment to published papers. As an alternative, some (small) datasets are placed on free data repositories (*e.g.*, Harvard Dataverse[27], VizieR Online Data Catalog by Centre de données astronomiques de Strasbourg[28]). The repositories provide the ability to create metadata and to assign DOI[29] numbers. However, the DOI numbers themselves need to be maintained and updated with new pointing information. Unfortunately, there are already cases when DOIs may end in a broken link.

There are also several archives that collect information (links) about the datasets, which may improve the discoverability of some datasets. Table 3 provides brief information about selected datasets. NASA also funds the development of the Virtual Solar Observatory (VSO) to improve the accessibility of heliophysics data. However, VSO only serves as an interface for connecting the user with the data providers. Data curation remains the responsibility of data providers. Currently, VSO does not include historical data about solar activity although some of the authors of this article had initiated conversations with the VSO team on this matter.

### *4.2. Formulation of standardized method for processing and preservation of historical data*

The study of long-term solar variability is closely linked to the availability and preservation of historical archives of solar observations. It was already crucial at the time of Rudolf Wolf when he gathered more than 100 years of historical data on sunspots back to the 1700s, and is even more crucial and complicated 200 years later. Muñoz-Jaramillo & Vaquero (2019) describe the data gaps that limit the accuracy of the SN and GN series, while Arlt & Vaquero (2020) describe the amount of information that could be retrieved from identified data sources that have not been made available in digital format yet. That encompasses numbers and drawings that have been identified, but are still in paper form, as well as numbers and drawings that are scanned, but not directly exploitable without investing manpower to extract the information.

[27] https://dataverse.harvard.edu/
[28] https://vizier.cds.unistra.fr/index.gml
[29] Digital Object Identifier

Table 3: Datasets of various solar data and their DOI/HTML links.

| Observable | Period | Link |
|---|---|---|
| NASA's Heliophysics Data Portal | Various | https://heliophysicsdata.gsfc.nasa.gov/websearch/dispatcher |
| NOAA.s NCEI solar data collection | Various | https://www.ngdc.noaa.gov/stp/SOLAR |
| Solar activity from the catalogs of the Zürich Observatory | 1887–1920 | https://doi.org/10.1007/s11207-022-02015-3 |
| BASS-2000: Solar survey archive | Various | https://bass2000.obspm.fr/home.php |
| Databases at the Debrecen Observatory | 1872–2014 | http://fenyi.solarobs.epss.hu/en/databases/Summary/ |
| Sunspot positions and areas | 1612–1614 | https://doi.org/10.1007/s11207-020-01752-7 |
| Sunspot number | 1900–1911 | https://doi.org/10.1002/asna.202013654 |
| Sunspot positions and areas | 1610–1613 | https://doi.org/10.1007/s11207-020-01604-4 |
| Sunspot positions | 1761, 1764–1777 | https://doi.org/10.1007/s11207-019-1466-y |
| Sunspot positions | 1761, 1764–1777 | https://doi.org/10.1007/s11207-019-1465-z |
| Sunspot positions | 1747 | https://doi.org/10.1002/asna.201913544 |
| Sunspot positions | 1680–1709 | https://doi.org/10.1002/asna.201813481 |
| Sunspot number (official time series) | 1700-present | https://www.sidc.be/silso/datafiles |
| Sunspot groups position | 1826–2005 | https://doi.org/10.1051/0004-6361/201629533 |
| Sunspot positions, areas, and group tilt angles | 1611–1631 | https://doi.org/10.1051/0004-6361/201629000 |
| Sunspot group tilts | various | https://doi.org/10.1016/j.asr.2016.03.002 |
| Sunspot areas and tilt angles | 1825–1867 | https://doi.org/10.1051/0004-6361/201527080 |
| Sunspot positions, polarity, and field strength (digitized MWO observations) | 1917–2016 | https://doi.org/10.25668/bkt9-4d24 |
| Sunspot positions, polarity, and field strength (from PASP publications) | 1920–1958 | https://doi.org/10.7910/DVN/A49B7Y |
| Synoptic maps of Ca II K line intensity | 1915–1985 | https://doi.org/10.7910/DVN/RQSEJ8 |
| Composite disk-integrated Ca II K emission | 1907–2016 | https://doi.org/10.7910/DVN/VF5BMO |
| Sunspot positions (NSO/Sac Peak) | 1947–2004 | https://doi.org/10.25668/9x5p-6d86 |
| NSO/Sac Peak flare patrol H$\alpha$ | 1966–2000 | https://nispdata.nso.edu/ftp/flare_patrol_h_alpha_sp/ |

*Continued on next page*

*Continued from previous page*

| Observable | Period | Link |
|---|---|---|
| NSO/Sac Peak spectroheliograph Ca K and H$\alpha$ | 1965–2002 | https://nispdata.nso.edu/ftp/Evans_spectroheliograms/ https://nispdata.nso.edu/ftp/ESF_SHG_cdrom/ |
| NSO/Sac Peak Ca II K-line monitoring program | Nov. 1976 - Oct. 2015 | https://nsosp-dev.nso.edu/node/15 |
| NSO Ca K indices from the Kitt Peak vacuum telescope | 1974–2013 | https://solis.nso.edu/kpvt/CaK_Indicies/K-line_stats.dat |
| NSO/SOLIS integrated sunlight spectrometer | 2006–2017 | https://doi.org/10.25668/61PJ-WH14 |
| Full disk H$\alpha$ images (GONG) | 2000–present | https://doi.org/10.25668/as28-7p13 |
| Combined database of sunspot magnetic fields (USSR-Russia) | 1957–1997 | http://www.gaoran.ru/database/mfbase/main_e.html |
| Pulkovo catalogue of solar activity (various solar features and indices) | 1932–1991 | http://www.gaoran.ru/database/csa/main_e.html |
| Sunspot magnetic fields (Crimean Astrophysical Observatory) | 1957–present | https://sun.crao.ru/observations/sunspots-magnetic-field |
| Sunspot drawings of the Specola Solare Ticinese | 1957–2023 | https://www.specola.ch/e/drawings.html https://sunspots.irsol.usi.ch/db/ |
| Sunspot Group Database of the Specola Solare Ticinese | 1957-2022 | https://doi.org/10.5281/zenodo.8117331 |
| Historical archive of sunspot observations (HASO) at the University of Extremadura (Spain) | Various | http://haso.unex.es/ |
| Archive of sunspot drawings at NOAA's NCEI | 1816, 1817, 1859, 1860, 1880–1919, 1942–2019 | http://www.ngdc.noaa.gov/stp/space-weather/solar-data/solar-imagery/photosphere/sunspot-drawings/ |
| Archive of sunspot drawings at Slovak Central Observatory Hurbanovo | 1967–present[a] | http://www.suh.sk/obs/aktivita/archivdraw.htm |
| Kodaikanal Solar Observatory data archive | 1907–2007 (CaK) 1912–1979 (Ha) 1904–2011 (white light) | https://kso.iiap.res.in/new |
| Solar observations from Mount Wilson Observatory (MWO) | various | http://obs.astro.ucla.edu/intro.html |
| Sunspot number and area | 1931–1933 | https://doi.org/10.1007/s11207-022-01992-9 |
| Stonyhurst College Observatory daily sunspot area measurements | 1886–1940 | https://doi.org/10.26093/cds/vizier.22560038 |
| Hemispheric sunspot number | 1935–1986 | https://doi.org/10.3847/1538-4357/ac5dc6 |
| Dcx (corrected Dst) index server | 1932–2022 | http://dcx.oulu.fi |
| Geomagnetic indices | 1868–present | https://www.ngdc.noaa.gov/geomag/indices/indices.html |

*Continued on next page*

*Continued from previous page*

| **Observable** | **Period** | **Link** |
|---|---|---|
| Sun-as-a-star magnetic field | 1968–2010 | https://www.ngdc.noaa.gov/stp/solar/sunasastar.html |
| Records of sunspot and aurora | CE 960–1279 | https://doi.org/10.1186/s40623-015-0250-y |
| Neutron monitor database | 1951-present | http://www01.nmdb.eu/data/ |
| Solar radio flux | 1947-present | https://www.ngdc.noaa.gov/stp/solar/solarradio.html |
| Royal Observatory, Greenwich – USAF/NOAA sunspot data | 1874–2016 | https://solarscience.msfc.nasa.gov/greenwch.shtml |
| Solar Electro-Optical Network (SEON, RSTN, SOON) | 1980–2013 | https://www.ncei.noaa.gov/products/space-weather/legacy-data/solar-electro-optical-network |
| SOONAR – Solar Optical Observing Network ARchive (H$\alpha$ data) | 2013–2021 | https://www.soonar.org/ |
| Virtual Solar Observatory | 1975–present | https://nso.virtualsolar.org/cgi/search |

[a] Only 2007-2023 are online

Since the recalibration in 2015 (Clette et al., 2016a) considerable efforts at recovering these data have been made by the WDC-SILSO team (Clette et al., 2021), Rainer Arlt (Ilarionov & Arlt, 2022; Vokhmyanin et al., 2021), Hisashi Hayakawa (Hayakawa et al., 2022, 2023), and Jose Vaquero and his team (Aparicio et al., 2022a,b; Carrasco et al., 2022a,b, 2021a,d,c,b,e,f,g), leading to hundreds of additional data points available for a compiled sunspot series with even more detailed information. Here we cite only the most recent ones. However, the community still lacks a common access/platform where all available data could be made accessible. In 2023, the WDC-SILSO was awarded a Belgian BRAIN grant[30] for the FARSUN project that will address exactly this problem. It is formulating and putting into action a method for gathering, processing, and preserving historical sunspot data.

Its goal is to make the raw historical sunspot data of national and international origin findable and accessible for all users. The project gathers, interprets, and valorizes the data. It includes data pre-processing, quality assessment, and standardization, as well as publicity towards end users. A detailed statistical study will provide quality criteria for these historical data, and the most pertinent criteria will be included in metadata describing the dataset.

This project extends across multiple fields: the WDC-SILSO expertise as curator of the International Sunspot Number is complemented by statistical expertise, expertise on historical datasets, Virtual Observatory (VO) expertise, time-series expertise, and a team of experts in optical characters recognition[31]. The output of this project will be a compilation of historical sunspot numbers that will be made available via standard VO tools defined by the International Virtual Observatory Alliance (IVOA[32]), and more specifically via an EPN-TAP (Europlanet-Table Access Protocol) service. This will allow this catalog to be findable (via the IVOA Registry) and accessible by queries from a variety of TAP clients. In addition, the standardization of this VO tool allows other tools (graphical viewers, editors, etc) to easily access the data, making them interoperable, while the rich catalog metadata will allow the data to be reusable, *i.e.*, the data will be FAIR-compliant[33]. Making these validated historical sunspot data collections FAIR will allow solar physicists, Earth-climate modelers, experts in statistics, or anyone with a keen interest in solar variability, to analyze this unique natural record and will ensure its sustainability in the long term, while the association of specifically developed metadata will enable homogeneous processing for future additions to the dataset.

Our community will benefit directly from the output of the FARSUN project and especially from the research on common metadata criteria. First, it will set up the base for the standardization of historical sunspot data, creating the first standardized metadata. Second, it will gather, process and preserve all this data, through the use of standard VO tools. And third, access to these data in a centralized way will greatly facilitate work within the community, but also with experts from related fields such as Earth climate, space climate or space weather, and all users of the data.

## 5. Continuity of long-term observations of the Sun

While this ISWAT S1 cluster concentrates on long-term solar variability, the continuity of modern-day observations over extended periods of time (synoptic observations) is critical in building the datasets that future researchers would call "historical data". Thus, for example, continuous observations are essential to study changes in solar differential rotation, the meridional flows, kinetic and magnetic helicities — all key ingredients for solar dynamo. A routine observation of Doppler velocities led to the discovery of so-called torsional oscillations, latitudinal bands with faster or slower solar rotation (Snodgrass & Howard, 1985). Spatially, the torsional oscillation pattern coincides with latitudes of sunspot emergence, but the pattern also precedes the active region development, giving an indication of extended solar cycle. There is also a separate poleward directed branch of torsional oscillations, which reaches the poles approximately at about the polar field reversal. In helioseismic derivations, this pattern has been observed for one complete solar cycle, and it seems to be confined mostly to the upper portion of the convection zone. At the beginning of solar cycle 25, however, the torsional oscillation pattern showed different behavior as compared with the previous cycle. We do not know yet if this is because of solar evolutionary changes, or some short-term abnormalities in these large-scale flows. Similar (and unexpected) changes in magnetic helicity were also observed. Synoptic observations would also provide necessary data for defining references for a "typical" state of solar activity and the various solar features. These observations will also inform us about any evolutionary and non-evolutionary changes in the Sun.

Currently, synoptic observations of the Sun in optical (visible) wavelength range are conducted by several observatories around the globe. There are also several worldwide networks in operation. Solar Observing Optical Network (SOON, Neidig et al., 1998) includes three stations situated in Southwestern USA, Western Australia, and southern Italy. SOON observations include determination of several parameters of solar active regions (class, area, heliographic location), and rapid imaging of their flare activity in the H$\alpha$ spectral line. Global Oscillations Network Group (GONG[34], Harvey et al., 1996; Hill, 2018) is a 6-site network with two instruments located in the USA, and other instruments in Western Australia, India, Spain (Canary Islands), and Chile. GONG observations include measurements of Doppler velocities for helioseismology derivations, line-of-sight magnetic field, and full disk H$\alpha$ imaging.

[30] Belgian Research Action through Interdisciplinary Networks: https://www.belspo.be/belspo/brain2-be/index_en.stm

[31] https://readcoop.eu/transkribus/

[32] http://www.ivoa.net/documents/TAP/20190927/REC-TAP-1.1.html

[33] Findability, Accessibility, Interoperability, and Reuse: https://www.go-fair.org/fair-principles/

[34] https://gong.nso.edu/

Other networks include Global High-Resolution H-alpha Network (GHN[35], Steinegger et al., 2000), an ad hoc network of H$\alpha$ instruments operated by different observatories. The Birmingham Solar-Oscillations Network (BiSON[36], Davies et al., 2014; Hale et al., 2016) is a world-wide network of six remotely operated ground-based telescopes, monitoring the globally coherent, core-penetrating modes of oscillation of the Sun.

Synoptic observations are also taken using spaceborn instruments such as (past) Solar and Heliospheric Observatory (SoHO) and Solar Dynamics Observatory. Unlike ground-based observatories, space-based instruments are designed for a shorter period of operations, although they could continue operations for extended periods as was the case with SoHO and SDO. For overview of other synoptic observations, and comparative advantages/disadvantages of ground-based and space-borne observations, see Pevtsov (2016). There is an extensive network of neutron monitors and radio telescopes. For additional information, see a Google map of groundbased solar observatories and neutron monitors.

Several networks are in different stages of development, including the Solar Activity Monitor Network (SAMNet, Erdélyi et al., 2022), Continuous H$\alpha$ Imaging Network (CHAIN[37], Ueno et al., 2010; Ishitsuka et al., 2014), the Solar Physics Research Integrated Network Group (SPRING, Gosain et al., 2018), and next generation GONG (ngGONG, Pevtsov et al., 2022). Unfortunately, many of these long-term instruments are aging and some are getting obsolete. Many facilities see a pattern of decreasing funding (Pevtsov & Clette, 2017).

## 6. Summary and Recommendations

This article provides an overview of our current understanding of different aspects of long-term variations of solar activity. In developing this understanding, historical records of solar activity such as sunspot observations play a key role. While significant progress has been made in improving sunspot and group numbers, this work needs to continue. There is a need for development of improved methods for creating time series of indices characterizing long-term solar activity. In addition to well-established SN and GN series, the value of other proxies such as sunspot/group areas needs to be investigated. See Section 2.1.4 for outstanding questions related to SN and GN time series. The improvements to historical times series depend critically on adding new data especially for periods when direct observations are limited. In that respect, preservation, recovery, digitization, long-term curation, and scientific exploration of historical data is essential. There is also a need to develop a better characterization of historical datasets in respect to their uniformity and error analysis. Long-term TSI time series has reached a community consensus. However, to develop SSI time series of similar quality as TSI would require longer SSI measurements with sufficient long-term stability. See Section 2.2.4 for outstanding questions related to solar total and spectral irradiance.

Outstanding questions for large-scale heliospheric parameters/structure can be found in Section 2.3.4. Solving the open flux problem and developing a better understanding of long-term evolution of the global structure of the heliosphere are some of the most important questions. High latitude in situ and remote observations would be extremely beneficial for achieving these goals.

There are several outstanding questions related to extreme solar events (see Section 2.4.4) including the unknown physics of extreme events, their possible impacts on our highly technological society, and, not least, resolving the apparent controversy in the level of flare activity based on solar proxies and direct observations of solar-analogues. To answer these questions, new precise datasets in both terrestrial proxies and stellar observations are needed, along with the development of sophisticated analysis methods and new models. Currently, there is a lack of models for extreme events.

In modeling of solar dynamos, further improvements need to be made in global 3D simulations to address shortcomings of current models. The interplay between small-scale and large-scale dynamos, role of magnetic helicity, and the ability of the Babcock-Leighton mechanism to explain the diversity of stellar scaling laws self-consistently are other outstanding questions for making progress in dynamo theory and simulations and to improve the long-term predictability of the solar cycle. See Sections 3.1.3 and 3.2.2 for outstanding questions related to solar dynamo and solar cycle prediction.

Our current approaches to understanding the effects of exoplanetary space weather on habitability of exoplanets need to be revised to include the secular evolution of magnetism of the host star and the planet, and the interaction of stellar magnetized winds with planetary atmospheres. See Section 3.3.3 for outstanding questions related to solar-planetary interactions.

Finally, it is imperative that long-term synoptic observations of the Sun continue for a period of time comparable to at least two full magnetic cycles (about 44 years, or longer). Given the importance of such observations to society and the global impact of space weather, these observations should include strong international collaborations backed by sufficient targeted funding by the National funding agencies.

## 7. Acknowledgments

The National Solar Observatory is operated by the Association of Universities for Research in Astronomy (AURA), Inc., under a cooperative agreement with the National Science Foundation. The Center of Excellence in Space Sciences India (CESSI) is funded by the Ministry of Education, Government of India. C.S. is funded by the Council of Scientific and Industrial Research, Government of India through grant number 09/921(0334)/2020-EMR-I. A.S.B, B.P. and A.S. acknowledges funding by the European Research Council (ERC) under grant #810238 Whole Sun, by the European Space Agency (ESA) under the Swesnet project and by the French Space Agency (CNES) Solar Orbiter &

[35] https://www.bbso.njit.edu/Research/Halpha/
[36] bison.ph.bham.ac.uk
[37] https://www.kwasan.kyoto-u.ac.jp/CHAIN/

Space Weather grants and CNRS/INSU Sun-Earth research program, and by the french Agence Nationale de la Recherche (ANR) under grant STORMGENESIS ANR-22-CE31-0013-01. L.L. gratefully acknowledges funding from the Belgian Federal Science Policy Office (BELSPO) through the BRAIN DeepSun project (B2/191/P2/DeepSun) and FARSUN project (B2/233/P2/FARSUN) and the Solar-Terrestrial Centre of Excellence, a collaboration between the Royal Observatory of Belgium, the Royal Meteorological Institute, and the Royal Belgian Institute for Space Aeronomy funded by BELSPO. I.U. acknowledges the support from the Academy of Finland (project ESPERA 321882). Y.A.N. acknowledges the support from Grant 075-15-2020-780 of the Ministry of Science and Higher Education of the Russian Federation. C.C. acknowledges funding by NASA Living with the Star (LWS 80NSSC20K1819). M.A.D. acknowledges partial support from NASA LWS grant 80NSSC19K0079 and SWO2R award 80NSSC20K0290.

Several authors are members of the international teams "Solar Extreme Events: Setting Up a Paradigm" (team #510), "Modeling Space Weather And Total Solar Irradiance Over The Past Century" (team #475), "Reconstructing Solar and Heliospheric Magnetic Field Evolution Over the Past Century" (team #420), and "Recalibration of Sunspot Number Series" (team #417) supported by the International Space Science Institute (ISSI), Bern, Switzerland and ISSI-Beijing, China. Fruitful discussions by members of the International Astronomical Union's Inter-Division B-E Working Group on Coordination of Synoptic Observations of the Sun (https://www.iau.org/science/scientific_bodies/working_groups/255/) are also acknowledged.

## Appendix A. Acronyms

| | |
|---|---|
| **ACRIM** | Active Cavity Radiometer Irradiance Monitor |
| **ATLAS-3** | Atmospheric Laboratory for Applications and Science – 3 |
| **BCE** | Before Current Era |
| **BRAIN** | Belgian Research Action through Interdisciplinary Networks |
| **BiSON** | Birmingham Solar-Oscillations Network |
| **CE** | Current Era |
| **CHAIN** | Continuous H$\alpha$ Imaging Network |
| **CME** | Coronal Mass Ejection |
| **COSPAR** | Committee on Space Research |
| **DIARAD** | SoHO/VIRGO/Differential Absolute Radiometer |
| **DOI** | Digital Object Identifier |
| **ENA** | Energetic Neutral Atoms |
| **EPN-TAP** | Europlanet-Table Access Protocol |
| **ESPE** | Extreme Solar Particle Event |
| **FAIR** | Findability, Accessibility, Interoperability, and Reuse |
| **FARSUN** | Findability and Accessibility of historical (1610–1980) Raw Sunspot Numbers |
| **GCR** | Galactic Cosmic Ray |
| **GHN** | Global high-resolution H-alpha Network |
| **GLE** | Ground Level Enhancement |
| **GN** | Group Number |
| **GOES** | Geostationary Operational Environmental Satellite |
| **GONG** | Global Oscillations Network Group |
| **HMF** | Heliospheric Magnetic Field |
| **HMI** | SDO/Heliospheric and Magnetic Imager |
| **ISWAT** | International Space Weather Action Teams |
| **iPATH** | improved PATH |
| **IVOA** | International Virtual Observatory Alliance |
| **LISM** | Local Interstellar Medium |
| **MHD** | Magnetohydrodynamics |
| **MWO** | Mount Wilson Observatory |
| **NCEI** | National Centers for Environmental Information |
| **ngGONG** | next generation GONG |
| **NSO** | National Solar Observatory |
| **OSF** | Open Solar Flux |
| **PATH** | Particle Acceleration and Transport in the Heliosphere |
| **PMOD** | Physikalisch-Meteorologisches Observatorium Davos |
| **PMOV6** | SoHO/VIRGO/Physikalisch-Meteorologisches Observatorium radiometer Version 6 |
| **ROB** | Royal Observatory of Belgium |
| **SAMNet** | Solar Activity Monitor Network |
| **SATIRE-3D** | Spectral and Total Irradiance Reconstruction for the Satellite Era – 3D |
| **SDO** | Solar Dynamics Observatory |
| **SEP** | Solar Energetic Particle |

| | |
|---|---|
| **SFT** | Surface Flux Transport |
| **SILSO** | Sunspot Index and Long-term Solar Observations |
| **SIM** | SORCE/Solar Irradiance Monitor |
| **SN** | Sunspot Number |
| **SOLSTICE** | Solar Stellar Irradiance Comparison Experiment |
| **SOON** | Solar Observing Optical Network |
| **SORCE** | Solar Radiation and Climate Experiment |
| **SPRING** | Solar Physics Research Integrated Network Group |
| **SSI** | Spectral Solar Irradiance |
| **SoHO** | Solar and Heliospheric Observatory |
| **StEP** | Stellar Energetic Particle |
| **TIM** | SORCE/Total Irradiance Monitor |
| **TSIS-1** | Total and Spectral Solar Irradiance Sensor – 1 |
| **TSI** | Total Solar Irradiance |
| **VIRGO** | SoHO/Variability of solar Irradiance and Gravity Oscillations |
| **VO** | Virtual Observatory |
| **VSO** | Virtual Solar Observatory |
| **WDC** | World Data Center |
| **WHI** | Whole Heliosphere Interval |
| **XRS** | GOES/X-Ray Sensor |

## References


Aartsen, M. G., Abbasi, R., Ackermann, M. et al. (2021). Measurements of the time-dependent cosmic-ray Sun shadow with seven years of IceCube data: Comparison with the Solar cycle and magnetic field models. *Physical Review D*, *103*(4), 042005. doi:10.1103/PhysRevD.103.042005.

Abdusamatov, Kh. I. (2007). Optimal prediction of the peak of the next 11-year activity cycle and of the peaks of several succeeding cycles on the basis of long-term variations in the solar radius or solar constant. *Kinematics and Physics of Celestial Bodies*, *23*(3), 97–100. doi:10.3103/S0884591307030026.

Abreu, J. A., Beer, J., Ferriz-Mas, A. et al. (2012). Is there a planetary influence on solar activity? *Astronomy & Astrophysics*, *548*, A88. doi:10.1051/0004-6361/201219997.

Acero, F. J., Gallego, M. C., García, J. A. et al. (2018). Extreme value theory applied to the millennial sunspot number series. *The Astrophysical Journal*, *853*(1), 80. doi:10.3847/1538-4357/aaa406.

Airapetian, V. S., Barnes, R., Cohen, O. et al. (2020). Impact of space weather on climate and habitability of terrestrial-type exoplanets. *International Journal of Astrobiology*, *19*(2), 136–194. doi:10.1017/S1473550419000132.

Amenomori, M., Ayabe, S., Caidong et al. (2000). A study of the shadowing of galactic cosmic rays by the Sun in a quiet phase of solar activity with the Tibet air shower array. *The Astrophysical Journal*, *541*(2), 1051. doi:10.1086/309479.

Aparicio, A. J. P., Carrasco, V. M. S., Gallego, M. C. et al. (2022a). Hemispheric sunspot number from the Madrid Astronomical Observatory for the period 1935–1986. *The Astrophysical Journal*, *931*(1), 52. doi:10.3847/1538-4357/ac5dc6.

Aparicio, A. J. P., Carrasco, V. M. S., Gallego, M. C. et al. (2022b). A sunspot catalog by Rafael Carrasco at the Madrid Astronomical Observatory for the period 1931 – 1933. *Solar Physics*, *297*(5), 58. doi:10.1007/s11207-022-01992-9.

Arlt, R., & Vaquero, J. M. (2020). Historical sunspot records. *Living Reviews in Solar Physics*, *17*(1), 1. doi:10.1007/s41116-020-0023-y.

Attia, A.-F., Ismail, H. A., & Basurah, H. M. (2013). A neuro-fuzzy modeling for prediction of solar cycles 24 and 25. *Astrophysics and Space Science*, *344*(1), 5–11. doi:10.1007/s10509-012-1300-6.

Aulanier, G., Démoulin, P., Schrijver, C. J. et al. (2013). The standard flare model in three dimensions: II. Upper limit on solar flare energy. *Astronomy & Astrophysics*, *549*, A66. doi:10.1051/0004-6361/201220406.

Axford, W. I., Leer, E., & Skadron, G. (1977). The acceleration of cosmic rays by shock waves. In *Proceedings of the 15th International Cosmic Ray Conference* (pp. 132–137). Budapest, Hungary: Hungarian Academy of Sciences volume 11. URL: https://ui.adsabs.harvard.edu/abs/1977ICRC...11..132A.

Babcock, H. W. (1961). The topology of the Sun's magnetic field and the 22-year cycle. *The Astrophysical Journal*, *133*, 572–587. doi:10.1086/147060.

Ball, W. T., Unruh, Y. C., Krivova, N. A. et al. (2012). Reconstruction of total solar irradiance 1974–2009. *Astronomy & Astrophysics*, *541*, A27. doi:10.1051/0004-6361/201118702.

Basak, A., & Nandy, D. (2021). Modelling the imposed magnetospheres of Mars-like exoplanets: Star–planet interactions and atmospheric losses. *Monthly Notices of the Royal Astronomical Society*, *502*(3), 3569–3581. doi:10.1093/mnras/stab225.

Beer, J., McCracken, K., & von Steiger, R. (2012). *Cosmogenic Radionuclides: Theory and Applications in the Terrestrial and Space Environment*. Physics of Earth and Space Environments. Berlin, Germany: Springer. doi:10.1007/978-3-642-14651-0.

Beer, J., Tobias, S. M., & Weiss, N. O. (2018). On long-term modulation of the Sun's magnetic cycle. *Monthly Notices of the Royal Astronomical Society*, *473*(2), 1596–1602. doi:10.1093/mnras/stx2337.

Bell, A. R. (1978a). The acceleration of cosmic rays in shock fronts – I. *Monthly Notices of the Royal Astronomical Society*, *182*(2), 147–156. doi:10.1093/mnras/182.2.147.

Bell, A. R. (1978b). The acceleration of cosmic rays in shock fronts – II. *Monthly Notices of the Royal Astronomical Society*, *182*(3), 443–455. doi:10.1093/mnras/182.3.443.

Belov, A., Kurt, V., Mavromichalaki, H. et al. (2007). Peak-size distributions of proton fluxes and associated soft X-ray flares. *Solar Physics*, *246*(2), 457–470. doi:10.1007/s11207-007-9071-x.

Berdyugina, S. V. (2005). Starspots: A key to the stellar dynamo. *Living Reviews in Solar Physics*, *2*(1–62), 8. doi:10.12942/lrsp-2005-8.

Bhattacharya, S., Lefèvre, L., Hayakawa, H. et al. (2023). Scale transfer in 1849: Heinrich Schwabe to Rudolf Wolf. *Solar Physics*, *298*(1), 12. doi:10.1007/s11207-022-02103-4.

Bhattacharya, S., Teague, E. T. H., Fay, S. et al. (2021). A modern reconstruction of Richard Carrington's observations (1853–1861). *Solar Physics*, *296*(8), 118. doi:10.1007/s11207-021-01864-8.

Bhowmik, P., Jiang, J., Upton, L. et al. (2023). Physical Models for Solar Cycle Predictions. *Space Science Reviews*, *219*(5), 40. doi:10.1007/s11214-023-00983-x. arXiv:2303.12648.

Bhowmik, P., & Nandy, D. (2018). Prediction of the strength and timing of sunspot cycle 25 reveal decadal-scale space environmental conditions. *Nature Communications*, *9*(1–10), 5209. doi:10.1038/s41467-018-07690-0.

Biswas, A., Karak, B. B., Usoskin, I. et al. (2023). Long-term modulation of solar cycles. *Space Science Reviews*, *219*(3), 19. doi:10.1007/s11214-023-00968-w.

Blackman, E. G., & Brandenburg, A. (2002). Dynamic nonlinearity in large-scale dynamos with shear. *The Astrophysical Journal*, *579*(1), 359–373. doi:10.1086/342705.

Blandford, R. D., & Ostriker, J. P. (1978). Particle acceleration by astrophysical shocks. *The Astrophysical Journal*, *221*, L29–L32. doi:10.1086/182658.

Brandenburg, A., & Giampapa, M. S. (2018). Enhanced stellar activity for slow

antisolar differential rotation? *The Astrophysical Journal Letters*, *855*(2), L22. doi:10.3847/2041-8213/aab20a.

Brandenburg, A., & Subramanian, K. (2005). Astrophysical magnetic fields and nonlinear dynamo theory. *Physics Reports*, *417*(1), 1–209. doi:10.1016/j.physrep.2005.06.005.

Brehm, N., Bayliss, A., Christl, M. et al. (2021). Eleven-year solar cycles over the last millennium revealed by radiocarbon in tree rings. *Nature Geoscience*, *14*(1), 10–15. doi:10.1038/s41561-020-00674-0.

Brehm, N., Christl, M., Knowles, T. D. J. et al. (2022). Tree-rings reveal two strong solar proton events in 7176 and 5259 BCE. *Nature Communications*, *13*(1), 1196. doi:10.1038/s41467-022-28804-9.

Brun, A. S., & Browning, M. K. (2017). Magnetism, dynamo action and the solar-stellar connection. *Living Reviews in Solar Physics*, *14*(1), 4. doi:10.1007/s41116-017-0007-8.

Brun, A. S., Browning, M. K., Dikpati, M. et al. (2015a). Recent advances on solar global magnetism and variability. *Space Science Reviews*, *196*(1), 101–136. doi:10.1007/s11214-013-0028-0.

Brun, A. S., García, R. A., Houdek, G. et al. (2015b). The solar-stellar connection. *Space Science Reviews*, *196*(1), 303–356. doi:10.1007/s11214-014-0117-8.

Brun, A. S., Hung, C. P., Fournier, A. et al. (2019). A solar cycle 25 prediction based on 4D-var data assimilation approach. *Proceedings of the International Astronomical Union*, *15*(S354), 138–146. doi:10.1017/S1743921320003993.

Brun, A. S., Strugarek, A., Noraz, Q. et al. (2022). Powering stellar magnetism: Energy transfers in cyclic dynamos of Sun-like stars. *The Astrophysical Journal*, *926*(1), 21. doi:10.3847/1538-4357/ac469b.

Bushby, P. J. (2006). Zonal flows and grand minima in a solar dynamo model. *Monthly Notices of the Royal Astronomical Society*, *371*(2), 772–780. doi:10.1111/j.1365-2966.2006.10706.x.

Cameron, R. H., Jiang, J., Schmitt, D. et al. (2010). Surface flux transport modeling for solar cycles 15–21: Effects of cycle-dependent tilt angles of sunspot groups. *The Astrophysical Journal*, *719*(1), 264–270. doi:10.1088/0004-637X/719/1/264.

Cameron, R. H., Jiang, J., & Schüssler, M. (2016). Solar cycle 25: Another moderate cycle? *The Astrophysical Journal Letters*, *823*(2), L22. doi:10.3847/2041-8205/823/2/L22.

Carrasco, V. M. S., Gallego, M. C., & Vaquero, J. M. (2020). Number of sunspot groups from the Galileo–Scheiner controversy revisited. *Monthly Notices of the Royal Astronomical Society*, *496*(2), 2482–2492. doi:10.1093/mnras/staa1633.

Carrasco, V. M. S., Gallego, M. C., Villalba Álvarez, J. et al. (2021a). A reanalysis of the number of sunspot groups recorded by Pierre Gassendi in the cycle before the Maunder minimum. *Solar Physics*, *296*(4), 59. doi:10.1007/s11207-021-01809-1.

Carrasco, V. M. S., Gallego, M. C., Villalba Álvarez, J. et al. (2021b). Analyses of early sunspot records by Jean Tarde (1615 – 1617) and Jan Smogulecki (1621 – 1625). *Solar Physics*, *296*(11), 170. doi:10.1007/s11207-021-01905-2.

Carrasco, V. M. S., Hayakawa, H., Kuroyanagi, C. et al. (2021c). Strong evidence of low levels of solar activity during the Maunder minimum. *Monthly Notices of the Royal Astronomical Society*, *504*(4), 5199–5204. doi:10.1093/mnras/stab1155.

Carrasco, V. M. S., Muñoz-Jaramillo, A., Gallego, M. C. et al. (2022a). Revisiting Christoph Scheiner's sunspot records: A new perspective on solar activity of the early telescopic era. *The Astrophysical Journal*, *927*(2), 193. doi:10.3847/1538-4357/ac52ee.

Carrasco, V. M. S., Muñoz-Jaramillo, A., Nogales, J. M. et al. (2021d). Sunspot catalog (1921–1935) and area series (1886–1940) from the Stonyhurst College Observatory. *The Astrophysical Journal Supplement Series*, *256*(2), 38. doi:10.3847/1538-4365/ac24a7.

Carrasco, V. M. S., Munoz-Jaramillo, A., Nogales, J. M. et al. (2022b). SCO daily sunspot area measurements (1886-1940). Vizier Online Data Catalog. doi:10.26093/cds/vizier.22560038.

Carrasco, V. M. S., Nogales, J. M., Vaquero, J. M. et al. (2021e). A note on the sunspot and prominence records made by Angelo Secchi during the period 1871–1875. *Journal of Space Weather and Space Climate*, *11*, 51. doi:10.1051/swsc/2021033.

Carrasco, V. M. S., Pevtsov, A. A., Nogales, J. M. et al. (2021f). The sunspot drawing collection of the National Solar Observatory at Sacramento Peak (1947–2004). *Solar Physics*, *296*(1), 3. doi:10.1007/s11207-020-01746-5.

Carrasco, V. M. S., Vaquero, J. M., & Gallego, M. C. (2021g). A forgotten sunspot record during the Maunder minimum (Jean Charles Gallet, 1677). *Publications of the Astronomical Society of Japan*, *73*(3), 747–752. doi:10.1093/pasj/psab035.

Carrington, R. C. (1863). *Observations of the Spots on the Sun: From November 9, 1853, to March 24, 1861, Made at Redhill*. London, UK: Williams and Norgate. URL: https://ui.adsabs.harvard.edu/abs/1863oss..book.....C.

Chapman, G. A., Cookson, A. M., & Dobias, J. J. (1996). Variations in total solar irradiance during solar cycle 22. *Journal of Geophysical Research: Space Physics*, *101*(A6), 13541–13548. doi:10.1029/96JA00683.

Chapman, G. A., Cookson, A. M., & Preminger, D. G. (2013). Modeling total solar irradiance with San Fernando observatory ground-based photometry: Comparison with ACRIM, PMOD, and RMIB composites. *Solar Physics*, *283*(2), 295–305. doi:10.1007/s11207-013-0233-8.

Charbonneau, P. (2020). Dynamo models of the solar cycle. *Living Reviews in Solar Physics*, *17*(1), 4. doi:10.1007/s41116-020-00025-6.

Charbonneau, P. (2022). External forcing of the solar dynamo. *Frontiers in Astronomy and Space Sciences*, *9*, 853676. URL: https://www.frontiersin.org/articles/10.3389/fspas.2022.853676.

Charbonneau, P., Christensen-Dalsgaard, J., Henning, R. et al. (1999). Helioseismic constraints on the structure of the solar tachocline. *The Astrophysical Journal*, *527*(1), 445–460. doi:10.1086/308050.

Chatzistergos, T., Ermolli, I., Giorgi, F. et al. (2020a). Modelling solar irradiance from ground-based photometric observations. *Journal of Space Weather and Space Climate*, *10*, 45. doi:10.1051/swsc/2020047.

Chatzistergos, T., Ermolli, I., Krivova, N. A. et al. (2022a). Scrutinising the relationship between plage areas and sunspot areas and numbers. *Astronomy & Astrophysics*, *667*, A167. doi:10.1051/0004-6361/202244913.

Chatzistergos, T., Ermolli, I., Krivova, N. A. et al. (2020b). Analysis of full-disc Ca II K spectroheliograms - III. Plage area composite series covering 1892–2019. *Astronomy & Astrophysics*, *639*, A88. doi:10.1051/0004-6361/202037746.

Chatzistergos, T., Krivova, N. A., & Ermolli, I. (2022b). Full-disc Ca II K observations—A window to past solar magnetism. *Frontiers in Astronomy and Space Sciences*, *9*, 1038949. doi:10.3389/fspas.2022.1038949.

Chatzistergos, T., Krivova, N. A., Ermolli, I. et al. (2021). Reconstructing solar irradiance from historical Ca II K observations - I. Method and its validation. *Astronomy & Astrophysics*, *656*, A104. doi:10.1051/0004-6361/202141516.

Chatzistergos, T., Krivova, N. A., & Yeo, K. L. (2023). Long-term changes in solar activity and irradiance. doi:10.48550/arXiv.2303.03046.

Chatzistergos, T., Usoskin, I. G., Kovaltsov, G. A. et al. (2017). New reconstruction of the sunspot group numbers since 1739 using direct calibration and "backbone" methods. *Astronomy & Astrophysics*, *602*, A69. doi:10.1051/0004-6361/201630045.

Cionco, R. G., Kudryavtsev, S. M., & Soon, W. W.-H. (2023). Tidal forcing on the sun and the 11-year solar-activity cycle. *Solar Physics*, *298*(5), 70. doi:10.1007/s11207-023-02167-w.

Clette, F., Berghmans, D., Vanlommel, P. et al. (2007). From the Wolf number to the International Sunspot Index: 25 years of SIDC. *Advances in Space Research*, *40*(7), 919–928. doi:10.1016/j.asr.2006.12.045.

Clette, F., Cliver, E. W., Lefèvre, L. et al. (2015). Revision of the sunspot number(s). *Space Weather*, *13*(9), 529–530. doi:10.1002/2015SW001264.

Clette, F., Cliver, E. W., Lefèvre, L. et al. (2016a). Preface to topical issue: Recalibration of the sunspot number. *Solar Physics*, *291*(9), 2479–2486. doi:10.1007/s11207-016-1017-8.

Clette, F., & Lefèvre, L. (2012). Are the sunspots really vanishing? - Anomalies in solar cycle 23 and implications for long-term models and proxies. *Journal of Space Weather and Space Climate*, *2*, A06. doi:10.1051/swsc/2012007.

Clette, F., & Lefèvre, L. (2016). The new sunspot number: Assembling all corrections. *Solar Physics*, *291*(9), 2629–2651. doi:10.1007/s11207-016-1014-y.

Clette, F., Lefèvre, L., Bechet, S. et al. (2021). Reconstruction of the sunspot number source database and the 1947 Zurich discontinuity. *Solar Physics*, *296*(9), 137. doi:10.1007/s11207-021-01882-6.

Clette, F., Lefèvre, L., Cagnotti, M. et al. (2016b). The revised Brussels–Locarno sunspot number (1981 – 2015). *Solar Physics*, *291*(9), 2733–2761. doi:10.1007/s11207-016-0875-4.

Clette, F., Lefèvre, L., Chatzistergos, T. et al. (2023). Recalibration of the sunspot-number: Status report. *Solar Physics*, *298*(3), 44. doi:10.1007/s11207-023-02136-3.

Clette, F., Svalgaard, L., Vaquero, J. M. et al. (2014). Revisiting the sunspot number. *Space Science Reviews*, *186*(1), 35–103. doi:10.1007/s11214-014-0074-2.

Cliver, E. W. (2015). The extended cycle of solar activity and the Sun's 22-year magnetic cycle. In A. Balogh, H. Hudson, K. Petrovay, & R. von Steiger (Eds.), *The Solar Activity Cycle: Physical Causes and Consequences* Space Sciences Series of ISSI (pp. 169–189). New York, NY: Springer. doi:10.1007/978-1-4939-2584-1_6.

Cliver, E. W. (2016). Comparison of new and old sunspot number time series. *Solar Physics*, *291*(9), 2891–2916. doi:10.1007/s11207-016-0929-7.

Cliver, E. W., & D'Huys, E. (2018). Size distributions of solar proton events and their associated soft X-ray flares: Application of the maximum likelihood estimator. *The Astrophysical Journal*, *864*(1), 48. doi:10.3847/1538-4357/aad043.

Cliver, E. W., & Ling, A. G. (2016). The discontinuity circa 1885 in the group sunspot number. *Solar Physics*, *291*(9), 2763–2784. doi:10.1007/s11207-015-0841-6.

Cliver, E. W., Schrijver, C. J., Shibata, K. et al. (2022). Extreme solar events. *Living Reviews in Solar Physics*, *19*(1), 2. doi:10.1007/s41116-022-00033-8.

Coddington, O., Lean, J. L., Pilewskie, P. et al. (2016). A solar irradiance climate data record. *Bulletin of the American Meteorological Society*, *97*(7), 1265–1282. doi:10.1175/BAMS-D-14-00265.1.

Coddington, O. M., Richard, E. C., Harber, D. et al. (2021). The TSIS-1 hybrid solar reference spectrum. *Geophysical Research Letters*, *48*(12), e2020GL091709. doi:10.1029/2020GL091709.

Covas, E., Peixinho, N., & Fernandes, J. (2019). Neural network forecast of the sunspot butterfly diagram. *Solar Physics*, *294*(3), 24. doi:10.1007/s11207-019-1412-z.

Cowling, T. G. (1933). The magnetic field of sunspots. *Monthly Notices of the Royal Astronomical Society*, *94*(1), 39–48. doi:10.1093/mnras/94.1.39.

Dani, T., & Sulistiani, S. (2019). Prediction of maximum amplitude of solar cycle 25 using machine learning. *Journal of Physics: Conference Series*, *1231*(1), 012022. doi:10.1088/1742-6596/1231/1/012022.

Das, S. B., Basak, A., Nandy, D. et al. (2019). Modeling star–planet interactions in far-out planetary and exoplanetary systems. *The Astrophysical Journal*, *877*(2), 80. doi:10.3847/1538-4357/ab18ad.

Dasi-Espuig, M., Solanki, S. K., Krivova, N. A. et al. (2010). Sunspot group tilt angles and the strength of the solar cycle. *Astronomy & Astrophysics*, *518*, A7. doi:10.1051/0004-6361/201014301.

Davies, G. R., Chaplin, W. J., Elsworth, Y. et al. (2014). BiSON data preparation: A correction for differential extinction and the weighted averaging of contemporaneous data. *Monthly Notices of the Royal Astronomical Society*, *441*(4), 3009–3017. doi:10.1093/mnras/stu803.

Dayeh, M. A., Allegrini, F., DeMajistre, R. et al. (2014). Spectral evolution of energetic neutral atom emissions at the heliospheric poles as measured by IBEX during its first three years. *The Astrophysical Journal*, *797*(1), 57. doi:10.1088/0004-637X/797/1/57.

Dayeh, M. A., Zirnstein, E. J., Desai, M. I. et al. (2019). Variability in the position of the IBEX ribbon over nine years: More observational evidence for a secondary ENA source. *The Astrophysical Journal*, *879*(2), 84. doi:10.3847/1538-4357/ab21c1.

Dayeh, M. A., Zirnstein, E. J., Fuselier, S. A. et al. (2022). Evolution of the heliotail lobes over a solar cycle as measured by IBEX. *The Astrophysical Journal Supplement Series*, *261*(2), 27. doi:10.3847/1538-4365/ac714e.

De Jager, C., & Versteegh, G. J. M. (2005). Do planetary motions drive solar variability? *Solar Physics*, *229*(1), 175–179. doi:10.1007/s11207-005-4086-7.

DeLand, M. T., & Cebula, R. P. (2008). Creation of a composite solar ultraviolet irradiance data set. *Journal of Geophysical Research: Space Physics*, *113*(A11), A11103. doi:10.1029/2008JA013401.

DeLand, M. T., Floyd, L. E., Marchenko, S. et al. (2019). Creation of the GSFCSSI2 composite solar spectral irradiance data set. *Earth and Space Science*, *6*(7), 1284–1298. doi:10.1029/2019EA000616.

DeRosa, M. L., Brun, A. S., & Hoeksema, J. T. (2012). Solar magnetic field reversals and the role of dynamo families. *The Astrophysical Journal*, *757*(1), 96. doi:10.1088/0004-637X/757/1/96.

Dewitte, S., Crommelynck, D., & Joukoff, A. (2004). Total solar irradiance observations from DIARAD/VIRGO. *Journal of Geophysical Research: Space Physics*, *109*(A2), A02102. doi:10.1029/2002JA009694.

Dikpati, M., & Charbonneau, P. (1999). A Babcock-Leighton flux transport dynamo with solar-like differential rotation. *The Astrophysical Journal*, *518*(1), 508–520. doi:10.1086/307269.

Dodd, M. S., Papineau, D., Grenne, T. et al. (2017). Evidence for early life in Earth's oldest hydrothermal vent precipitates. *Nature*, *543*(7643), 60–64. doi:10.1038/nature21377.

D'Silva, S., & Choudhuri, A. R. (1993). A theoretical model for tilts of bipolar magnetic regions. *Astronomy and Astrophysics*, *272*, 621–633. URL: https://ui.adsabs.harvard.edu/abs/1993A&A...272..621D/abstract.

Du, Z., & Du, S. (2006). The relationship between the amplitude and descending time of a solar activity cycle. *Solar Physics*, *238*(2), 431–437. doi:10.1007/s11207-006-0175-5.

Dudok de Wit, T. (2022). Detecting undocumented trends in solar irradiance observations. *Journal of Space Weather and Space Climate*, *12*, 10. doi:10.1051/swsc/2021041.

Dudok de Wit, T., Kopp, G., Fröhlich, C. et al. (2017). Methodology to create a new total solar irradiance record: Making a composite out of multiple data records. *Geophysical Research Letters*, *44*(3), 1196–1203. doi:10.1002/2016GL071866.

Dudok de Wit, T., Lefèvre, L., & Clette, F. (2016). Uncertainties in the sunspot numbers: Estimation and implications. *Solar Physics*, *291*(9), 2709–2731. doi:10.1007/s11207-016-0970-6.

Eddy, J. A. (1976). The Maunder Minimum: The reign of Louis XIV appears to have been a time of real anomaly in the behavior of the sun. *Science*, *192*(4245), 1189–1202. doi:10.1126/science.192.4245.1189.

Emslie, A. G., Dennis, B. R., Shih, A. Y. et al. (2012). Global energetics of thirty-eight large solar eruptive events. *The Astrophysical Journal*, *759*(1), 71. doi:10.1088/0004-637X/759/1/71.

Engelbrecht, N. E., Effenberger, F., Florinski, V. et al. (2022). Theory of cosmic ray transport in the heliosphere. *Space Science Reviews*, *218*(4), 33. doi:10.1007/s11214-022-00896-1.

Erdélyi, R., Korsós, M. B., Huang, X. et al. (2022). The Solar Activity Monitor Network – SAMNet. *Journal of Space Weather and Space Climate*, *12*, 2. doi:10.1051/swsc/2021025.

Ermolli, I., Caccin, B., Centrone, M. et al. (2003). Modeling solar irradiance variations through full-disk images and semi-empirical atmospheric models. *Memorie della Societa Astronomica Italiana*, *74*, 603–606. URL: https://ui.adsabs.harvard.edu/abs/2003MmSAI..74..603E.

Ermolli, I., Criscuoli, S., & Giorgi, F. (2011). Recent results from optical synoptic observations of the solar atmosphere with ground-based instruments. *Contributions of the Astronomical Observatory Skalnate Pleso*, *41*(2), 73–84. URL: https://ui.adsabs.harvard.edu/abs/2011CoSka..41...73E.

Ermolli, I., Matthes, K., Dudok de Wit, T. et al. (2013). Recent variability of the solar spectral irradiance and its impact on climate modelling. *Atmospheric Chemistry and Physics*, *13*(8), 3945–3977. doi:10.5194/acp-13-3945-2013.

Espuña Fontcuberta, A., Ghosh, A., Chatterjee, S. et al. (2023). Forecasting solar cycle 25 with physical model-validated recurrent neural networks. *Solar Physics*, *298*(1), 8. doi:10.1007/s11207-022-02104-3.

Feehrer, C. E. (2000). Dances with wolfs: A short history of sunspot indices — aavso. URL: https://www.aavso.org/dances-wolfs-short-history-sunspot-indices.

Feynman, J., & Crooker, N. U. (1978). The solar wind at the turn of the century. *Nature*, *275*(5681), 626–627. doi:10.1038/275626a0.

Fligge, M., Solanki, S. K., & Unruh, Y. C. (2000). Modelling irradiance variations from the surface distribution of the solar magnetic field. *Astronomy and Astrophysics*, *353*, 380–388. URL: https://ui.adsabs.harvard.edu/abs/2000A&A...353..380F/abstract.

Floyd, L., Rottman, G., Deland, M. et al. (2003). 11 years of solar UV irradiance measurements from UARS. In A. Wilson (Ed.), *Solar Variability as an Input to the Earth's Environment* (pp. 195–203). Noordwijk, Netherlands: ESA Publications Division volume 535 of *ESA Special Publication*. URL: https://ui.adsabs.harvard.edu/abs/2003ESASP.535..195F.

Fontenla, J. M., Avrett, E., Thuillier, G. et al. (2006). Semiempirical models of the solar atmosphere. I. The quiet- and active sun photosphere at moderate resolution. *The Astrophysical Journal*, *639*(1), 441–458. doi:10.1086/499345.

Fontenla, J. M., Harder, J., Livingston, W. et al. (2011). High-resolution solar spectral irradiance from extreme ultraviolet to far infrared. *Journal of Geophysical Research: Atmospheres*, *116*(D20), D20108. doi:10.1029/2011JD016032.

Foukal, P. (1993). The curious case of the Greenwich faculae. *Solar Physics*, *148*(2), 219–232. doi:10.1007/BF00645087.

Foukal, P., & Lean, J. (1988). Magnetic modulation of solar luminosity by photospheric activity. *The Astrophysical Journal*, *328*, 347–357. doi:10.1086/166297.

Friedli, T. K. (2016). Sunspot observations of Rudolf Wolf from 1849 – 1893. *Solar Physics*, *291*(9), 2505–2517. doi:10.1007/s11207-016-0907-0.

Fröhlich, C. (2006). Solar irradiance variability since 1978. *Space Science Reviews*, *125*(1), 53–65. doi:10.1007/s11214-006-9046-5.

Fröhlich, C. (2012). Total solar irradiance observations. *Surveys in Geophysics*, *33*(3), 453–473. doi:10.1007/s10712-011-9168-5.

Fröhlich, C. (2013). Solar radiometry. In M. C. E. Huber, A. Pauluhn, J. L. Culhane, J. G. Timothy, K. Wilhelm, & A. Zehnder (Eds.), *Observing Photons in Space: A Guide to Experimental Space Astronomy* ISSI Scientific Report Series (pp. 565–581). New York, NY: Springer. doi:10.1007/978-1-4614-7804-1_32.

Fu, S., Jiang, Y., Airapetian, V. et al. (2019). Effect of star rotation rate on the characteristics of energetic particle events. *The Astrophysical Journal Letters*, *878*(2), L36. doi:10.3847/2041-8213/ab271d.

Georgieva, K., Kilçik, A., Nagovitsyn, Yu. et al. (2017). The ratio between the number of sunspot and the number of sunspot groups. *Geomagnetism and Aeronomy*, *57*(7), 776–782. doi:10.1134/S001679321707009X.

Gilman, P. A. (1983). Dynamically consistent nonlinear dynamos driven by convection in a rotating spherical shell. II - Dynamos with cycles and strong feedbacks. *The Astrophysical Journal Supplement Series*, *53*, 243–268. doi:10.1086/190891.

Gizon, L., Cameron, R. H., Pourabdian, M. et al. (2020). Meridional flow in the Sun's convection zone is a single cell in each hemisphere. *Science*, *368*(6498), 1469–1472. doi:10.1126/science.aaz7119.

Glatzmaier, G. A. (1984). Numerical simulations of stellar convective dynamos. I. The model and method. *Journal of Computational Physics*, *55*(3), 461–484. doi:10.1016/0021-9991(84)90033-0.

Gleissberg, W. (1939). A long-periodic fluctuation of the sun-spot numbers. *The Observatory*, *62*, 158–159. URL: https://ui.adsabs.harvard.edu/abs/1939Obs....62..158G.

Gopalswamy, N. (2018). Extreme solar eruptions and their space weather consequences. In N. Buzulukova (Ed.), *Extreme Events in Geospace* (pp. 37–63). Amsterdam, Netherlands: Elsevier. doi:10.1016/B978-0-12-812700-1.00002-9.

Gosain, S., Roth, M., Hill, F. et al. (2018). Design of a next generation synoptic solar observing network: Solar physics research integrated network group (SPRING). In C. J. Evans, L. Simard, & H. Takami (Eds.), *Ground-Based and Airborne Instrumentation for Astronomy VII* (p. 107024H). Bellingham, WA: SPIE volume 10702 of *SPIE Proceedings*. doi:10.1117/12.2306555.

Green, L. M., Török, T., Vršnak, B. et al. (2018). The origin, early evolution and predictability of solar eruptions. *Space Science Reviews*, *214*(1), 46. doi:10.1007/s11214-017-0462-5.

Gronoff, G., Arras, P., Baraka, S. et al. (2020). Atmospheric escape processes and planetary atmospheric evolution. *Journal of Geophysical Research: Space Physics*, *125*(8), e2019JA027639. doi:10.1029/2019JA027639.

Gruntman, M., Roelof, E. C., Mitchell, D. G. et al. (2001). Energetic neutral atom imaging of the heliospheric boundary region. *Journal of Geophysical Research: Space Physics*, *106*(A8), 15767–15781. doi:10.1029/2000JA000328.

Güdel, M. (2007). The sun in time: Activity and environment. *Living Reviews in Solar Physics*, *4*(1), 3. doi:10.12942/lrsp-2007-3.

Gupta, S., Basak, A., & Nandy, D. (2023). Impact of Changing Stellar and Planetary Magnetic Fields on (Exo)planetary Environments and Atmospheric Mass Loss. *The Astrophysical Journal*, *953*(1), 70. doi:10.3847/1538-4357/acd93b. arXiv:2303.04770.

Gutiérrez, M., Masip, M., & Muñoz, S. (2022). The solar disk at high energies. *The Astrophysical Journal*, *941*(1), 86. doi:10.3847/1538-4357/aca020.

Haberreiter, M., Schöll, M., Dudok de Wit, T. et al. (2017). A new observational solar irradiance composite. *Journal of Geophysical Research: Space Physics*, *122*(6), 5910–5930. doi:10.1002/2016JA023492.

Haigh, J. D. (2007). The Sun and the Earth's climate. *Living Reviews in Solar Physics*, *4*(1), 2. doi:10.12942/lrsp-2007-2.

Hale, S. J., Howe, R., Chaplin, W. J. et al. (2016). Performance of the Birmingham Solar-Oscillations Network (BiSON). *Solar Physics*, *291*(1), 1–28. doi:10.1007/s11207-015-0810-0.

Han, Y. B., & Yin, Z. Q. (2019). A decline phase modeling for the prediction of solar cycle 25. *Solar Physics*, *294*(8), 107. doi:10.1007/s11207-019-1494-7.

Harder, J. W., Fontenla, J. M., Pilewskie, P. et al. (2009). Trends in solar spectral irradiance variability in the visible and infrared. *Geophysical Research Letters*, *36*(7), L07801. doi:10.1029/2008GL036797.

Harra, L., Andretta, V., Appourchaux, T. et al. (2022). A journey of exploration to the polar regions of a star: Probing the solar poles and the heliosphere from high helio-latitude. *Experimental Astronomy*, *54*(2), 157–183. doi:10.1007/s10686-021-09769-x.

Harvey, J. W., Hill, F., Hubbard, R. P. et al. (1996). The Global Oscillation Network Group (GONG) project. *Science*, *272*(5266), 1284–1286. doi:10.1126/science.272.5266.1284.

Harvey, K. L. (1993). *Magnetic Bipoles on the Sun*. Ph.D. thesis Utrecht University. URL: https://ui.adsabs.harvard.edu/abs/1993PhDT.....241H.

Hathaway, D. H. (2015). The solar cycle. *Living Reviews in Solar Physics*, *12*(1), 4. doi:10.1007/lrsp-2015-4.

Hathaway, D. H., & Upton, L. A. (2016). Predicting the amplitude and hemispheric asymmetry of solar cycle 25 with surface flux transport. *Journal of Geophysical Research: Space Physics*, *121*(11), 10744–10753. doi:10.1002/2016JA023190.

Hathaway, D. H., & Wilson, R. M. (2004). What the sunspot record tells us about space climate. *Solar Physics*, *224*(1), 5–19. doi:10.1007/s11207-005-3996-8.

Hayakawa, H., Hattori, K., Sôma, M. et al. (2022). An overview of sunspot observations in 1727–1748. *The Astrophysical Journal*, *941*(2), 151. doi:10.3847/1538-4357/ac6671.

Hayakawa, H., Suzuki, D., Mathieu, S. et al. (2023). Sunspot observations at Kawaguchi Science Museum: 1972 – 2013. *Geoscience Data Journal*, *10*(1), 87–98. doi:10.1002/gdj3.158.

Hazra, G., Choudhuri, A. R., & Miesch, M. S. (2017). A theoretical study of the build-up of the Sun's polar magnetic field by using a 3D kinematic dynamo model. *The Astrophysical Journal*, *835*(1), 39. doi:10.3847/1538-4357/835/1/39.

Hazra, G., Nandy, D., Kitchatinov, L. et al. (2023). Mean Field Models of Flux Transport Dynamo and Meridional Circulation in the Sun and Stars. *Space Science Reviews*, *219*(5), 39. doi:10.1007/s11214-023-00982-y. arXiv:2302.09390.

Hazra, S., & Nandy, D. (2016). A proposed paradigm for solar cycle dynamics mediated via turbulent pumping of magnetic flux in Babcock–Leighton-type solar dynamos. *The Astrophysical Journal*, *832*(1), 9. doi:10.3847/0004-637X/832/1/9.

Hazra, S., & Nandy, D. (2019). The origin of parity changes in the solar cycle. *Monthly Notices of the Royal Astronomical Society*, *489*(3), 4329–4337. doi:10.1093/mnras/stz2476.

Hazra, S., Passos, D., & Nandy, D. (2014). A stochastically forced time delay solar dynamo model: Self-consistent recovery from a Maunder-like grand minimum necessitates a mean-field alpha effect. *The Astrophysical Journal*, *789*(1), 5. doi:10.1088/0004-637X/789/1/5.

Hazra, S., Réville, V., Perri, B. et al. (2021). Modeling solar wind variations over an 11 year cycle with Alfvén wave dissipation: A parameter study. *The Astrophysical Journal*, *910*(2), 90. doi:10.3847/1538-4357/abe12e.

Heerikhuisen, J., Pogorelov, N. V., Florinski, V. et al. (2008). The effects of a $\kappa$-distribution in the heliosheath on the global heliosphere and ENA flux at 1 AU. *The Astrophysical Journal*, *682*(1), 679–689. doi:10.1086/588248.

Hickey, J. R., Stowe, L. L., Jacobowitz, H. et al. (1980). Initial solar irradiance determinations from Nimbus 7 cavity radiometer measurements. *Science*, *208*(4441), 281–283. doi:10.1126/science.208.4441.281.

Hill, F. (2018). The Global Oscillation Network Group facility—An example of research to operations in space weather. *Space Weather*, *16*(10), 1488–1497. doi:10.1029/2018SW002001.

Hiremath, K. M. (2008). Prediction of solar cycle 24 and beyond. *Astrophysics and Space Science*, *314*(1), 45–49. doi:10.1007/s10509-007-9728-9.

Holm, S. (2015). Prudence in estimating coherence between planetary, solar and climate oscillations. *Astrophysics and Space Science*, *357*(2), 106. doi:10.1007/s10509-015-2334-3.

Horstmann, G. M., Mamatsashvili, G., Giesecke, A. et al. (2023). Tidally forced

planetary waves in the tachocline of solar-like stars. *The Astrophysical Journal*, *944*(1), 48. doi:10.3847/1538-4357/aca278.

Hotta, H., Kusano, K., & Shimada, R. (2022). Generation of solar-like differential rotation. *The Astrophysical Journal*, *933*(2), 199. doi:10.3847/1538-4357/ac7395.

Hoyt, D. V., & Schatten, K. H. (1998a). Group sunspot numbers: A new solar activity reconstruction. *Solar Physics*, *179*(1), 189–219. doi:10.1023/A:1005007527816.

Hoyt, D. V., & Schatten, K. H. (1998b). Group sunspot numbers: A new solar activity reconstruction. *Solar Physics*, *181*(2), 491–491. doi:10.1023/A:1005056326158.

Hu, J., Airapetian, V. S., Li, G. et al. (2022). Extreme energetic particle events by superflare-associated CMEs from solar-like stars. *Science Advances*, *8*(12), eabi9743. doi:10.1126/sciadv.abi9743.

Hu, J., Li, G., Ao, X. et al. (2017). Modeling particle acceleration and transport at a 2-D CME-driven shock. *Journal of Geophysical Research: Space Physics*, *122*(11), 10938–10963. doi:10.1002/2017JA024077.

Hu, J., Li, G., Fu, S. et al. (2018). Modeling a single SEP event from multiple vantage points using the iPATH model. *The Astrophysical Journal*, *854*(2), L19. doi:10.3847/2041-8213/aaabc1.

Hudson, H. S., Silva, S., Woodard, M. et al. (1982). The effects of sunspots on solar irradiance. *Solar Physics*, *76*(2), 211–219. doi:10.1007/BF00170984.

Hung, C. P., Brun, A. S., Fournier, A. et al. (2017). Variational estimation of the large-scale time-dependent meridional circulation in the Sun: Proofs of concept with a solar mean field dynamo model. *The Astrophysical Journal*, *849*(2), 160. doi:10.3847/1538-4357/aa91d1.

Iijima, H., Hotta, H., Imada, S. et al. (2017). Improvement of solar-cycle prediction: Plateau of solar axial dipole moment. *Astronomy & Astrophysics*, *607*, L2. doi:10.1051/0004-6361/201731813.

Illarionov, E., & Arlt, R. (2022). Reconstruction of the solar activity from the catalogs of the Zurich Observatory. *Solar Physics*, *297*(7), 79. doi:10.1007/s11207-022-02015-3.

Ishitsuka, J., Asai, A., Morita, S. et al. (2014). Within the international collaboration CHAIN: A summary of events observed with Flare Monitoring Telescope (FMT) in Peru. *Sun and Geosphere*, *9*, 85–96. URL: https://ui.adsabs.harvard.edu/abs/2014SunGe...9...85I.

Izenman, A. J. (1985). J. R. Wolf and the Zürich sunspot relative numbers. *The Mathematical Intelligencer*, *7*(1), 27–33. doi:10.1007/BF03023002.

Javaraiah, J. (2015). Long-term variations in the north–south asymmetry of solar activity and solar cycle prediction, III: Prediction for the amplitude of solar cycle 25. *New Astronomy*, *34*, 54–64. doi:10.1016/j.newast.2014.04.001.

Jha, B. K., Karak, B. B., Mandal, S. et al. (2020). Magnetic field dependence of bipolar magnetic region tilts on the Sun: Indication of tilt quenching. *The Astrophysical Journal Letters*, *889*(1), L19. doi:10.3847/2041-8213/ab665c.

Jiang, J., Cameron, R., Schmitt, D. et al. (2009). Modeling the Sun's open magnetic flux and the heliospheric current sheet. *The Astrophysical Journal*, *709*(1), 301–307. doi:10.1088/0004-637X/709/1/301.

Jiang, J., Hathaway, D. H., Cameron, R. H. et al. (2014). Magnetic flux transport at the solar surface. *Space Science Reviews*, *186*(1), 491–523. doi:10.1007/s11214-014-0083-1.

Jose, P. D. (1965). Sun's motion and sunspots. *The Astronomical Journal*, *70*, 193–200. doi:10.1086/109714.

Jouve, L., & Brun, A. S. (2007). On the role of meridional flows in flux transport dynamo models. *Astronomy & Astrophysics*, *474*(1), 239–250. doi:10.1051/0004-6361:20077070.

Jouve, L., Gastine, T., & Lignières, F. (2015). Three-dimensional evolution of magnetic fields in a differentially rotating stellar radiative zone. *Astronomy & Astrophysics*, *575*, A106. doi:10.1051/0004-6361/201425240.

Jouve, L., Proctor, M. R. E., & Lesur, G. (2010). Buoyancy-induced time delays in Babcock-Leighton flux-transport dynamo models. *Astronomy & Astrophysics*, *519*, A68. doi:10.1051/0004-6361/201014455.

Kakad, B., Kumar, R., & Kakad, A. (2020). Randomness in sunspot number: A clue to predict solar cycle 25. *Solar Physics*, *295*(6), 88. doi:10.1007/s11207-020-01655-7.

Kallenrode, M.-B. (1997). The temporal and spatial development of MeV proton acceleration at interplanetary shocks. *Journal of Geophysical Research: Space Physics*, *102*(A10), 22347–22363. doi:10.1029/97JA01678.

Kane, R. P. (2007). Solar cycle predictions based on extrapolation of spectral components: An update. *Solar Physics*, *246*(2), 487–493. doi:10.1007/s11207-007-9059-6.

Karachik, N. V., Pevtsov, A. A., & Nagovitsyn, Y. A. (2019). The effect of telescope aperture, scattered light and human vision on early measurements of sunspot and group numbers. *Monthly Notices of the Royal Astronomical Society*, *488*(3), 3804–3809. doi:10.1093/mnras/stz1936.

Karak, B. B., & Choudhuri, A. R. (2013). Studies of grand minima in sunspot cycles by using a flux transport solar dynamo model. *Research in Astronomy and Astrophysics*, *13*(11), 1339–1357. doi:10.1088/1674-4527/13/11/005.

Kazachenko, M. D., Lynch, B. J., Welsch, B. T. et al. (2017). A database of flare ribbon properties from the Solar Dynamics Observatory. I. Reconnection flux. *The Astrophysical Journal*, *845*(1), 49. doi:10.3847/1538-4357/aa7ed6.

Knobloch, E., Tobias, S. M., & Weiss, N. O. (1998). Modulation and symmetry changes in stellar dynamos. *Monthly Notices of the Royal Astronomical Society*, *297*(4), 1123–1138. doi:10.1046/j.1365-8711.1998.01572.x.

Kochukhov, O., Hackman, T., Lehtinen, J. J. et al. (2020). Hidden magnetic fields of young suns. *Astronomy & Astrophysics*, *635*, A142. doi:10.1051/0004-6361/201937185.

Koldobskiy, S., Mekhaldi, F., Kovaltsov, G. et al. (2023). Multiproxy reconstructions of integral energy spectra for extreme solar particle events of 7176 BCE, 660 BCE, 775 CE, and 994 CE. *Journal of Geophysical Research: Space Physics*, *128*(3), e2022JA031186. doi:10.1029/2022JA031186.

Kopp, G. (2016). Magnitudes and timescales of total solar irradiance variability. *Journal of Space Weather and Space Climate*, *6*, A30. doi:10.1051/swsc/2016025.

Kopp, G., Krivova, N., Wu, C. J. et al. (2016). The impact of the revised sunspot record on solar irradiance reconstructions. *Solar Physics*, *291*(9), 2951–2965. doi:10.1007/s11207-016-0853-x.

Kopp, G., Lawrence, G., & Rottman, G. (2005). The total irradiance monitor (TIM): Science results. *Solar Physics*, *230*(1), 129–139. doi:10.1007/s11207-005-7433-9.

Kóta, J. (2000). Diffusion of energetic particles in focusing fields. *Journal of Geophysical Research: Space Physics*, *105*(A2), 2403–2411. doi:10.1029/1999JA900469.

Krivova, N. A., Solanki, S. K., Fligge, M. et al. (2003). Reconstruction of solar irradiance variations in cycle 23: Is solar surface magnetism the cause? *Astronomy & Astrophysics*, *399*(1), L1–L4. doi:10.1051/0004-6361:20030029.

Krivova, N. A., Solanki, S. K., & Floyd, L. (2006). Reconstruction of solar UV irradiance in cycle 23. *Astronomy & Astrophysics*, *452*(2), 631–639. doi:10.1051/0004-6361:20064809.

Krivova, N. A., Solanki, S. K., Hofer, B. et al. (2021). Modelling the evolution of the Sun's open and total magnetic flux. *Astronomy & Astrophysics*, *650*, A70. doi:10.1051/0004-6361/202140504.

Krymsky, G. F. (1977). A regular mechanism for the acceleration of charged particles on the front of a shock wave. *Akademiia Nauk SSSR Doklady (Reports of the Academy of Sciences of the USSR)*, *234*, 1306–1308.

Küker, M., Arlt, R., & Rüdiger, G. (1999). The Maunder minimum as due to magnetic lambda -quenching. *Astronomy and Astrophysics*, *343*, 977–982. URL: https://ui.adsabs.harvard.edu/abs/1999A&A...343..977K/abstract.

Kumar, R., Jouve, L., & Nandy, D. (2019). A 3D kinematic Babcock Leighton solar dynamo model sustained by dynamic magnetic buoyancy and flux transport processes. *Astronomy & Astrophysics*, *623*, A54. doi:10.1051/0004-6361/201834705.

Labonville, F., Charbonneau, P., & Lemerle, A. (2019). A dynamo-based forecast of solar cycle 25. *Solar Physics*, *294*(6), 82. doi:10.1007/s11207-019-1480-0.

Lammer, H. (2013). *Origin and Evolution of Planetary Atmospheres: Implications for Habitability*. SpringerBriefs in Astronomy. Berlin, Germany: Springer. doi:10.1007/978-3-642-32087-3.

Lee, M. A., & Ryan, J. M. (1986). Time-dependent coronal shock acceleration of energetic solar flare particles. *The Astrophysical Journal*, *303*, 829–842. doi:10.1086/164131.

Lee III, R. B., Gibson, M. A., Wilson, R. S. et al. (1995). Long-term total solar irradiance variability during sunspot cycle 22. *Journal of Geophysical Research: Space Physics*, *100*(A2), 1667–1675. doi:10.1029/94JA02897.

Leighton, R. B. (1969). A magneto-kinematic model of the solar cycle. *The Astrophysical Journal*, *156*, 1–26. doi:10.1086/149943.

Lemerle, A., & Charbonneau, P. (2017). A coupled 2 × 2D Babcock–Leighton solar dynamo model. II. Reference dynamo solutions. *The Astrophysical Journal*, *834*(2), 133. doi:10.3847/1538-4357/834/2/133.

Li, F. Y., Kong, D. F., Xie, J. L. et al. (2018). Solar cycle characteristics and their application in the prediction of cycle 25. *Journal of Atmospheric and Solar-Terrestrial Physics*, *181*, 110–115. doi:10.1016/j.jastp.2018.10.014.

Li, G., Zank, G. P., & Rice, W. K. M. (2003). Energetic particle acceleration and transport at coronal mass ejection–driven shocks. *Journal of Geophysical Research: Space Physics*, *108*(A2), SSH 10. doi:10.1029/2002JA009666.

Li, G., Zank, G. P., & Rice, W. K. M. (2005). Acceleration and transport of heavy ions at coronal mass ejection-driven shocks. *Journal of Geophysical Research: Space Physics*, *110*(A6), A06104. doi:10.1029/2004JA010600.

Li, K. J., Feng, W., & Li, F. Y. (2015). Predicting the maximum amplitude of solar cycle 25 and its timing. *Journal of Atmospheric and Solar-Terrestrial Physics*, *135*, 72–76. doi:10.1016/j.jastp.2015.09.010.

Linden, T., Beacom, J. F., Peter, A. H. G. et al. (2022). First observations of solar disk gamma rays over a full solar cycle. *Physical Review D*, *105*(6), 063013. doi:10.1103/PhysRevD.105.063013.

Linker, J. A., Caplan, R. M., Downs, C. et al. (2017). The open flux problem. *The Astrophysical Journal*, *848*(1), 70. doi:10.3847/1538-4357/aa8a70.

Linsky, J. L., Wood, B. E., Youngblood, A. et al. (2020). The relative emission from chromospheres and coronae: Dependence on spectral type and age*. *The Astrophysical Journal*, *902*(1), 3. doi:10.3847/1538-4357/abb36f.

Lockwood, M., & Owens, M. J. (2011). Centennial changes in the heliospheric magnetic field and open solar flux: The consensus view from geomagnetic data and cosmogenic isotopes and its implications. *Journal of Geophysical Research: Space Physics*, *116*(A4), A04109. doi:10.1029/2010JA016220.

Lockwood, M., Owens, M. J., & Barnard, L. (2014). Centennial variations in sunspot number, open solar flux, and streamer belt width: 2. Comparison with the geomagnetic data. *Journal of Geophysical Research: Space Physics*, *119*(7), 5183–5192. doi:10.1002/2014JA019972.

Lockwood, M., Owens, M. J., Barnard, L. et al. (2016a). Tests of sunspot number sequences: 2. Using geomagnetic and auroral data. *Solar Physics*, *291*(9), 2811–2828. doi:10.1007/s11207-016-0913-2.

Lockwood, M., Scott, C. J., Owens, M. J. et al. (2016b). Tests of sunspot number sequences: 1. Using ionosonde data. *Solar Physics*, *291*(9), 2785–2809. doi:10.1007/s11207-016-0855-8.

Lopes, I., Passos, D., Nagy, M. et al. (2014). Oscillator models of the solar cycle. *Space Science Reviews*, *186*(1), 535–559. doi:10.1007/s11214-014-0066-2.

Lorenzo-Oliveira, D., Freitas, F. C., Meléndez, J. et al. (2018). The solar twin planet search - the age-chromospheric activity relation. *Astronomy & Astrophysics*, *619*, A73. doi:10.1051/0004-6361/201629294.

Luhmann, J. G., Ledvina, S. A., Krauss-Varban, D. et al. (2007). A heliospheric simulation-based approach to SEP source and transport modeling. *Advances in Space Research*, *40*(3), 295–303. doi:10.1016/j.asr.2007.03.089.

Luhmann, J. G., Ledvina, S. A., Odstrcil, D. et al. (2010). Cone model-based SEP event calculations for applications to multipoint observations. *Advances in Space Research*, *46*(1), 1–21. doi:10.1016/j.asr.2010.03.011.

Maehara, H., Shibayama, T., Notsu, S. et al. (2012). Superflares on solar-type stars. *Nature*, *485*(7399), 478–481. doi:10.1038/nature11063.

Marubashi, K. (1997). Interplanetary magnetic flux ropes and solar filaments. In N. Crooker, J. A. Joselyn, & J. Feynman (Eds.), *Coronal Mass Ejections* (pp. 147–156). Washington, D.C.: American Geophysical Union (AGU) volume 99 of *Geophysical Monograph Series*. doi:10.1029/GM099p0147.

Matt, S. P., Brun, A. S., Baraffe, I. et al. (2015). The mass-dependence of angular momentum evolution in Sun-like stars. *The Astrophysical Journal Letters*, *799*(2), L23. doi:10.1088/2041-8205/799/2/L23.

McComas, D. J., Allegrini, F., Bochsler, P. et al. (2009). IBEX—Interstellar Boundary Explorer. *Space Science Reviews*, *146*(1), 11–33. doi:10.1007/s11214-009-9499-4.

McComas, D. J., Bzowski, M., Dayeh, M. A. et al. (2020). Solar cycle of imaging the global heliosphere: Interstellar Boundary EXplorer (IBEX) observations from 2009–2019. *The Astrophysical Journal Supplement Series*, *248*(2), 26. doi:10.3847/1538-4365/ab8dc2.

McComas, D. J., Ebert, R. W., Elliott, H. A. et al. (2008). Weaker solar wind from the polar coronal holes and the whole Sun. *Geophysical Research Letters*, *35*(18), L18103. doi:10.1029/2008GL034896.

McComas, D. J., Elliott, H. A., Schwadron, N. A. et al. (2003). The three-dimensional solar wind around solar maximum. *Geophysical Research Letters*, *30*(10), 24. doi:10.1029/2003GL017136.

Mekhaldi, F., Muscheler, R., Adolphi, F. et al. (2015). Multiradionuclide evidence for the solar origin of the cosmic-ray events of AD 774/5 and 993/4. *Nature Communications*, *6*(1), 8611. doi:10.1038/ncomms9611.

Miesch, M. S., & Teweldebirhan, K. (2016). A three-dimensional Babcock–Leighton solar dynamo model: Initial results with axisymmetric flows. *Advances in Space Research*, *58*(8), 1571–1588. doi:10.1016/j.asr.2016.02.018.

Mininni, P. D., Gómez, D. O., & Mindlin, G. B. (2000). Stochastic relaxation oscillator model for the solar cycle. *Physical Review Letters*, *85*(25), 5476–5479. doi:10.1103/PhysRevLett.85.5476.

Miyahara, H., Kitazawa, K., Nagaya, K. et al. (2010). Is the Sun heading for another Maunder minimum? - Precursors of the grand solar minima. *Journal of Cosmology*, *8*, 1970–1982. URL: https://ui.adsabs.harvard.edu/abs/2010JCos....8.1970M.

Miyake, F., Masuda, K., & Nakamura, T. (2013). Another rapid event in the carbon-14 content of tree rings. *Nature Communications*, *4*(1), 1748. doi:10.1038/ncomms2783.

Miyake, F., Nagaya, K., Masuda, K. et al. (2012). A signature of cosmic-ray increase in ad 774–775 from tree rings in Japan. *Nature*, *486*(7402), 240–242. doi:10.1038/nature11123.

Miyake, F., Usoskin, I., & Poluianov, S. (Eds.) (2019). *Extreme Solar Particle Storms: The Hostile Sun*. 2514-3433. Bristol, UK: IOP Publishing. doi:10.1088/2514-3433/ab404a.

Moffatt, H. K. (1978). *Magnetic Field Generation in Electrically Conducting Fluids*. Cambridge Monographs on Mechanics and Applied Mathematics. Cambrige, UK: University Press. URL: https://ui.adsabs.harvard.edu/abs/1978mfge.book.....M.

Montillet, J.-P., Finsterle, W., Kermarrec, G. et al. (2022). Data fusion of total solar irradiance composite time series using 41 years of satellite measurements. *Journal of Geophysical Research: Atmospheres*, *127*(13), e2021JD036146. doi:10.1029/2021JD036146.

Muñoz-Jaramillo, A., Dasi-Espuig, M., Balmaceda, L. A. et al. (2013). Solar cycle propagation, memory, and prediction: Insights from a century of magnetic proxies. *The Astrophysical Journal Letters*, *767*(2), L25. doi:10.1088/2041-8205/767/2/L25.

Muñoz-Jaramillo, A., Nandy, D., & Martens, P. C. H. (2010). Magnetic quenching of turbulent diffusivity: Reconciling mixing-length theory estimates with kinematic dynamo models of the solar cycle. *The Astrophysical Journal Letters*, *727*(1), L23. doi:10.1088/2041-8205/727/1/L23.

Muñoz-Jaramillo, A., & Vaquero, J. M. (2019). Visualization of the challenges and limitations of the long-term sunspot number record. *Nature Astronomy*, *3*(3), 205–211. doi:10.1038/s41550-018-0638-2.

Müller, D., Cyr, O. C. S., Zouganelis, I. et al. (2020). The Solar Orbiter mission - Science overview. *Astronomy & Astrophysics*, *642*, A1. doi:10.1051/0004-6361/202038467.

Mursula, K., Manoharan, P., Nandy, D. et al. (2013). Long-term solar activity and its implications to the heliosphere, geomagnetic activity, and the Earth's climate - Preface to the Special Issue on Space Climate. *Journal of Space Weather and Space Climate*, *3*, A21. doi:10.1051/swsc/2013043.

Nagovitsyn, Y. A., & Georgieva, K. (2017). Versions of time series for classical solar indices and an adequate description of solar activity. *Geomagnetism and Aeronomy*, *57*(7), 783–787. doi:10.1134/S0016793217070131.

Nagovitsyn, Y. A., & Osipova, A. A. (2021). Average annual total sunspot area in the last 410 yr: The most probable values and limits of their uncertainties. *Monthly Notices of the Royal Astronomical Society*, *505*(1), 1206–1212. doi:10.1093/mnras/stab1328.

Nagovitsyn, Y. A., & Pevtsov, A. A. (2020). Duffing oscillator model of solar cycles. *The Astrophysical Journal Letters*, *888*(2), L26. doi:10.3847/2041-8213/ab6335.

Nagy, M., Lemerle, A., Labonville, F. et al. (2017). The effect of "rogue" active regions on the solar cycle. *Solar Physics*, *292*(11), 167. doi:10.1007/s11207-017-1194-0.

Namekata, K., Maehara, H., Honda, S. et al. (2022). Probable detection of an eruptive filament from a superflare on a solar-type star. *Nature Astronomy*, *6*(2), 241–248. doi:10.1038/s41550-021-01532-8.

Nandy, D. (2002). Constraints on the solar internal magnetic field from a buoyancy driven solar dynamo. *Astrophysics and Space Science*, *282*(1), 209–219. doi:10.1023/A:1021632522168.

Nandy, D. (2004). Exploring magnetic activity from the Sun to the stars. *Solar*

*Physics*, *224*(1), 161–169. doi:10.1007/s11207-005-4990-x.

Nandy, D. (2021). Progress in solar cycle predictions: Sunspot cycles 24–25 in perspective. *Solar Physics*, *296*(3), 54. doi:10.1007/s11207-021-01797-2.

Nandy, D., & Choudhuri, A. R. (2002). Explaining the latitudinal distribution of sunspots with deep meridional flow. *Science*, *296*(5573), 1671–1673. doi:10.1126/science.1070955.

Nandy, D., & Martens, P. C. H. (2007). Space Climate and the Solar–Stellar connection: What can we learn from the stars about long-term solar variability? *Advances in Space Research*, *40*(7), 891–898. doi:10.1016/j.asr.2007.01.079.

Nandy, D., Martens, P. C. H., Obridko, V. et al. (2021). Solar evolution and extrema: Current state of understanding of long-term solar variability and its planetary impacts. *Progress in Earth and Planetary Science*, *8*(1), 40. doi:10.1186/s40645-021-00430-x.

Nataf, H.-C. (2022). Tidally synchronized solar dynamo: A rebuttal. *Solar Physics*, *297*(8), 107. doi:10.1007/s11207-022-02038-w.

Nataf, H.-C. (2023). Response to comment on "Tidally synchronized solar dynamo: A rebuttal". *Solar Physics*, *298*(3), 33. doi:10.1007/s11207-023-02128-3.

National Academies of Sciences, Engineering, and Medicine (2021). *Pathways to Discovery in Astronomy and Astrophysics for the 2020s*. Washington, D.C.: National Academies Press. doi:10.17226/26141.

Neidig, D., Wiborg, P., Confer, M. et al. (1998). The USAF Improved Solar Observing Optical Network (ISOON) and its impact on solar synoptic data bases. In K. S. Balasubramaniam, J. Harvey, & D. Rabin (Eds.), *Synoptic Solar Physics* (pp. 519–528). San Francisco: Astronomical Society of the Pacific volume 140 of *Astronomical Society of the Pacific Conference Series*. URL: https://ui.adsabs.harvard.edu/abs/1998ASPC..140..519N.

Nèmec, N.-E., Shapiro, A. I., Işık, E. et al. (2022). Faculae cancel out on the surfaces of active suns. *The Astrophysical Journal Letters*, *934*(2), L23. doi:10.3847/2041-8213/ac8155.

Ng, C. K., Reames, D. V., & Tylka, A. J. (2003). Modeling shock-accelerated solar energetic particles coupled to interplanetary Alfvén waves. *The Astrophysical Journal*, *591*(1), 461–485. doi:10.1086/375293.

Notsu, Y., Maehara, H., Honda, S. et al. (2019). Do *Kepler* Superflare Stars Really Include Slowly Rotating Sun-like Stars?—Results Using APO 3.5 m Telescope Spectroscopic Observations and *Gaia* -DR2 Data. *The Astrophysical Journal*, *876*(1), 58. doi:10.3847/1538-4357/ab14e6.

Obridko, V. N., & Vaisberg, O. L. (2017). On the history of the solar wind discovery. *Solar System Research*, *51*(2), 165–169. doi:10.1134/S0038094617020058.

Okamoto, S., Notsu, Y., Maehara, H. et al. (2021). Statistical properties of superflares on solar-type stars: Results using all of the Kepler primary mission data. *The Astrophysical Journal*, *906*(2), 72. doi:10.3847/1538-4357/abc8f5.

Okhlopkov, V. P. (2016). The gravitational influence of Venus, the Earth, and Jupiter on the 11-year cycle of solar activity. *Moscow University Physics Bulletin*, *71*(4), 440–446. doi:10.3103/S0027134916040159.

Okoh, D. I., Seemala, G. K., Rabiu, A. B. et al. (2018). A hybrid regression-neural network (HR-NN) method for forecasting the solar activity. *Space Weather*, *16*(9), 1424–1436. doi:10.1029/2018SW001907.

Ossendrijver, M. (2003). The solar dynamo. *The Astronomy and Astrophysics Review*, *11*(4), 287–367. doi:10.1007/s00159-003-0019-3.

Owens, B. (2013). Long-term research: Slow science. *Nature*, *495*(7441), 300–303. doi:10.1038/495300a.

Owens, M. J., Arge, C. N., Crooker, N. U. et al. (2008). Estimating total heliospheric magnetic flux from single-point in situ measurements. *Journal of Geophysical Research: Space Physics*, *113*(A12), A12103. doi:10.1029/2008JA013677.

Owens, M. J., Cliver, E., McCracken, K. G. et al. (2016). Near-Earth heliospheric magnetic field intensity since 1750: 1. Sunspot and geomagnetic reconstructions. *Journal of Geophysical Research: Space Physics*, *121*(7), 6048–6063. doi:10.1002/2016JA022529.

Owens, M. J., & Lockwood, M. (2012). Cyclic loss of open solar flux since 1868: The link to heliospheric current sheet tilt and implications for the Maunder Minimum. *Journal of Geophysical Research: Space Physics*, *117*(A4), A04102. doi:10.1029/2011JA017193.

Owens, M. J., Lockwood, M., Riley, P. et al. (2018). Long-term variations in the heliosphere. *Proceedings of the International Astronomical Union*, *13*(S340), 108–114. doi:10.1017/S1743921318000972.

Owens, M. J., Usoskin, I., & Lockwood, M. (2012). Heliospheric modulation of galactic cosmic rays during grand solar minima: Past and future variations. *Geophysical Research Letters*, *39*(19), L19102. doi:10.1029/2012GL053151.

Paleari, C. I., Mekhaldi, F., Adolphi, F. et al. (2022). Cosmogenic radionuclides reveal an extreme solar particle storm near a solar minimum 9125 years BP. *Nature Communications*, *13*(1), 214. doi:10.1038/s41467-021-27891-4.

Parker, E. N. (1955). Hydromagnetic dynamo models. *The Astrophysical Journal*, *122*, 293–314. doi:10.1086/146087.

Passos, D., Nandy, D., Hazra, S. et al. (2014). A solar dynamo model driven by mean-field alpha and Babcock-Leighton sources: Fluctuations, grand-minima-maxima, and hemispheric asymmetry in sunspot cycles. *Astronomy & Astrophysics*, *563*, A18. doi:10.1051/0004-6361/201322635.

Penza, V., Caccin, B., Ermolli, I. et al. (2003). Modeling solar irradiance variations through PSPT images and semiempirical models. In A. Wilson (Ed.), *Solar Variability as an Input to the Earth's Environment* (pp. 299–302). Noordwijk, Netherlands: ESA Publications Division volume 535 of *ESA Special Publication*. URL: https://ui.adsabs.harvard.edu/abs/2003ESASP.535..299P.

Peristykh, A. N., & Damon, P. E. (2003). Persistence of the Gleissberg 88-year solar cycle over the last ~12,000 years: Evidence from cosmogenic isotopes. *Journal of Geophysical Research: Space Physics*, *108*(A1), SSH 1. doi:10.1029/2002JA009390.

Perri, B., Brun, A. S., Réville, V. et al. (2018). Simulations of solar wind variations during an 11-year cycle and the influence of north–south asymmetry. *Journal of Plasma Physics*, *84*(5), 765840501. doi:10.1017/S0022377818000880.

Perri, B., Brun, A. S., Strugarek, A. et al. (2020). Impact of solar magnetic field amplitude and geometry on cosmic rays diffusion coefficients in the inner heliosphere. *Journal of Space Weather and Space Climate*, *10*, 55. doi:10.1051/swsc/2020057.

Pevtsov, A., Griffin, E., Grindlay, J. et al. (2019). Historical astronomical data: Urgent need for preservation, digitization enabling scientific exploration. doi:10.48550/arXiv.1903.04839 White paper submitted to ASTRO2020 Decadal Survey.

Pevtsov, A. A. (2016). The need for synoptic solar observations from the ground. In I. Dorotovic, C. Fischer, & M. Temmer (Eds.), *Coimbra Solar Physics Meeting: Ground-based Solar Observations in the Space Instrumentation Era* (pp. 71–85). San Francisco: Astronomical Society of the Pacific volume 504 of *ASP Conf. Ser.*. URL: https://ui.adsabs.harvard.edu/abs/2016ASPC..504...71P.

Pevtsov, A. A., Bertello, L., Tlatov, A. G. et al. (2014). Cyclic and long-term variation of sunspot magnetic fields. *Solar Physics*, *289*(2), 593–602. doi:10.1007/s11207-012-0220-5.

Pevtsov, A. A., & Clette, F. (2017). To understand future solar activity, one has to know the past. *Eos*, *98*. doi:10.1029/2017EO083277.

Pevtsov, A. A., Martinez-Pillet, V., Gilbert, H. et al. (2022). Helio2024 science white paper: ngGONG – Future ground-based facilities for research in heliophysics and space weather operational forecast. doi:10.48550/arXiv.2211.06712 White paper submitted to Decadal Survey for Solar and Space Physics (Heliophysics) 2024-2033.

Pinto, R. F., Brun, A. S., Jouve, L. et al. (2011). Coupling the solar dynamo and the corona: Wind properties, mass, and momentum losses during an activity cycle. *The Astrophysical Journal*, *737*(2), 72. doi:10.1088/0004-637X/737/2/72.

Pishkalo, M. I. (2008). Preliminary prediction of solar cycles 24 and 25 based on the correlation between cycle parameters. *Kinematics and Physics of Celestial Bodies*, *24*(5), 242–247. doi:10.3103/S0884591308050036.

Poluianov, S., & Usoskin, I. (2014). Critical analysis of a hypothesis of the planetary tidal influence on solar activity. *Solar Physics*, *289*(6), 2333–2342. doi:10.1007/s11207-014-0475-0.

Poluianov, S. V., Usoskin, I. G., Mishev, A. L. et al. (2017). GLE and sub-GLE redefinition in the light of high-altitude polar neutron monitors. *Solar Physics*, *292*(11), 176. doi:10.1007/s11207-017-1202-4.

Preminger, D. G., Walton, S. R., & Chapman, G. A. (2002). Photometric quantities for solar irradiance modeling. *Journal of Geophysical Research: Space Physics*, *107*(A11), 1354. doi:10.1029/2001JA009169.

Quassim, M. S., Attia, A.-F., & Elminir, H. K. (2007). Forecasting the peak amplitude of the 24th and 25th sunspot cycles and accompanying

geomagnetic activity. *Solar Physics*, *243*(2), 253–258. doi:10.1007/s11207-007-0447-8.

Rajaguru, S. P., & Antia, H. M. (2015). Meridional circulation in the solar convection zone: Time–distance helioseismic inferences from four years of hmi/sdo observations. *The Astrophysical Journal*, *813*(2), 114. doi:10.1088/0004-637X/813/2/114.

Rankin, J. S., Bindi, V., Bykov, A. M. et al. (2022). Galactic cosmic rays throughout the heliosphere and in the very local interstellar medium. *Space Science Reviews*, *218*(5), 42. doi:10.1007/s11214-022-00912-4.

Raynaud, R., & Tobias, S. M. (2016). Convective dynamo action in a spherical shell: Symmetries and modulation. *Journal of Fluid Mechanics*, *799*, R6. doi:10.1017/jfm.2016.407.

Reames, D. V. (1990). Energetic particles from impulsive solar flares. *The Astrophysical Journal Supplement Series*, *73*, 235–251. doi:10.1086/191456.

Reames, D. V., & Ng, C. K. (1998). Streaming-limited intensities of solar energetic particles. *The Astrophysical Journal*, *504*(2), 1002–1005. doi:10.1086/306124.

Reames, D. V., & Ng, C. K. (2010). Streaming-limited intensities of solar energetic particles on the intensity plateau. *The Astrophysical Journal*, *723*(2), 1286–1293. doi:10.1088/0004-637X/723/2/1286.

Reiners, A., Shulyak, D., Käpylä, P. J. et al. (2022). Magnetism, rotation, and nonthermal emission in cool stars - Average magnetic field measurements in 292 M dwarfs. *Astronomy & Astrophysics*, *662*, A41. doi:10.1051/0004-6361/202243251.

Reinhold, T., Shapiro, A. I., Solanki, S. K. et al. (2022). Measuring periods in aperiodic light curves—Applying the GPS method to infer the rotation periods of solar-like stars. *The Astrophysical Journal Letters*, *938*(1), L1. doi:10.3847/2041-8213/ac937a.

Reinhold, T., Shapiro, A. I., Solanki, S. K. et al. (2020). The Sun is less active than other solar-like stars. *Science*, *368*(6490), 518–521. doi:10.1126/science.aay3821.

Reisenfeld, D. B., Bzowski, M., Funsten, H. O. et al. (2021). A three-dimensional map of the heliosphere from IBEX. *The Astrophysical Journal Supplement Series*, *254*(2), 40. doi:10.3847/1538-4365/abf658.

Réville, V., & Brun, A. S. (2017). Global solar magnetic field organization in the outer corona: Influence on the solar wind speed and mass flux over the cycle. *The Astrophysical Journal*, *850*(1), 45. doi:10.3847/1538-4357/aa9218.

Réville, V., Brun, A. S., Matt, S. P. et al. (2015). The effect of magnetic topology on thermally driven wind: Toward a general formulation of the braking law. *The Astrophysical Journal*, *798*(2), 116. doi:10.1088/0004-637X/798/2/116.

Ribas, I. (2009). The Sun and stars as the primary energy input in planetary atmospheres. *Proceedings of the International Astronomical Union*, *5*(S264), 3–18. doi:10.1017/S1743921309992298.

Rigozo, N. R., Souza Echer, M. P., Evangelista, H. et al. (2011). Prediction of sunspot number amplitude and solar cycle length for cycles 24 and 25. *Journal of Atmospheric and Solar-Terrestrial Physics*, *73*(11), 1294–1299. doi:10.1016/j.jastp.2010.09.005.

Ringnes, T. S., & Jensen, E. (1960). On the relation between magnetic fields and areas of sunspots in the interval 1917-56. *Astrophysica Norvegica*, *7*(4), 99–121. URL: https://ui.adsabs.harvard.edu/abs/1960ApNr....7..99R.

Roberts, P. H. (1972). Kinematic dynamo models. *Philosophical Transactions of the Royal Society of London Series A*, *272*, 663–698. doi:10.1098/rsta.1972.0074.

Saha, C., Chandra, S., & Nandy, D. (2022). Evidence of persistence of weak magnetic cycles driven by meridional plasma flows during solar grand minima phases. *Monthly Notices of the Royal Astronomical Society: Letters*, *517*(1), L36–L40. doi:10.1093/mnrasl/slac104.

Sanz-Forcada, J., Micela, G., Ribas, I. et al. (2011). Estimation of the XUV radiation onto close planets and their evaporation. *Astronomy & Astrophysics*, *532*, A6. doi:10.1051/0004-6361/201116594.

Sanz-Forcada, J., Stelzer, B., Coffaro, M. et al. (2019). Multi-wavelength variability of the young solar analog $\iota$ Horologii - X-ray cycle, star spots, flares and UV emission. *Astronomy & Astrophysics*, *631*, A45. doi:10.1051/0004-6361/201935703.

Saur, J., Grambusch, T., Duling, S. et al. (2013). Magnetic energy fluxes in sub-Alfvénic planet star and moon planet interactions. *Astronomy & Astrophysics*, *552*, A119. doi:10.1051/0004-6361/201118179.

Scafetta, N. (2012). Does the Sun work as a nuclear fusion amplifier of planetary tidal forcing? A proposal for a physical mechanism based on the mass-luminosity relation. *Journal of Atmospheric and Solar-Terrestrial Physics*, *81–82*, 27–40. doi:10.1016/j.jastp.2012.04.002.

Scafetta, N., Willson, R. C., Lee, J. N. et al. (2019). Modeling quiet solar luminosity variability from TSI satellite measurements and proxy models during 1980–2018. *Remote Sensing*, *11*(21), 2569. doi:10.3390/rs11212569.

Schmieder, B. (2018). Extreme solar storms based on solar magnetic field. *Journal of Atmospheric and Solar-Terrestrial Physics*, *180*, 46–51. doi:10.1016/j.jastp.2017.07.018.

Schmutz, W. K. (2021). Changes in the total solar irradiance and climatic effects. *Journal of Space Weather and Space Climate*, *11*, 40. doi:10.1051/swsc/2021016.

Schrijver, C. J., Kauristie, K., Aylward, A. D. et al. (2015). Understanding space weather to shield society: A global road map for 2015–2025 commissioned by COSPAR and ILWS. *Advances in Space Research*, *55*(12), 2745–2807. doi:10.1016/j.asr.2015.03.023.

See, V., Matt, S. P., Folsom, C. P. et al. (2019). Estimating magnetic filling factors from Zeeman–Doppler magnetograms. *The Astrophysical Journal*, *876*(2), 118. doi:10.3847/1538-4357/ab1096.

Shapiro, A. I., Solanki, S. K., Krivova, N. A. et al. (2017). The nature of solar brightness variations. *Nature Astronomy*, *1*(9), 612–616. doi:10.1038/s41550-017-0217-y.

Shapiro, A. I., Solanki, S. K., Krivova, N. A. et al. (2014). Variability of Sun-like stars: Reproducing observed photometric trends. *Astronomy & Astrophysics*, *569*, A38. doi:10.1051/0004-6361/201323086.

Shibayama, T., Maehara, H., Notsu, S. et al. (2013). Superflares on solar-type stars observed with Kepler. iI. statistical properties of superflares. *The Astrophysical Journal Supplement Series*, *209*(1), 5. doi:10.1088/0067-0049/209/1/5.

Singh, A. K., & Bhargawa, A. (2017). An early prediction of 25th solar cycle using Hurst exponent. *Astrophysics and Space Science*, *362*(11), 199. doi:10.1007/s10509-017-3180-2.

Smith, E. J., & Balogh, A. (1995). Ulysses observations of the radial magnetic field. *Geophysical Research Letters*, *22*(23), 3317–3320. doi:10.1029/95GL02826.

Snodgrass, H. B., & Howard, R. (1985). Torsional oscillations of the Sun. *Science*, *228*(4702), 945–952. doi:10.1126/science.228.4702.945.

Sokół, J. M., Bzowski, M., Tokumaru, M. et al. (2013). Heliolatitude and time variations of solar wind structure from in situ measurements and interplanetary scintillation observations. *Solar Physics*, *285*(1), 167–200. doi:10.1007/s11207-012-9993-9.

Sokół, J. M., Dayeh, M. A., Fuselier, S. A. et al. (2021). Breathing of the heliosphere. *The Astrophysical Journal*, *922*(2), 250. doi:10.3847/1538-4357/ac21cd.

Solanki, S. K., Krivova, N. A., & Haigh, J. D. (2013). Solar irradiance variability and climate. *Annual Review of Astronomy and Astrophysics*, *51*(1), 311–351. doi:10.1146/annurev-astro-082812-141007.

Solanki, S. K., Schüssler, M., & Fligge, M. (2000). Evolution of the Sun's large-scale magnetic field since the Maunder minimum. *Nature*, *408*(6811), 445–447. doi:10.1038/35044027.

Solanki, S. K., Usoskin, I. G., Kromer, B. et al. (2004). Unusual activity of the Sun during recent decades compared to the previous 11,000 years. *Nature*, *431*(7012), 1084–1087. doi:10.1038/nature02995.

Spruit, H. C. (2002). Dynamo action by differential rotation in a stably stratified stellar interior. *Astronomy & Astrophysics*, *381*(3), 923–932. doi:10.1051/0004-6361:20011465.

Stefani, F., Giesecke, A., Weber, N. et al. (2016). Synchronized helicity oscillations: A link between planetary tides and the solar cycle? *Solar Physics*, *291*(8), 2197–2212. doi:10.1007/s11207-016-0968-0.

Stefani, F., Giesecke, A., & Weier, T. (2019). A model of a tidally synchronized solar dynamo. *Solar Physics*, *294*(5), 60. doi:10.1007/s11207-019-1447-1.

Stefani, F., Stepanov, R., & Weier, T. (2021). Shaken and stirred: When Bond meets Suess–de Vries and Gnevyshev–Ohl. *Solar Physics*, *296*(6), 88. doi:10.1007/s11207-021-01822-4.

Steinegger, M., Denker, C., Goode, P. R. et al. (2000). The new Global High-resolution H$\alpha$ Network: First observations and first results. In A. Wilson (Ed.), *Proceedings of the 1st Solar & Space Weather Euroconference, "The Solar Cycle and Terrestrial Climate"* (pp. 617–622). Noordwijk, Netherlands: ESA Publications Division volume 463 of *ESA Special Publica-*

*tion*. URL: https://ui.adsabs.harvard.edu/abs/2000ESASP.463..617S.

Strugarek, A. (2017). Models of star-planet magnetic interaction. In H. J. Deeg, & J. A. Belmonte (Eds.), *Handbook of Exoplanets* (pp. 1–23). New York, NY: Springer International Publishing. doi:10.1007/978-3-319-30648-3_25-1.

Strugarek, A., Beaudoin, P., Charbonneau, P. et al. (2017). Reconciling solar and stellar magnetic cycles with nonlinear dynamo simulations. *Science*, *357*(6347), 185–187. doi:10.1126/science.aal3999.

Suess, H. E. (1980). The radiocarbon record in tree rings of the last 8000 years. *Radiocarbon*, *22*(2), 200–209. doi:10.1017/S0033822200009462.

Sukhodolov, T., Usoskin, I., Rozanov, E. et al. (2017). Atmospheric impacts of the strongest known solar particle storm of 775 AD. *Scientific Reports*, *7*(1), 45257. doi:10.1038/srep45257.

Svalgaard, L., Cagnotti, M., & Cortesi, S. (2017). The effect of sunspot weighting. *Solar Physics*, *292*(2), 34. doi:10.1007/s11207-016-1024-9.

Svalgaard, L., & Cliver, E. W. (2005). The IDV index: Its derivation and use in inferring long-term variations of the interplanetary magnetic field strength. *Journal of Geophysical Research: Space Physics*, *110*(A12), A12103. doi:10.1029/2005JA011203.

Svalgaard, L., & Cliver, E. W. (2010). Heliospheric magnetic field 1835–2009. *Journal of Geophysical Research: Space Physics*, *115*(A9), A09111. doi:10.1029/2009JA015069.

Svalgaard, L., & Schatten, K. H. (2016). Reconstruction of the sunspot group number: The backbone method. *Solar Physics*, *291*(9), 2653–2684. doi:10.1007/s11207-015-0815-8.

Tagirov, R. V., Shapiro, A. I., Krivova, N. A. et al. (2019). Readdressing the UV solar variability with SATIRE-S: Non-LTE effects. *Astronomy & Astrophysics*, *631*, A178. doi:10.1051/0004-6361/201935121.

Talafha, M., Nagy, M., Lemerle, A. et al. (2022). Role of observable nonlinearities in solar cycle modulation. *Astronomy & Astrophysics*, *660*, A92. doi:10.1051/0004-6361/202142572.

Tapping, K. F., & Charrois, D. P. (1994). Limits to the accuracy of the 10.7 cm flux. *Solar Physics*, *150*(1), 305–315. doi:10.1007/BF00712892.

Temmer, M., Rybák, J., Bendík, P. et al. (2006). Hemispheric sunspot numbers and from 1945–2004: Catalogue and N-S asymmetry analysis for solar cycles 18–23. *Astronomy & Astrophysics*, *447*(2), 735–743. doi:10.1051/0004-6361:20054060.

Thuillier, G., Floyd, L., Woods, T. N. et al. (2004). Solar irradiance reference spectra for two solar active levels. *Advances in Space Research*, *34*(2), 256–261. doi:10.1016/j.asr.2002.12.004.

Tjus, J. B., Desiati, P., Döpper, N. et al. (2020). Cosmic-ray propagation around the Sun: Investigating the influence of the solar magnetic field on the cosmic-ray Sun shadow. *Astronomy & Astrophysics*, *633*, A83. doi:10.1051/0004-6361/201936306.

Tlatov, A. G. (2013). Long-term variations in sunspot characteristics. *Geomagnetism and Aeronomy*, *53*(8), 953–956. doi:10.1134/S0016793213080264.

Tlatov, A. G., & Pevtsov, A. A. (2017). On the timing of the next great solar activity minimum. *Advances in Space Research*, *60*(5), 1108–1114. doi:10.1016/j.asr.2017.05.009.

Tobias, S. M. (1996). Grand minima in nonlinear dynamos. *Astronomy and Astrophysics*, *307*, L21–L24. URL: https://ui.adsabs.harvard.edu/abs/1996A&A...307L..21T/abstract.

Tobias, S. M. (1997). The solar cycle: Parity interactions and amplitude modulation. *Astronomy and Astrophysics*, *322*, 1007–1017. URL: https://ui.adsabs.harvard.edu/abs/1997A&A...322.1007T.

Tobias, S. M. (1998). Relating stellar cycle periods to dynamo calculations. *Monthly Notices of the Royal Astronomical Society*, *296*(3), 653–661. doi:10.1046/j.1365-8711.1998.01412.x.

Tobias, S. M. (2002). Modulation of solar and stellar dynamos. *Astronomische Nachrichten (Astronomical News)*, *323*(3-4), 417–423. doi:10.1002/1521-3994(200208)323:3/4<417::AID-ASNA417>3.0.CO;2-U.

Tobias, S. M. (2021). The turbulent dynamo. *Journal of Fluid Mechanics*, *912*, P1. doi:10.1017/jfm.2020.1055.

Tylka, A. J., Reames, D. V., & Ng, C. K. (1999). Observations of systematic temporal evolution in elemental composition during gradual solar energetic particle events. *Geophysical Research Letters*, *26*(14), 2141–2144. doi:10.1029/1999GL900458.

Ueno, S., Shibata, K., Ichimoto, K. et al. (2010). Continuous H-Alpha Imaging Network project (CHAIN) with ground- based solar telescopes for space weather research. *African Skies*, *14*, 17–20. URL: https://ui.adsabs.harvard.edu/abs/2010AfrSk..14...17U.

Upton, L. A., & Hathaway, D. H. (2018). An updated solar cycle 25 prediction with AFT: The modern minimum. *Geophysical Research Letters*, *45*(16), 8091–8095. doi:10.1029/2018GL078387.

Usoskin, I. G. (2023). A history of solar activity over millennia. *Living Reviews in Solar Physics*, *20*(1), 2. doi:10.1007/s41116-023-00036-z.

Usoskin, I. G., Koldobskiy, S. A., Kovaltsov, G. A. et al. (2020). Revisited reference solar proton event of 23 February 1956: Assessment of the cosmogenic-isotope method sensitivity to extreme solar events. *Journal of Geophysical Research: Space Physics*, *125*(6), e2020JA027921. doi:10.1029/2020JA027921.

Usoskin, I. G., Koldobskiy, S. A., Poluianov, S. V. et al. (2023). Consistency of the average flux of solar energetic particles over timescales of years to megayears. *Astronomy & Astrophysics*, *670*, L22. doi:10.1051/0004-6361/202245810.

Usoskin, I. G., Kovaltsov, G. A., Lockwood, M. et al. (2016). A new calibrated sunspot group series since 1749: Statistics of active day fractions. *Solar Physics*, *291*(9), 2685–2708. doi:10.1007/s11207-015-0838-1.

Usoskin, I. G., Kromer, B., Ludlow, F. et al. (2013). The AD775 cosmic event revisited: The Sun is to blame. *Astronomy & Astrophysics*, *552*, L3. doi:10.1051/0004-6361/201321080.

Usoskin, I. G., Solanki, S. K., Krivova, N. A. et al. (2021). Solar cyclic activity over the last millennium reconstructed from annual 14C data. *Astronomy & Astrophysics*, *649*, A141. doi:10.1051/0004-6361/202140711.

Uusitalo, J., Arppe, L., Hackman, T. et al. (2018). Solar superstorm of AD 774 recorded subannually by Arctic tree rings. *Nature Communications*, *9*(1), 3495. doi:10.1038/s41467-018-05883-1.

Vainio, R., & Laitinen, T. (2007). Monte Carlo simulations of coronal diffusive shock acceleration in self-generated turbulence. *The Astrophysical Journal*, *658*(1), 622–630. doi:10.1086/510284.

Van Hollebeke, M. A. I., Ma Sung, L. S., & McDonald, F. B. (1975). The variation of solar proton energy spectra and size distribution with heliolongitude. *Solar Physics*, *41*(1), 189–223. doi:10.1007/BF00152967.

Vaquero, J. M. (2007). Historical sunspot observations: A review. *Advances in Space Research*, *40*(7), 929–941. doi:10.1016/j.asr.2007.01.087. arXiv:astro-ph/0702068.

Vaquero, J. M., Svalgaard, L., Carrasco, V. M. S. et al. (2016). A revised collection of sunspot group numbers. *Solar Physics*, *291*(9), 3061–3074. doi:10.1007/s11207-016-0982-2.

Vaquero, J. M., & Trigo, R. M. (2014). Revised group sunspot number values for 1640, 1652, and 1741. *Solar Physics*, *289*(3), 803–808. doi:10.1007/s11207-013-0360-2.

Vaquero, J. M., & Vázquez, M. (2009). *The Sun Recorded through History: Scientific Data Extracted from Historical Documents* volume 361. Berlin, Germany: Springer. doi:10.1007/978-0-387-92789-3.

Varela, J., Brun, A. S., Zarka, P. et al. (2022). MHD study of extreme space weather conditions for exoplanets with Earth-like magnetospheres: On habitability conditions and radio-emission. *Space Weather*, *20*(11), e2022SW003164. doi:10.1029/2022SW003164.

Vasilyev, V., Reinhold, T., Shapiro, A. I. et al. (2022). Superflares on solar-like stars: A new method for identifying the true flare sources in photometric surveys. *Astronomy & Astrophysics*, *668*, A167. doi:10.1051/0004-6361/202244422.

Verkhoglyadova, O. P., Li, G., Zank, G. P. et al. (2010). Understanding large SEP events with the PATH code: Modeling of the 13 December 2006 SEP event. *Journal of Geophysical Research: Space Physics*, *115*(A12), A12103. doi:10.1029/2010JA015615.

Verkhoglyadova, O. P., Li, G., Zank, G. P. et al. (2009). Using the PATH code for modeling gradual sep events in the inner heliosphere. *The Astrophysical Journal*, *693*(1), 894–900. doi:10.1088/0004-637X/693/1/894.

Veronig, A. M., Odert, P., Leitzinger, M. et al. (2021). Indications of stellar coronal mass ejections through coronal dimmings. *Nature Astronomy*, *5*(7), 697–706. doi:10.1038/s41550-021-01345-9.

Vidotto, A. A., Gregory, S. G., Jardine, M. et al. (2014). Stellar magnetism: Empirical trends with age and rotation. *Monthly Notices of the Royal Astronomical Society*, *441*(3), 2361–2374. doi:10.1093/mnras/stu728.

Vieira, L. E. A., & Solanki, S. K. (2010). Evolution of the solar magnetic flux on time scales of years to millenia. *Astronomy & Astrophysics*, *509*, A100. doi:10.1051/0004-6361/200913276.

Vieira, L. E. A., Solanki, S. K., Krivova, N. A. et al. (2011). Evolution of the

solar irradiance during the Holocene. *Astronomy & Astrophysics*, *531*, A6. doi:10.1051/0004-6361/201015843.

Vokhmyanin, M., Arlt, R., & Zolotova, N. (2021). Sunspot positions and areas from observations by Cigoli, Galilei, Cologna, Scheiner, and Colonna in 1612 – 1614. *Solar Physics*, *296*(1), 4. doi:10.1007/s11207-020-01752-7.

von Steiger, R. (2008). The solar wind throughout the solar cycle. In A. Balogh, L. J. Lanzerotti, & S. T. Suess (Eds.), *The Heliosphere through the Solar Activity Cycle* Springer Praxis Books (pp. 41–78). Berlin, Germany: Springer. doi:10.1007/978-3-540-74302-6_3.

Waldmeier, M. (1968). Die Beziehung zwischen der Sonnenflecken-relativzahl und der Gruppenzahl (The relationship between sunspot relative number and group number). *Astron. Mitteil. Eidgn. Sternw. Zürich (Astronomical Notes of the ETH Observatory Zürich)*, (285), 1–8.

Wang, Y.-M., & Lean, J. L. (2021). A new reconstruction of the Sun's magnetic field and total irradiance since 1700. *The Astrophysical Journal*, *920*(2), 100. doi:10.3847/1538-4357/ac1740.

Wang, Y.-M., Lean, J. L., & Sheeley, N. R., Jr. (2005). Modeling the Sun's magnetic field and irradiance since 1713. *The Astrophysical Journal*, *625*(1), 522–538. doi:10.1086/429689.

Wang, Y.-M., & Sheeley, N. R., Jr. (1995). Solar implications of Ulysses interplanetary field measurements. *The Astrophysical Journal*, *447*(2), L143–L146. doi:10.1086/309578.

Warnecke, J., Käpylä, P. J., Käpylä, M. J. et al. (2016). Influence of a coronal envelope as a free boundary to global convective dynamo simulations. *Astronomy & Astrophysics*, *596*, A115. doi:10.1051/0004-6361/201526131.

Warnecke, J., Rheinhardt, M., Tuomisto, S. et al. (2018). Turbulent transport coefficients in spherical wedge dynamo simulations of solar-like stars. *Astronomy & Astrophysics*, *609*, A51. doi:10.1051/0004-6361/201628136.

Webb, D. F. (2002). CMEs and the solar cycle variation in their geoeffectiveness. In A. Wilson (Ed.), *Proceedings of the SOHO 11 Symposium on From Solar Min to Max: Half a Solar Cycle with SOHO* (pp. 409–419). Noordwijk, Netherlands: ESA Publications Division volume 508 of *ESA Special Publication*. doi:92-9092-818-2.

Wei, X. (2022). Tidal dynamo in solar-like close binary stars. *Monthly Notices of the Royal Astronomical Society*, *513*(4), 5474–5476. doi:10.1093/mnras/stac1323.

Weiss, N. O., & Tobias, S. M. (2016). Supermodulation of the Sun's magnetic activity: The effects of symmetry changes. *Monthly Notices of the Royal Astronomical Society*, *456*(3), 2654–2661. doi:10.1093/mnras/stv2769.

Weisshaar, E., Cameron, R. H., & Schüssler, M. (2023). No evidence for synchronization of the solar cycle by a "clock". *Astronomy & Astrophysics*, *671*, A87. doi:10.1051/0004-6361/202244997.

Wenzel, K. P., Marsden, R. G., Page, D. E. et al. (1992). The ULYSSES mission. *Astronomy and Astrophysics Supplement Series*, *92*, 207–219. URL: https://ui.adsabs.harvard.edu/abs/1992A&AS...92..207W.

Wenzler, T., Solanki, S. K., Krivova, N. A. et al. (2006). Reconstruction of solar irradiance variations in cycles 21–23 based on surface magnetic fields. *Astronomy & Astrophysics*, *460*(2), 583–595. doi:10.1051/0004-6361:20065752.

Willamo, T., Usoskin, I. G., & Kovaltsov, G. A. (2017). Updated sunspot group number reconstruction for 1749–1996 using the active day fraction method. *Astronomy & Astrophysics*, *601*, A109. doi:10.1051/0004-6361/201629839.

Willson, R. C. (1997). Total solar irradiance trend during solar cycles 21 and 22. *Science*, *277*(5334), 1963–1965. doi:10.1126/science.277.5334.1963.

Willson, R. C., Gulkis, S., Janssen, M. et al. (1981). Observations of solar irradiance variability. *Science*, *211*(4483), 700–702. doi:10.1126/science.211.4483.700.

Willson, R. C., & Hudson, H. S. (1988). Solar luminosity variations in solar cycle 21. *Nature*, *332*(6167), 810–812. doi:10.1038/332810a0.

Willson, R. C., & Mordvinov, A. V. (2003). Secular total solar irradiance trend during solar cycles 21–23. *Geophysical Research Letters*, *30*(5), 1199. doi:10.1029/2002GL016038.

Wilmot-Smith, A. L., Martens, P. C. H., Nandy, D. et al. (2005). Low-order stellar dynamo models. *Monthly Notices of the Royal Astronomical Society*, *363*(4), 1167–1172. doi:10.1111/j.1365-2966.2005.09514.x.

Wilmot-Smith, A. L., Nandy, D., Hornig, G. et al. (2006). A time delay model for solar and stellar dynamos. *The Astrophysical Journal*, *652*(1), 696–708. doi:10.1086/508013.

Wolf, R. (1848). *Nachrichten von Der Sternwarte in Bern (Bulletin of the Observatory in Bern)*. doi:10.3931/e-rara-2007.

Wolf, R. (1851). Auszug aus einem Schreiben des Herrn Professors Rudolf Wolf, Directors der Sternwarte in Bern, an den Herausgeber (Excerpt from a letter from Professor Rudolf Wolf, director of the observatory in Bern, to the publisher). *Astronomische Nachrichten (Astronomical News)*, *32*(13), 193–194. doi:10.1002/asna.18510321306.

Wolf, R. (1856). Mittheilungen über die Sonnenflecken I. *Astron. Mitteil. Eidgn. Sternw. Zürich*, *1*, 3–13. URL: https://ui.adsabs.harvard.edu/abs/1856MiZur...1....3W.

Wolf, R. (1859). Extract of a letter from Prof. R. Wolf, of Zurich, to Mr. Carrington, dated Jan. 12, 1859. *Monthly Notices of the Royal Astronomical Society*, *19*(3), 85–86. doi:10.1093/mnras/19.3.85.

Wolff, C. L., & Patrone, P. N. (2010). A new way that planets can affect the sun. *Solar Physics*, *266*(2), 227–246. doi:10.1007/s11207-010-9628-y.

Woods, T. N., Chamberlin, P. C., Harder, J. W. et al. (2009). Solar irradiance reference spectra (SIRS) for the 2008 whole heliosphere interval (WHI). *Geophysical Research Letters*, *36*(1), L01101. doi:10.1029/2008GL036373.

Woods, T. N., & DeLand, M. T. (2021). An improved solar spectral irradiance composite record. *Earth and Space Science*, *8*(8), e2021EA001740. doi:10.1029/2021EA001740.

Woods, T. N., Eparvier, F. G., Harder, J. et al. (2018). Decoupling solar variability and instrument trends using the multiple same-irradiance-level (MuSIL) analysis technique. *Solar Physics*, *293*(5), 76. doi:10.1007/s11207-018-1294-5.

Woods, T. N., Harder, J. W., Kopp, G. et al. (2022). Solar-cycle variability results from the Solar Radiation and Climate Experiment (SORCE) mission. *Solar Physics*, *297*(4), 43. doi:10.1007/s11207-022-01980-z.

Wu, C.-J., Krivova, N. A., Solanki, S. K. et al. (2018). Solar total and spectral irradiance reconstruction over the last 9000 years. *Astronomy & Astrophysics*, *620*, A120. doi:10.1051/0004-6361/201832956.

Yeates, A. R., Nandy, D., & Mackay, D. H. (2008). Exploring the physical basis of solar cycle predictions: Flux transport dynamics and persistence of memory in advection- versus diffusion-dominated solar convection zones. *The Astrophysical Journal*, *673*(1), 544–556. doi:10.1086/524352.

Yeo, K. L., Krivova, N. A., Solanki, S. K. et al. (2014). Reconstruction of total and spectral solar irradiance from 1974 to 2013 based on KPVT, SoHO/MDI, and SDO/HMI observations. *Astronomy & Astrophysics*, *570*, A85. doi:10.1051/0004-6361/201423628.

Yeo, K. L., Solanki, S. K., & Krivova, N. A. (2020a). How faculae and network relate to sunspots, and the implications for solar and stellar brightness variations. *Astronomy & Astrophysics*, *639*, A139. doi:10.1051/0004-6361/202037739.

Yeo, K. L., Solanki, S. K., Krivova, N. A. et al. (2020b). The dimmest state of the Sun. *Geophysical Research Letters*, *47*(19), e2020GL090243. doi:10.1029/2020GL090243.

Yeo, K. L., Solanki, S. K., Norris, C. M. et al. (2017). Solar irradiance variability is caused by the magnetic activity on the solar surface. *Physical Review Letters*, *119*(9), 091102. doi:10.1103/PhysRevLett.119.091102.

Yoshimura, H. (1975). Solar-cycle dynamo wave propagation. *The Astrophysical Journal*, *201*, 740–748. doi:10.1086/153940.

Zahn, J.-P., Brun, A. S., & Mathis, S. (2007). On magnetic instabilities and dynamo action in stellar radiation zones. *Astronomy & Astrophysics*, *474*(1), 145–154. doi:10.1051/0004-6361:20077653.

Zank, G. P., Rice, W. K. M., & Wu, C. C. (2000). Particle acceleration and coronal mass ejection driven shocks: A theoretical model. *Journal of Geophysical Research: Space Physics*, *105*(A11), 25079–25095. doi:10.1029/1999JA000455.

Zarka, P. (2007). Plasma interactions of exoplanets with their parent star and associated radio emissions. *Planetary and Space Science*, *55*(5), 598–617. doi:10.1016/j.pss.2006.05.045.

Zirnstein, E. J., Heerikhuisen, J., McComas, D. J. et al. (2018). Simulation of the solar wind dynamic pressure increase in 2014 and its effect on energetic neutral atom fluxes from the heliosphere. *The Astrophysical Journal*, *859*(2), 104. doi:10.3847/1538-4357/aac016.

Zirnstein, E. J., Shrestha, B. L., McComas, D. J. et al. (2022). Oblique and rippled heliosphere structures from the Interstellar Boundary Explorer. *Nature Astronomy*, *6*(12), 1398–1413. doi:10.1038/s41550-022-01798-6.

**Declaration of interests**

☒ The authors declare that they have no known competing financial interests or personal relationships that could have appeared to influence the work reported in this paper.

☐ The authors declare the following financial interests/personal relationships which may be considered as potential competing interests: